Review

Shaping Clean Water Futures with Carbon-Based Nanomaterials: A Comprehensive Review

Ganesh Gollavelli * and Yong-Chien Ling *

Posted Date: 7 October 2025

doi: 10.20944/preprints202510.0466.v1

Keywords: carbon-based nanomaterials; wastewater treatment; adsorption; membrane separation; photocatalytic degradation; systematic thinking and precautionary principle

 doi:10.20944/preprints202510.0466.v1

Review

Shaping Clean Water Futures with Carbon-Based Nanomaterials: A Comprehensive Review

Ganesh Gollavelli [1,*] and Yong-Chien Ling [2,*]

[1] Aurora Deemed to be University, India

[2] National Tsing Hua University, Taiwan

* Correspondence: ganesh@aurora.edu.in or ganeshgollavelli@gmail.com (G.G.); ycling@mx.nthu.edu (Y.-C.L.); Tel.: 886-0933737928

Abstract

The thorough analysis in this review examines current advancements in carbon-based nanomaterials (CBNs) intended for wastewater treatment, with an emphasis on how they are used to alleviate the world's problems with water scarcity and pollution. We highlight the fullerenes, carbon dots (CDs), carbon nanotubes (CNTs), graphene, graphene oxide (GO), reduced graphene oxide (RGO), and their composites, for OD, ID, 2D, and 3D materials. Because of their unique properties, CBNs are useful tools for eliminating pollutants, toxins, and pathogens from wastewater. This review emphasizes the most significant wastewater treatment techniques such as adsorption, membrane separation, and photocatalytic degradation of the pollutants based on CBNs. Apart from this, we also highlight the performance statistics and environmental impacts as well as future perspective. Sustainable practices pay attention to concerns about CBNs targeted for wastewater treatment as well as systematic thinking and precautionary principle are indispensable considerations.

Keywords: carbon-based nanomaterials; wastewater treatment; adsorption; membrane separation; photocatalytic degradation; systematic thinking and precautionary principle

1. Introduction

The rise in human population, industrialization, domestic wastewater, agricultural practices, and careless utilization of providing safe potable water have been daunting. This situation created an alarming situation globally with immediate effect. Water covers more than 71% of the planet's surface, meaning that just over one percent of it is fit for human use. Population growth is predicted to increase water consumption by 55% by 2050, while the global water shortfall is predicted to rise to 40% by 2030 [1]. According to the World Water Development Report 2020, by the United Nations, approximately four billion people experienced acute water dearth for at least one month of the year [2]. World Health Organization statistics revealed that among four people, one does not have an availability to safe potable water. The situation is worse in underdeveloped and low income countries. The lack of this vital resource was a factor in 6% of fatalities in 2017 was recorded [3]. In order to fulfill the growing demand, it is crucial to ensure the sustainable use of water, which might be achieved by creating efficient wastewater treatment techniques. The increasing of wastewater generation has been daunting to scientists, researchers, and engineers worldwide and the remediation of water pollutants in a sustainable and economic manner to generate clean water is a difficult issue [4].

Generally, wastewater can be defined as used water, and there are several types of it, such as domestic sewage waste, industrial wastewater, and agricultural wastewater. Which contain the most prominent pollutants, like organic (dyes, pesticides,) , inorganic (heavy metals), and biological pollutants (bacteria, and viruses). The most important treatment methods to treat the wastewater are physical (sedimentation and aeration), chemical (neutralization, adsorption, precipitation, disinfection, and ion-exchange), biological (aerobic, anaerobic and composting), and advanced

 doi:10.20944/preprints202510.0466.v1

wastewater treatment technologies (desalination, membrane filtration, and ultraviolet irradiation). Though we have several methods, it is very imperative to design the best treatment method or improve the existing methodologies [5–7].

Nanotechnology shows great promise in various disciplines, including wastewater purification technologies. Nanomaterials (NMs) with their tunable small sizes, high surface area, tailored physiochemical properties, and ease of surface functionalization, present unique prospects to create more efficient adsorbents, catalysts, membranes, and redox active media for wastewater purification and eradication. Various pollutants such as organic and inorganic toxins (heavy metals, dyes, pesticides, and solvents), biological hazards (bacteria, fungus, virus, and algae) which make diseases like cancer, typhoid, cholera, and dengue could be efficiently removed from wastewater by using NMs [8,9].

CNTs have been considered as some of the best among the plethora of NMs available today due to their astonishing capabilities in variety of applications, such as water treatment, environment, electronics, optical, catalysis, and biomedical use. Their versatility lie in preparation, economic availability, and interesting properties like high surface area and tunable functionality, distinguished surface morphology and porosity. In this review, we highlighted various NMs, from 0D fullerenes, CDs, 1D CNTs, 2D graphene, and GO materials for wastewater treatment, along with their advantages and future challenges [10–16]. We also made an excellent discussion on the performance of every material discussed above for the most prominent treatment methods such as adsorption, membrane separation, and catalytic catalytic degradation of the pollutants. The systematic discussion of the review can be seen in Scheme 1.

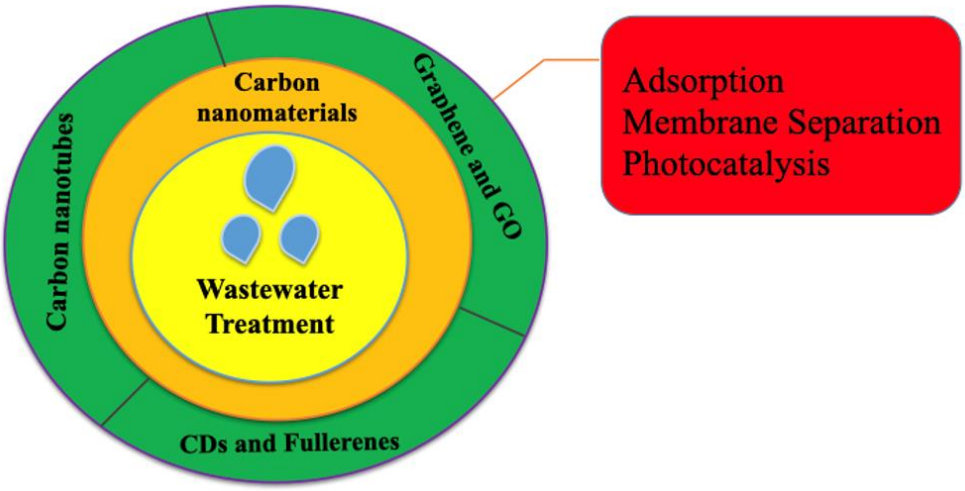

Scheme 1. Wastewater treatment by carbon nanomaterials.

2. Types of Wastewater and Pollutants

The wastewater can be defined as water which can be produced from various sources, like domestic waste, industrial and agricultural used water. Based on the origin, it could be called a point source or a scattered source of contamination. Examples for point source pollutants are sewage discharge, which originated from a single point of discharge. Whereas the scattered or dispersed pollutants enter the wastewater body from a vast range of origins. Examples are agricultural sources of waste like pesticides, animal feces, fertilizers, and pathogens. Industrial sources such as microplastics, radioactive hazards, oils, heavy metals, and organic dyes, heat from power plant cooling water are some other examples to dispersed sources of pollutants. In general, the wastewater are classified as domestic, industrial, and agricultural sources containing pollutants of heavy metals, organics and pathogens as in Figure 1 [17].

 doi:10.20944/preprints202510.0466.v1

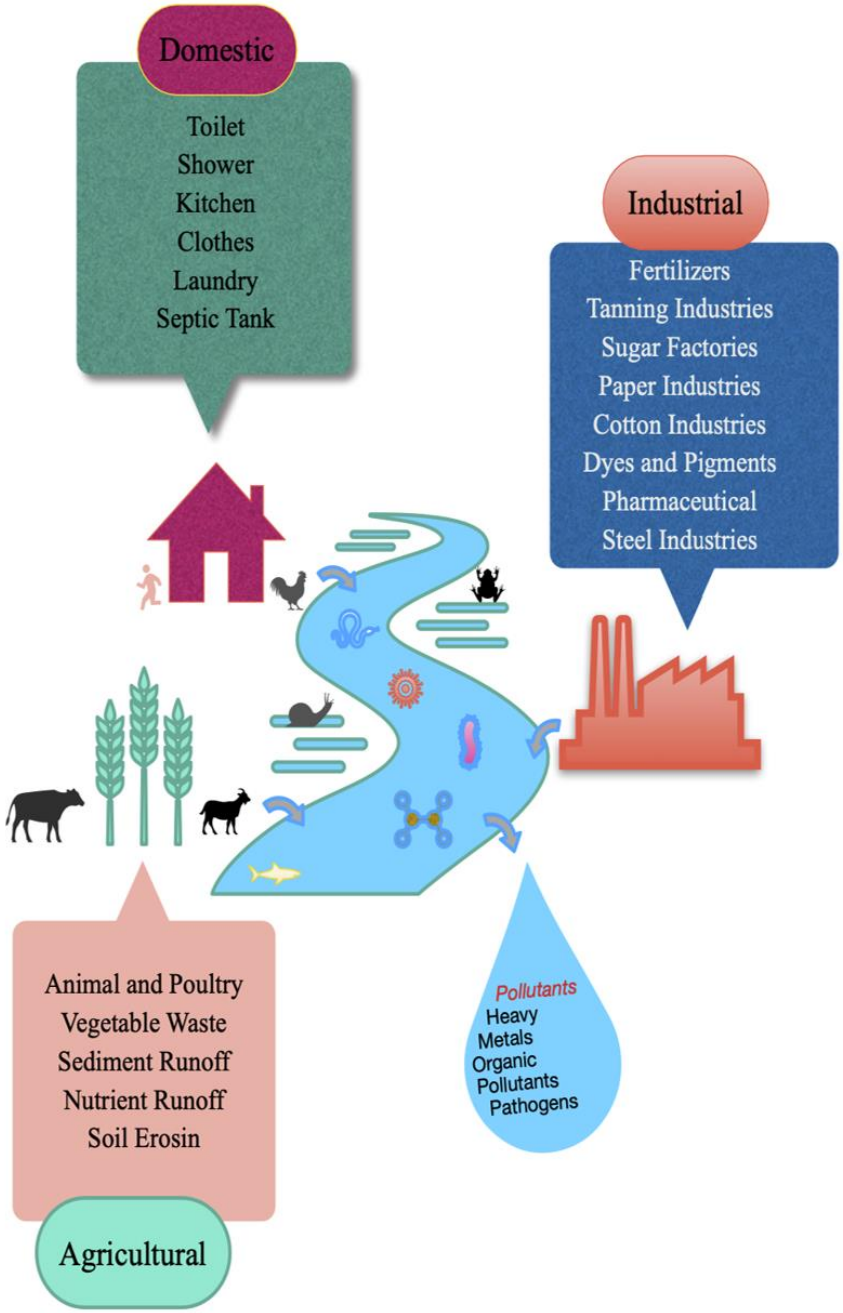

Figure 1. Wastewater sources and their pollutants.

Wastewater consists of a number of microorganisms like bacteria, viruses, and protozoa as well as toxic materials like radionuclides, heavy metals, and trace elements. Moreover, wastewater is the main root of water-borne illnesses, including cholera and typhoid, which can be fatal. Many children have died as a result of drinking contaminated water. Figure 2A depicts the types of contaminants in wastewater and, the principles of primary, secondary, and tertiary wastewater treatment in Figure 2B [18].

Preprints.org (www.preprints.org) | NOT PEER-REVIEWED | Posted: 7 October 2025 doi:10.20944/preprints202510.0466.v1

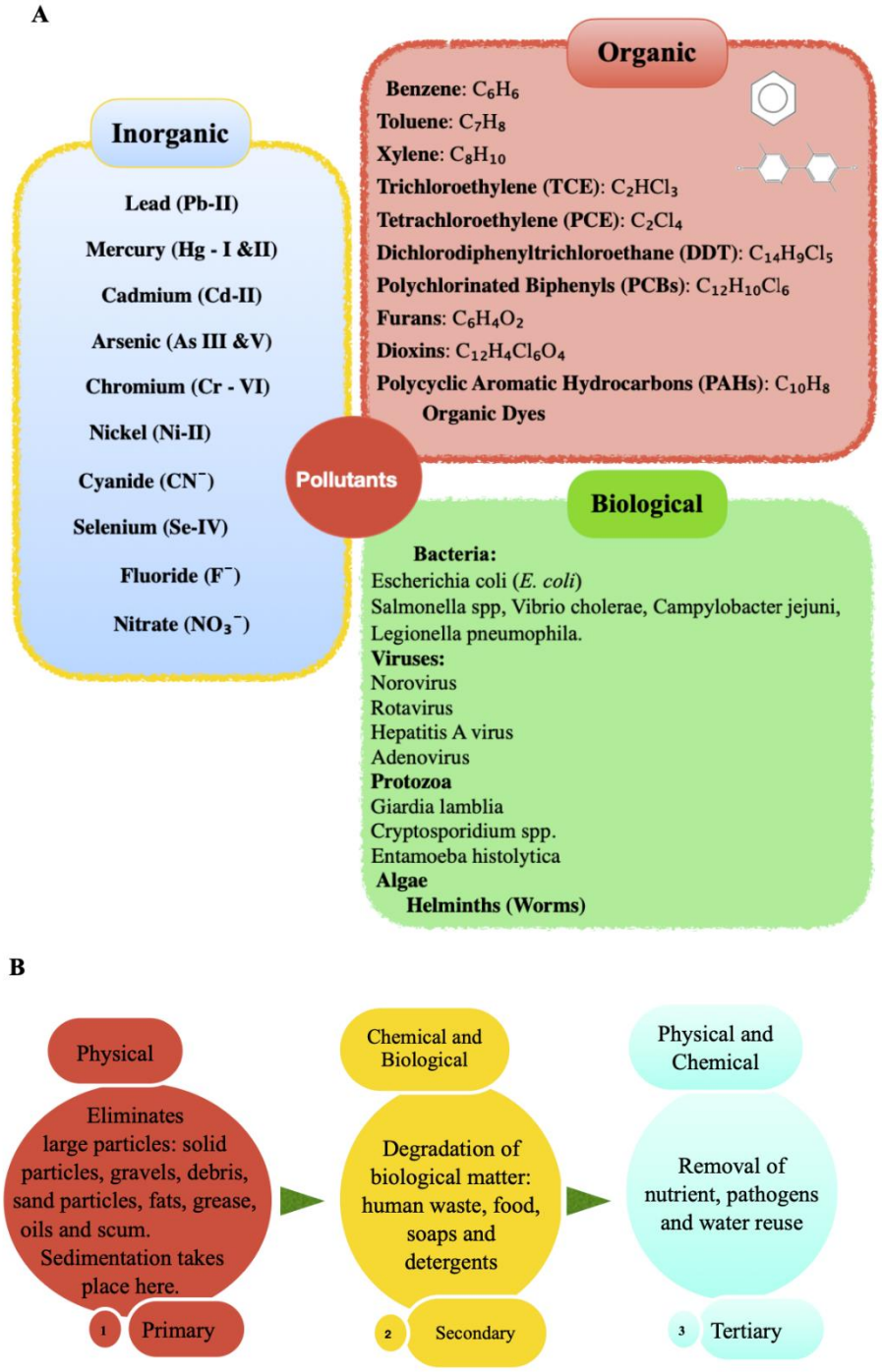

Figure 2. A Types of inorganic, organic, and biological pollutants in wastewater and B. principles for primary, secondary, and tertiary treatment of wastewater.

Wastewater treatment in the current days is crucial due to the adverse effects of pathogens and the risks of wastewater pollution on people, animals, and crops. To avoid the pollution of the environment, wastewater treatment on a personal and governmental level needs to be considered. Physical, chemical, and biological methods can be used to treat wastewater to purify it by eradicating the impurities. The impurities are classified as inorganic, organic, and biological. These impurities in the wastewater can be treated in three steps: 1. Primary treatment, where materials that float (scum) are removed by skimming, while settleable organic and inorganic solids are removed by sedimentation. In primary clarifiers, primary treatment eliminates the biochemical oxygen demand (BOD_5) about 25-50%, the total suspended solids (SS) of 50-70%, and the oil and grease about 65-70%. 2. Secondary treatment or subsequent treatment, which makes use of aerobic biological treatment to

 doi:10.20944/preprints202510.0466.v1

remove biodegradable pollutants in it. Aerobic microorganisms (mostly bacteria) carry out biological treatment in the presence of oxygen by breaking down the organic materials in the wastewater and creating additional microorganisms as well as inorganic end products (mainly carbon dioxide, ammonia and water).

When some wastewater components are unable to be eliminated by secondary treatment, tertiary and/or advanced wastewater treatment is utilized. Disinfection is frequently a part of tertiary treatment, and it usually entails injecting a chlorine solution. Other methods of disinfection include ozone and ultraviolet (UV) radiation. Chlorine and other disinfectants have varying bactericidal effects based on pH, interaction time, organic content, and temperature of effluent. The treated sludge can be buried in the land or used as fertilizer in agricultural sectors [1–3,19,20].

3. Carbon-Based Nanomaterials for Wastewater Treatment: Mechanism Insights

Carbon created uniqueness in the periodic table and has gained a good respect from the scientific world due to its versatility in bonding with hydrogen and other atoms to form a variety of chemical compounds, which have a great significance in various fields. Carbon is the 4th most available element in the universe and 15th on Earth's crust. Carbon belongs to the 4th group in the periodic table, electronegativity 2.55 (Pauling scale), atomic radius 0.09 14 nm, mass is 12 amu, and could exist in many isotopes, importantly ^{11}C, ^{12}C, ^{13}C, and ^{14}C. The melting and boiling points are 3652 °C and 4827 °C. Owing to these characteristics, the carbon reacts within itself by catenation and forms a variety of allotropes with unique features that amaze scientists. The outstanding characteristics of carbon have won many Nobel Prizes in various fields such as chemistry, physics, and medicine. Hence, the CBNs have been adopted in various disciplines of science, engineering, and technology [21,22].

A plethora of CBNs have been reported to date for water purification. Wood charcoal has been identified as the ancient carbon material used for early water purification since 3750 BC by the Egyptians and Sumerians. Sand and charcoal combinations are documented by the Hindu texts from 450 BC to serve the same purpose. After many systematic studies carried out by many pioneers, carbon black was commercialized for the purification of potable water in 1862. To date, activated carbon is the best ever-trusted carbon material in the water industry [23]. However, with the advancement in material science and nanotechnology, several nanocarbon materials have been reported for water treatment. Figure 3 illustrates that OD fullerenes, OD CDs, 1D CNTs, and 2D G (graphene), GO, and RGO are the most studied CBNs to provide better wastewater treatment solutions based on adsorption, membrane filtration, and photocatalysis mechanisms [11,24].

The significant properties of carbon nanomaterials for water treatment are: 1. High surface area, 2. High adsorption capacity, 3. Mechanical strength, 4. Light in weight, 5. Chemical stability in acid, 6. Easy and tunable chemical functionality by covalent and non-covalent interactions, 7. High pore volume in the case of activated carbon and carbon nanosponges, 8. Hydrophobicity (graphene) and hydrophilicity (GO and CDs), 9. Catalysis, 10. Simple and easy recovery of expensive metals by burning away the support, 11. Availability in different structures, 12. Economically available, 13. Low eco toxicity, 14. Industrial scale production, 15. High thermal stability, 16. Less density. These most important properties make the CNTs indispensable in water purification industries.

 doi:10.20944/preprints202510.0466.v1

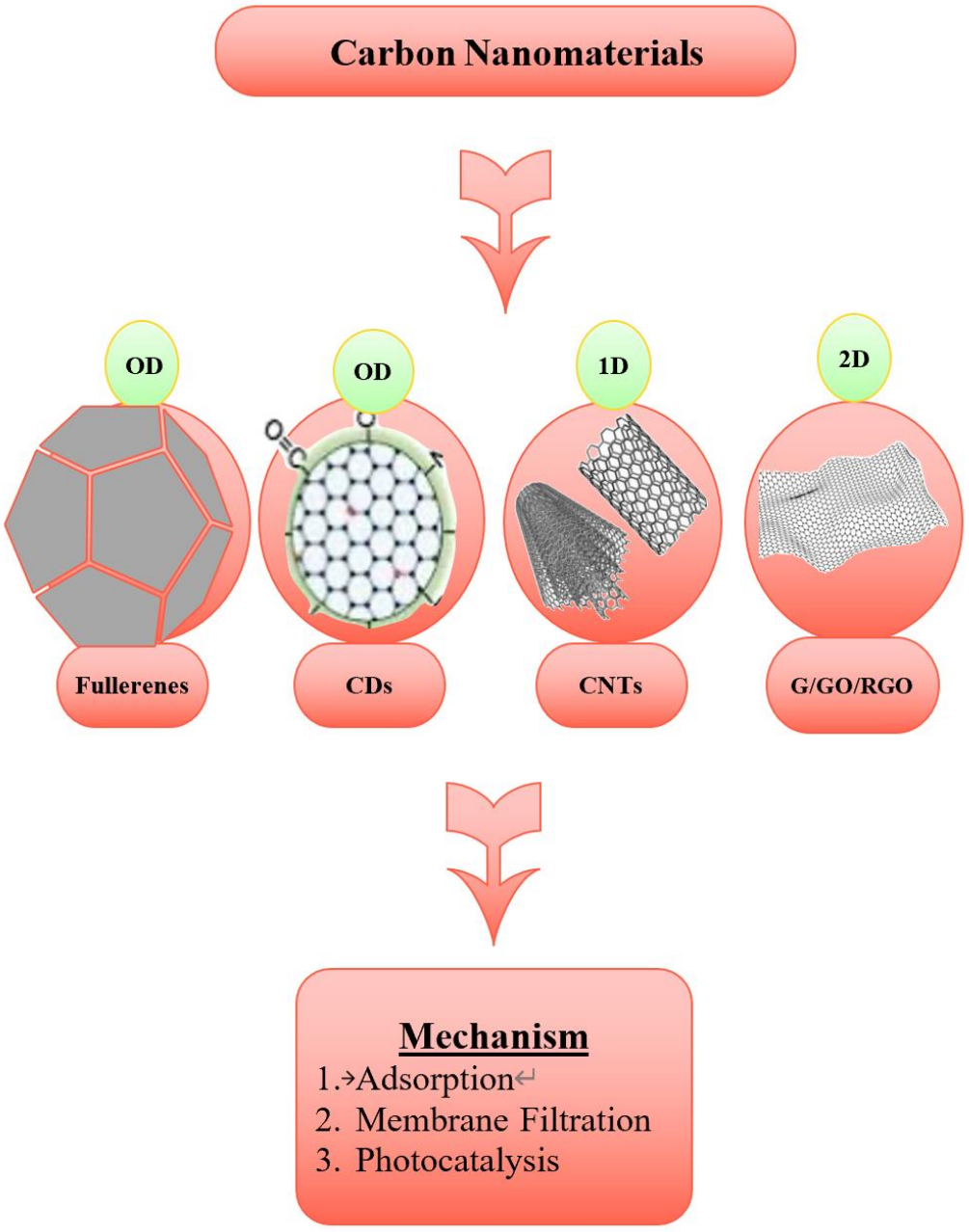

Figure 3. 0D Fullerenes, 0D CDs, 1D CNTs, 2D G/GO/RGO and corresponding wastewater treatment mechanism.

Nowadays, coagulation/flocculation, membrane filtration, photocatalytic degradation, biodegradation, advanced oxidation, ozonation, and adsorption are the methods used to detoxify wastewater containing organic /inorganic pollutants. Adsorption-based procedures are seen to be the most appropriate of these because of their high removal efficiency, ability to employ inexpensive adsorbents, and simplicity of usage. On the other hand, other methods, such photocatalytic degradation, release hydrocarbons, phenol, CO_2, and other organic molecules as secondary pollutants.

 doi:10.20944/preprints202510.0466.v1

3.1. Fullerenes for Water Treatment

3.1.1. Adsorption

The adsorption is a physicochemical method which takes place on surface of adsorbents, and is a common method to eradicate inorganic and organic pollutants from wastewater. The adsorption could be a physisorption or chemisorption. Where the physisorption is involved with π-π Interactions, weak, non-covalent interactions known as Van der Waals Forces, London dispersive forces, hydrogen bonding, and hydrophobic interactions. These interactions between adsorbent and adsorbate are very weak and happen in multilayers at low temperatures. The physorption is less specific and occurs with many types of pollutants. It is a reversible process in the presence of different temperatures, pressures, and p^H changes. In contrast, the chemisorption is a single-layered phenomenon where the adsorbent and adsorbate have strong interactions by forming a chemical bonds, like covalent, ionic, or metallic bonds. The interactions in chemisorptions are extremely specific towards adsorbates. Hence, limited to particular pollutants, and the surface functional groups and interaction sites play a pivotal role in this phenomenon. The adsorption energy is remarkably high compared with physorption, and the reversibility of adsorption is very low as there is a strong bonds between the adsorbent and adsorbate. This cause the limited reusability and recycling of the adsorbent. The quantity of adsorbent adsorbed on adsorbate can be expressed with the help of adsorption isotherms at constant temperature. Namely 1) Langmuir. 2) Freundlich. 3) Temkin. 4) Dubinin-Radushkevich (D-R), and 5) Brunauer-Emmett-Teller Isotherm which are expressed below in an order discussed.

1) $q_e / q_m = KL\ Ce / 1 + KL\ Ce$

2) $q_e = KF\ C_e^{1/n}$

3) $q_e = BT \ln (AT\ C_e)$

4) $q_e = q_m \exp^{(-beta\ (Ce)\ 1/n)}$

5) $C_e / q_e (1-C_e) = C / q_m$

The meaning of the terms are expressed as below.

q_e = Amount of adsorbate adsorbed per unit mass of adsorbent at equilibrium

q_m = Maximum adsorption capacity

KL = Langmuir constant

C_e = Adsorbate concentration at equilibrium

KF = Freundlich constant

n = Adsorption intensity related Freundlich expression

AT and BT = Temkin constant

C = BET constant

The amount and rate of adsorption of adsorbate rely on factors such as nature of adsorbate, adsorbent, surface area, porosity, time, temperature, pressure, and p^H of the solution.

Fullerenes are 0D carbon NMs discovered by the Richard Smalley, Robert Curl, and Harold Kroto in 1985, and won the noble prize in chemistry in 1996 [25,26]. The material also called as Buckminsterfullerene or Buckyball as its morphology looks like a soccer ball. The well-known form of fullerene existed in C60 with truncated icosahedron and other polygon structures in case of C70 it was in ellipsoidal shape. The carbon in fullerenes undergoes sp2 hybridization where every carbon form three sigma bonds and one π bond with the adjacent carbon atoms and made a stable networking structure [27]. Despite its stability, fullerenes undergoes various chemical reactions in a specific reaction condition and form desired compounds, composites and metal complexes. The Buckyballs are soluble in non-polar solvents like benzene, toluene etc. and are semiconductor in nature. Shows good electrical, optical, mechanical, and thermal properties. Hence, the fullerenes are used in nanotechnology, materials science, electronics, medicine, and environmental remediation

 doi:10.20944/preprints202510.0466.v1

[28,29]. In general, the adsorption phenomenon depends on surface area, but the fullerenes theoretical and reported surface area (~ 30 m^2/g) is less than compared with other CNTs such as graphene (~ 500-2000 m^2/g), CNTs (~ 1300-2000 m^2/g), GO (~ 500-1500 m^2/g) and CDs (~ 100-800 m^2/g) [30–34]. Based on this, and low solubility in water, fullerenes may not be a viable choice for water treatment, and not much literature was reported in the last five years. However, C60 was used to remove the organic pollutants due to the π-π and non-polar interactions between them. To assess the environmental impact of C60s, research has been done on the interactions of typical environmental pollutants with C60. Naphthalene and 1,2-dichlorobenzene, two hydrophobic pollutants were studied by their adsorption and desorption interactions with C60. The extent to which organic contaminants sorb into C60 aggregates is also significantly impacted by the same processes that induce the wetting and disaggregation of C60 particles. After being vigorously mixed in water, C60 dissolved in organic solvents like toluene can form stable nanoscale aggregates. They are called "nano-C60" because these C60 nanoscale particles create stable suspensions in water. Hysteresis is seen in the desorption of pollutants from stable nano-C60 solutions. A two compartment desorption model explains experimentally observed adsorption/desorption hysteresis: adsorption to external surfaces in contact with water comes first, followed by adsorption to internal surfaces within the aggregates [34]. Many diverse kinds of chemical compounds, such as N-methyl carbamates, phenols, polycyclic aromatic hydrocarbons, and amines can be adsorbed by fullerene with efficiencies that vary depending on the specific component and never go above 60%. For this reason, conventional sorbents such polyurethane foam or XAD-2 are more effective than C60. However, it can efficiently remove the organometallic compounds effectively than RP-C18 and silica gel 100 through the creation of neutral complexes or chelates [35]. In addition to π-π interactions in C60, the surface defects and inter lattice spacing will also help to hold the inorganic and organic pollutants are possible. Fullerenes were used by Alekseeva *et al*. either by itselves or in a composite film material based on polystyrene. They observe Cu^{2+} removal efficicacy is higher in the first scenario. It was discovered that a monomolecular layer has an adsorption capability of 14.6 mmol/g for Cu^{2+} [36]. Using fullerene alone may not be very efficient, but it can enhance the efficiency of adsorption by used as a composite. Upon adding 0.001-0.004% of fullerenes to activated carbons, the ability to absorb Pb^{2+} and Cu^{2+} rose by 1.5-2.5 times [37,38].

3.1.2. Membrane Separation

Fullerenes has good chemical stability, mechanical strength, and tunable surface functionality. Hence the Bucky balls can improve the strength, porosity, and affordability of nanocomposite membranes [39–41]. It has been found that enhancing the stability, water permeability, and solute selectivity of nanocomposite membranes requires careful consideration of the size, shape, and surface properties of fullerenes. Fullerene nanofillers have been used to give required pore sizes, high surface areas, and distinct surface functionalities in an effort to enhance the membrane's overall performance. It has been proposed that improving the surface chemistry of fullerene in polymer/fullerene nanocomposite membranes can lead to improved membrane stability [42].

Efficient salt removal from water, toxic ion separation, ion pair separation, recovering costly metals, and pathogenic microbe separation or deterioration have all been studied in relation to nanocomposite membranes of polymer/fullerenes [43]. Different metal ions including nickel, zinc, copper, cobalt, mercury, lead, arsenic, and cadmium can be recovered using the sorption approach [44,45]. The sorption capabilities of polymer/fullerene nanocomposite membranes towards metals might be influenced by surface imperfections and their design [46]. Additionally, the retention time of nanocomposite membranes showed excellent. In addition, functional hydroxy fullerene C60-based membrane was prepared with high water flux and Li^+/Mg^{2+} salt rejection [47]. Fullerene/GO/epoxy-based resins are prepared for water desalination. The membrane has shown the water flux of 10.9 L m^{-2} h^{-1} bar^{-1}. Nafion/C60 membrane composites were prepared with different weight ratios. The membrane composite has shown better water permeability than the nafion membrane alone. Here,

 doi:10.20944/preprints202510.0466.v1

the C60 in the nation matrix distrusts the polymer chain alignment and helps to allow the water molecules in it [48].

Polyamide membranes has gained exceptionally good success in the water industry [49]. A thin-film nanocomposite membrane for water treatment based on polyamide and hydroxy functional fullerene C60 was prepared by Plisko *et al*. [50]. They considered adding a 5 wt% nanofiller to the membranes and improved their antifouling characteristics and ability to remove organic materials. Prepared polyphenylene isophthalamide (PA) membranes modified with various fullerene derivatives such as hydroxy fullerene (HF)/fullerenol, carboxyfullerene (CF), and fullerene derivative with L-arginine (AF) with 5 wt% quantity. Characterized and assessed the composite features using SEM, XRD, AFM, sorption experiments, and contact angles. To estimate the impact of residual solvent on the membranes of PA and on their parameters, they designed pervaporation separation of industrially important methanol/toluene mixtures in two regimes to study the transport properties. The mixtures include different concentrations of azeotropic mixture and solely azeotropic mixture. The results are indicative of the fullerene derivative containing PA membrane has enhanced permeation flux than PA membrane alone. In the methanol and toluene mixture the permeate found 96% of methanol selectively in a PA containing 5 wt% fullerenes. See Figure 4A for fullerene functionalization on PA, and PV process to separate methanol/toluene mixture. Figure 4B of permeation flux and methanol feed in wt% reveal that the PA/HF has greater methanol flux than other PA membranes [51,52]. Penkova *et al*. prepared polysulfone and fullerene C60 mixed-matrix membranes. The membrane exhibited fine transport capabilities toward the pervaporation of an ethyl acetate-water mixture [53]. A molecular dynamic simulation study on graphene membranes shows that 100 % salt rejection, but the low intermolecular spacing hinders the water flux. More pressure is applied to enhance the water flow. The fillers between the GO layers enhances the water flux along with salt rejection in case of GO and fullerene membrane composites. Thus, there is a promise for cost-effective saltwater desalination by RO process using cross-sectional GO/C60 membrane, which has an elevated water flux and repels salt at low pressure [54]. A strategic GO interlayer with fixed spacing of 1.25 nm was prepared by adding C60 to produce GO/C60 on an alumina membrane. Their cross-sectional filtering capability was tested to dilate the desalination process effective area. The GO/C60 was prepared with epoxy. The as-prepared GO/C60 membrane achieved up to 10.85 L h^{-1} m^{-2} bar^{-1} water flux. At the same time, NaCl rejection rate reach up to 90%, which is enough to turn brackish water into potable water. Moreover, this GO/C60 membrane composite has a very good prospective for energy-efficient water desalination because it operates at low pressure (< 5 bar) and shows long-term stability [55]. Another simulation study based on non-equilibrium molecular dynamics reveal the probability of desalination of novel 2D C60. 100% salt rejection was observed towards various salts and at different operating pressures. The exceptional performance of 2D C60 was due to the presence of nano pores that form a network of hydrogen bonds among them. These studies can pave a new way of using these novel structures of 2D C60 in water desalination [56]. In addition to fullerene and GO composites, CDs another OD material and C60 polymer composites membranes were successfully fabricated for wastewater eradication [57].

Overall, the Bucky balls, GO and CDs based polymer membranes have shown interesting results in water purification.

3.1.3. Photocatalytic Degradation of Wastewater

It is well known that fullerenes and their blends are effective photocatalytic materials. Their photocatalytic mechanisms and functions are investigated. It performs three distinct tasks under various circumstances, namely that of electron donor, mediator of energy transfer, and receiver of electrons. In a fullerene composite, photogenerated electrons are produced on the valence band of the semiconductor material upon light excitation. The electrons are subsequently transferred to the fullerenes, which function as electron acceptors and transporters. Due to its short band gap (1.86 eV for C60 and 1.57 eV for C70) and visible light response, fullerene can operate as an energy transfer medium and directly produce $^1O_2$ for a reaction. Nevertheless, there is also an instance in which

 doi:10.20944/preprints202510.0466.v1

fullerenes function as e^- donors, transferring e^- to the semiconductor material when interacted with light, hence elevating the carrier transport rate and augmenting photocatalytic activity [58–60].

Fullerenes alone may not be an effective photocatalytic material. Hence, the fullerenes are functionalized with various photoactive semiconductive metal oxides such as TiO_2, ZnO, WO_3, CuO, and SnO_2. Here, the fullerene/metal oxide composite can show the synergistic photo effects to draw the better degradation by enhanced surface area, pollutant adsorption, interaction, photoactive catalytic sites, and tailored band gaps to the complete degradation without leaving the pollutants [61–63]. See Figure 4C for the semiconductor/fullerene photocatalyst synthesis methods, photocatalytic mechanism, and applications. TiO_2 is widely used photocatalyst due to its excellent photoelectronic qualities, potent oxidizing ability, and easy availability. TiO_2 large band gap (~3.2 eV) means only UV light can stimulate, which restricts its ability to use solar light efficiently. The quick recombination of photoinduced excitons can also limit TiO_2 photocatalytic effectiveness. Making the composite with fullerenes can enhance the charge separation of TiO_2 and redshift to enhance the visible light from UV region. Hence, visible light active photocatalysis is possible [64,65]. The polycarboxyic acid functionalized fullerenes mixed with TiO_2 composite was prepared using ultrasonication evaporation method to give TiO_2/fullerenes photocatalyst. Various spectroscopic and electron microscopic techniques are used to characterize the prepared materials. Figure 4D(a-c) SEM images reveal the aggregated spherical shapes of C60, TiO_2, and TiO_2/C60 composite. Whereas Figure 4D(d) HR-TEM image clearly depicts the TiO_2/C60 composites boundary and lattice spacings of TiO_2, confirms the formation of the composite, a photocatalyst. Figure 4E shows the schematic view of the TiO_2/C60 band gaps where one can see the large and small band gaps of the two materials and the photoelectrons generation upon visible light illumination. The light triggered electrons move to conduction band (CB) from valency band (VB). From CB of TiO_2 the e^- transfer to fullerenes CB and trigger the radical oxygen generation. The holes generated at VB interact with water and generate the hydroxyl radicals. The both reactive oxygen species interact with organic dye, RhB, and destruct the big carbon backbone into nonhazardous CO_2 and H_2O as final products. Figure 4F shows the adsorption and degradation of RhB efficiency by increasing the amount of C60. The best removal efficiencies are from 0.5 to 3 wt% of fullerenes. Which emphasizes the key role played by the C60 in semiconductor mediated photocatalysis. Figure 4G reveals excellent evidence of the photo stability of the composite. Where the catalysts adsorption and degradation capability is consistent up to five cycles [66]. The reduction of Cr (VI), oxidation of iodine, and 4-chlorophenol was conducted using Nb-TiO_2/fullerol. The obtained results are better than TiO_2, and Nb-TiO_2 catalysts [67]. TiO_2/polyhydroxyfullerene (PHF) for enhanced degradation and *E. coli* inactivation was observed. Many other TiO_2-fullerene composites are well demonstrated as well [68]. In addition, dye sensitized photoactive composites with TiO_2, ZnO, C60 and graphene was also studies for photodegradation performances towards various pollutants [69].

In addition to the TiO_2/C60 nanocomposites, ZnO and C60 developed a hybrid, when C60 molecules in a monomolecular layer state scattered on ZnO outer surface. The C60/ZnO nanoparticle composite hybrid photocatalyst demonstrated increased catalytic activity for the MB destruction, and the hybridization of C60 molecules effectively prevented ZnO from photocorroding and aggregation. The high migration efficiency of photoelectrons on the C60 and ZnO interface, caused by the interaction of C60 and ZnO nanoparticles with a conjugative π-system, was the source of the increased photocatalytic activity for C60-hybridized ZnO. The amount of which C60 molecules that were covered on the surface of ZnO nanoparticles significantly influenced the degree of photocatalytic activity increase. The best hybridization effect was discovered at a weight ratio of 1.5% (C60/ZnO). The efficacy of the composite is remarkably higher than the bare ZnO's performance [70]. The C60 enhanced the $ZnFe_2O_4$ photocatalytic activity also assists the degradation of norfloxacin and toxic Cr (VI) into Cr (III) [71]. The 4%fullerenes loaded WO_3 has shown high surface area, Visible light enhancement and diminished e^-/h^+ recombination [72]. Many other fullerene composites are successful in photocatalytic degradation/conversion of organic and inorganic pollutants into nonhazardous components [59–62].

 doi:10.20944/preprints202510.0466.v1

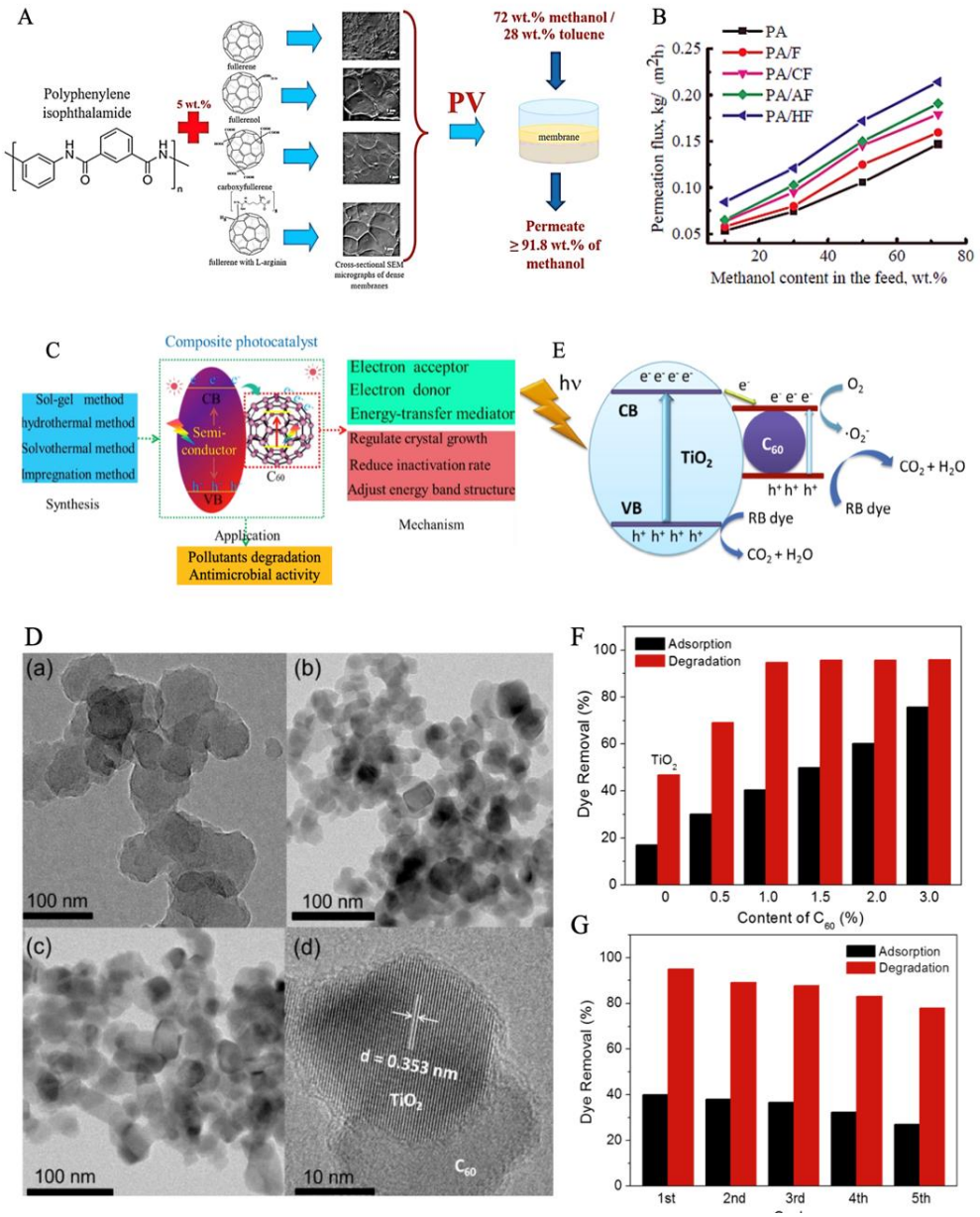

Figure 4. A.PV membranes made of polyphenylene isophthalamide modified with various kinds of fullerene C60 derivatives. B. Efficiency of permeation flux of PA and different fullerene derivatives based on methanol content in the feed. C. General synthesis methods, properties, and applications of fullerene semiconductor nanocomposite for photocatalytic applications. D. SEM of (a) Fullerenes, (b) TiO_2, (c) C60/TiO_2 nanocomposite and (d) HRTEM of C60/TiO_2 photocatalyst . E. TiO_2/Fullerene photocatalysis and their respective bandages to degrade the RhB dye into CO_2 and H_2O. F. Adsorption and degradation of RhB over C60/TiO_2 after 150 min. G. Number of cycles of adsorption and degradation of RhB over C60/TiO_2 composite. Reprinted/adapted with permission from Refs. [51,59,66]. Copyright 2019, , Copyright Elsevier, Copyright 2020, Copyright Elsevier and Copyright 2016, Copyright Elsevier.

3.2. Carbon Dots for Water Treatment

Similar to fullerenes, CDs are 0D materials discovered by Dr. Qian Ping and Dr. Xu Hongjie from Nanjing University in 2004. The structure and chemical composition are in Figure 5. Since then, they grab the interest of researchers around the globe in energy, environment, medicine, and sustainability. Diverse types of CDs such as carbon dots, graphene quantum dots (GQDs), carbon nanodots (CN-dots), and carbonized polymer dots (CP-dots) appeared. Based on the type of reaction and nature of precursor, assorted sizes and morphologies of the CDs can be prepared. The CDs can

 doi:10.20944/preprints202510.0466.v1

be prepared by top-down and bottom-up methods such as arc discharge, laser ablation, chemical oxidation, hydrothermal/solvothermal preparation, pyrolysis, and chemical vapor deposition techniques. Recently, green preparation of CDs from plant extracts and biomass conversion has been one of the best choice by the environmental scientists. The CDs are 1-10 nm in size and have exceptionally good optical properties like tunable luminescence with other unique properties like high surface area, abundant surface functional groups, good water dispensability and stability, and low toxicity. Figure 5 shows the structure (Figure 5A), general synthesis methods (Figure 5B), luminescence (Figure 5C), morphology, size, and chemical composition of CDs and GQDs (Figure 5D) [73,74]. The CDs have the capability towards various organic and inorganic pollutants. The CDs have tunable surface functionality that enable them to adsorb the contaminants efficiently through electrostatic attraction, π-π interaction, coordination, and chelation [75–78]. Here in this part, we are going to discuss the adsorption, membrane separation, photocatalysis of heavy metals and organic pollutants by above mentioned CDs, randomly.

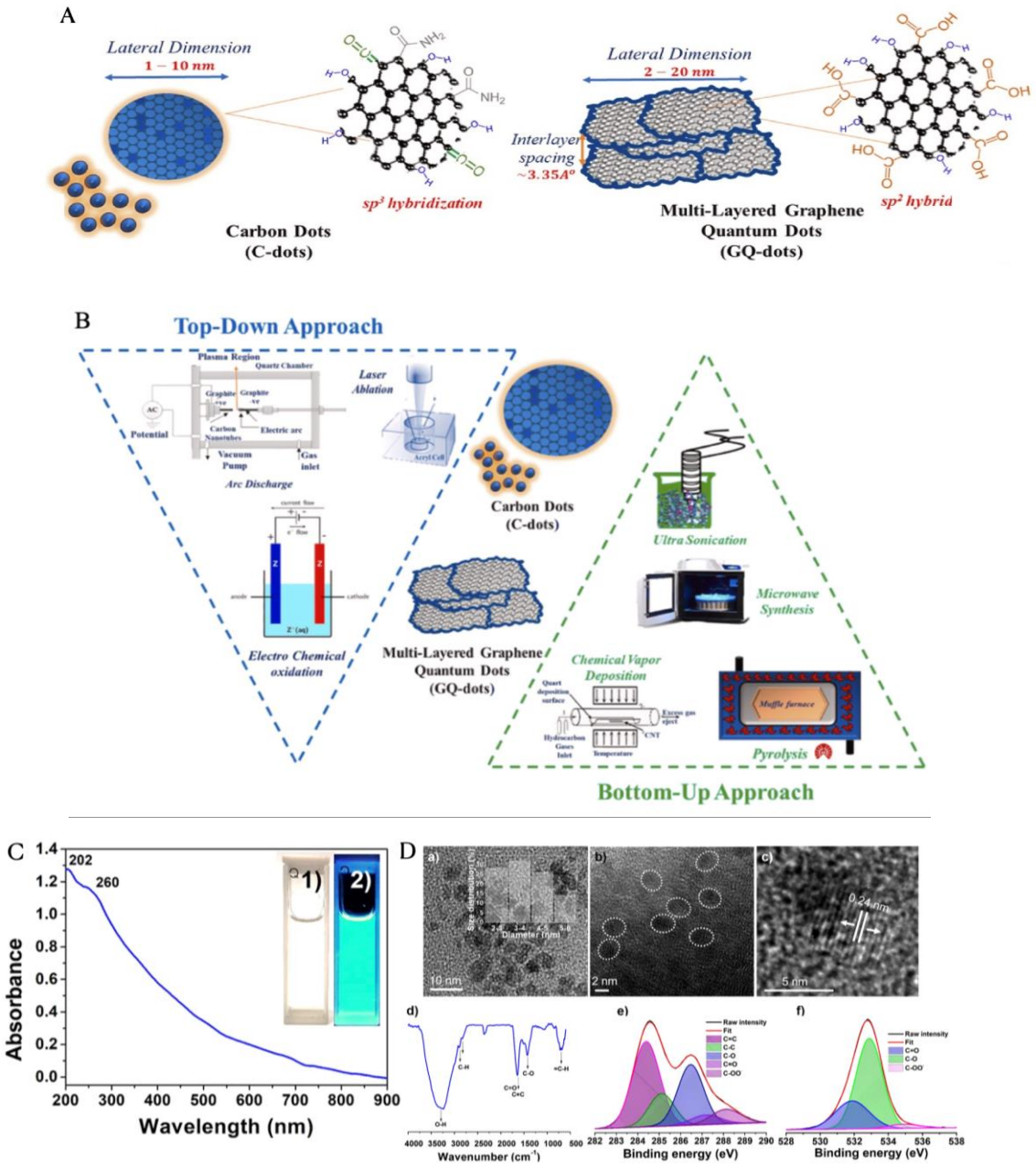

Figure 5. A. Structure of carbon dots with carbon, oxygen, and nitrogen functional groups with spherical dot structure. B. General synthesis methods. C. CDs sample under (1) day light and (2) presence of 365 nm UV light illumination. D. (a) Size, (b) shape, and (c) d-spacing of CDs from TEM. Chemical composition by (d) FTIR, (e-f)

 doi:10.20944/preprints202510.0466.v1

XPS. Reprinted/adapted with permission from Ref. [73,74]. Copyright 2024, Copyright Elsevier, and Copyright 2019, Copyright SCI Reports.

3.2.1. Adsorption

The problems associated with heavy metals/inorganic pollutants are serious concerns in the world of water technology, due to their adverse effects. The exceptional physicochemical features of heavy metal ions have led to their widespread applications in a diversified industry sectors. But when they were released into the environment without proper treatment, major pollution issues resulted. Therefore, it is desired but difficult to remove these harmful contaminants from water quickly and completely. The chemical makeup of CDs, their specific surface area, pore volumes, and the quantity of functional groups influenced the sorption capacity of CDs towards heavy metals. In addition to chemical chelation and electrostatic adhesion, physisorption between metal ions and the adsorbent can regulate the adsorption process of metal ions. Electrostatic interaction has been identified as a significant adsorption mechanism between metal ions and CDs-based adsorbents, owing to the abundance of negatively charged oxygen groups on CD surfaces. For example, nitrogen-doped CDs for the adsorption of Pb^{2+} and Cd^{2+} from wastewater were reported by Sabet and colleagues [79]. On the surfaces of CDs, negatively charged nitrogen functional groups and oxygenated functional groups can both function as active sites for metal ion adsorption at same time. Furthermore, it has been proposed that metal ions and CDs-composite interaction may be significantly influenced by electrostatic and π-π interactions [80].

Mahmoud *et al*. synthesized a sorbent based on microwave method. The goal of this work is to quickly synthesize CQDs via pyrolysis of starch-water systems under microwave irradiation in under 10 min. At 526 nm, the highest fluorescence emission of CQDs was apparent over the whole excitation wavelength of 390 nm. To prepare a novel nano CQDs@PAFP biosorbent, the CQDs designed to preoccupy the surface and pores of a polymeric material based on poly(anthranilic acid-formaldehyde-phthalic acid) (PAFP). CQDs@PAFP possessed a BET surface area of 28.79 m^2 g^{-1}. The maximum U(VI) reductions achieved by CQDs@PAFP nanobiosorbent ranged from 95.5 to 98.0% for 30 to 90 mg L^{-1}. The sorption process closely matched the Freundlich isotherm model and assigned to the pseudo-second-order model. CQDs@PAFP was a superior nanobiosorbent for removing U(VI) from seawater (96.0%) and wastewater (97.3%). The authors have validated CQDs@PAFP's outstanding reusability for effective multi-recovery of U(VI) from various water samples [81]. Other than PAFP, a CDs composite prepared with amine rich conductive polymers (poly(o-phenylene diamine) (PoPD)) with enhanced surface functional groups for better adsorption of heavy meals. Compared to previously reported conductive polymers, PoPD had a higher Cu^{2+} removal ratio (73.63%) and a higher CDs/PoPD ratio (88.16%). The Pb^{2+} and Cd^{2+} removal rates with CDs/PoPD were 98.97% and 77.48%, respectively. For Cu^{2+}, Pb^{2+}, and Cd^{2+} the highest adsorption capabilities of CDs/PoPD were 48.88, 53.44, and 36.20 mg / g, in that order. The amine and imine groups on the CDs/PoPD chain formed complexes with Cu^{2+}, Pb^{2+}, and Cd^{2+}as demonstrated by the results. The Langmuir adsorption isotherm model and the quasi-second-order kinetic model could account for these adsorption processes. According to the reusability test findings of the Cu^{2+} adsorption, CDs/PoPD had a regeneration effectiveness of 85.95% much higher than PoPD's [82]. A hybrid of N-CDs spherical shaped hydrogel particles (CGCDs) are fabricated by Perumal *et al*. for Hg^{+2}, Cd^{+2}, Pb^{+2}, and Cr^{+3} used for simultaneous removal from water [83]. To enable simultaneous fluorescence sensing and Cu^{2+} adsorption, cellulose, chitosan (CS), and polyvinyl alcohol (PVA) were crosslinked to create luminous CD-rooted polysaccharide hydrogel (CDs@CCP hydrogel) for Cu^{+2} elimination of 124.7 mg/g [84]. Cellulose based CD-hybrid was also reported recently to sense and remove Hg^{+2} with the adsorption efficacy of 290.70 mg/g. The hybrid has shown remarkable stability for about two months and retains the adsorption sites up to 80% even after five cycles of use [85]. Another composite, N-CDs with alginate (ALG@NCDs) prepared for Cu^{+2} eradication from waste soil water and the amount was 152.44 mg/g. ALG@NCDs exhibited a greater affinity for Cu^{+2} than for Pb^{+2}, Co^{+2}, Ni^{+2}, and Zn^{+2} according to the results of selective adsorption. The ALG@NCDs adsorption capability

 doi:10.20944/preprints202510.0466.v1

was maintained at 89% of its starting level following five adsorption-desorption experiments. Cu^{+2} mechanism of adsorption was also investigated using density functional theory [86]. In a similar type of investigation, the authors used cotton and a straightforward hydrothermal method to prepare a ternary composite of nanocellulose/CDs/magnesium hydroxide (CCMg). A mixture of density functional theory computations and experimental methods was used to study the removal mechanism of Cd^{2+} and Cu^{2+}. It was understood that hydrogen/dative bonds taken a prominent role in the interactions between each component of CCMg and $Cd(NO_3)_2$. The $Mg(OH)_2$ moiety preferentially enriches $Cd(NO_3)_2$, as demonstrated by computed thermodynamics, interfacial interactions, and charges. Following transformation, copper ions precipitate as basic sulfate, and of interest is that nanocellulose (NC) fixes the $CdCO_3$ precipitate on the surface by chemical interaction. CCMg has potential uses as a water treatment agent because of its strong adsorption action and straightforward recovery process [87]. Apart from these interesting reports on CDs, graphene CDs composites were also reported to effectively eradicate various organic and inorganic pollutants [88–90].

Organic dyes linked to industrial waste, such as methylene blue (MB), rhodamine B (RhB), crystal violet (CV) and others, are progressively causing pollution in water sources. These chemical dyes are extremely dangerous to the health of both people and animals. They can damage vital organs such as the liver, kidneys, reproductive system, brain, and central nervous system. They can also cause mutations and cancerous effects. Moreover, they have significant negative consequences on the ecosystem, such as inhibiting photosynthetic activity, decreasing solar penetration, consuming dissolved oxygen, and decreasing the recreational value of water bodies [91,92]. Hence, removal of the dyes from water is imperative. To investigate the adsorption of eco-hazardous MB dye, Basha *et al*. synthesized neem bark powder derived biobased CDs (BCDs) adducts. Figure 6A and B reveals the BCDs absorb the MB through in-situ precipitation reaction which involves electrostatic mechanism between the MB and BCDs. The impressive results included an adsorption capacity of 605 mg/g and a percentage of removal of 64.7%, which exceeded other solid-based adsorption methods reported in the literature. This system fits very well with the pseudo-second-order kinetics model and the Langmuir isotherm. Gibbs free energy change (ΔG), a determined thermodynamic parameter, was negative, suggesting an exothermic, physisorption-based mechanism that occurs spontaneously. By employing ethyl alcohol as the solvent to effectively extract and recover the MB dye (64%), the system's regenerative capacity was further proven. With the use of this technique, valuable cationic organic dye compounds can be effectively recovered from contaminated environments [93].

Prepared a CDs crosslinked chitosan/microcrystalline cellulose (CS/MCC/CA-CDs) sponge. The sponge has a tangled fiber structure with a bundle made of hydrogen bonds connecting the CA-CDs to the CS/MCC composite matrix. The entangled fiber bundle units provide abundant active adsorption sites for the dye molecules to be collected. At p^H-10 and 298 K, the CS/MCC/CA-CDs sponge had an adsorption capacity of 306.8 mg/g toward MB [94]. Anthracene is classified as a stable polycyclic aromatic hydrocarbon (PAH). Carbon-based compounds like biochar cannot effectively adsorb anthracene in aqueous phase. Chitosan (CS)-decorated CDs obtained from the acid treatment of coconut shell biochar (MCSB/CDs) are effectively manufactured and eleminated anthracene from aqueous solutions. Within 60 min, h-CDs/MCSB demonstrated a 95% removal efficiency and rapid anthracene adsorption with a notable sorption capacity (Q_{max} = 49.26 mg/g) [95]. In a recent report, You *et al*. presented a straightforward casting technique, a polyvinyl alcohol/chitosan-based polymer CDs [PVA/P(CS-g-CA)CDs] composite film was created for dye eradication. With an increased adsorption capacity of 433.24 mg/g, the composite film demonstrated steady adsorption of acid blue 93 (AB93) at pH 2 to 9. Even after five cycles, the adsorption complied with the Langmuir rule with an effectiveness of over 89% [96]. To successfully remove MB dye from an aqueous solution, non-metal elements were used to dope up CQDs with nitrogen and sulfur (N, S-CQDs), then loaded into hexagonal mesoporous silicon (HMS). The hydrothermal method of N, S-CQD was synthesized using the amino acids cysteine and histidine as the raw materials. Maximum MB adsorption capability and

 doi:10.20944/preprints202510.0466.v1

removal efficiency were found to be 370.4 mg/g and 97%, respectively. The good selective behavior of N,S-CQDs/HMS for MB adsorption was demonstrated by the elimination of MB when placed close to RhB and Reactive Black 5 dyes. Four repeated adsorption–desorption cycles would provide for a well-recycled adsorbent with appropriate activity. The findings showed that the N, S-CQDs/HMS's porous characteristics, surface area, charge characteristics, bandgap reduction, and quantum yield were crucial elements that influenced dye adsorption [97]. Besides the above CDs and composites, metal doped CDs for mitigating various pollutants [98], mesoporous silica decorated CDs for methoxy-DDT [99], CDs-liposome-Au catalysts for 4-nitrophenol reduction [100], CDs with g-C_3N_4-FeNi-BTC for antibiotics and microplastic eradication [101], and CDs-hydrogels for perfluorooctane sulfonate eradication was reported successfully [102]. Apart from these findings, various GCDs have successfully reported on various pollutants removal [103–105]. Among the above discussed CDs and their composites, BCDs have shown remarkable removal efficacy of 605 mg/g than adsorbents reported.

3.2.2. Membrane Filtration

The membrane separation process has had remarkable expansion over the last few decades, making it one of the growing technologies. Because of its superior performance over traditional separation technology, it has caught the interest of researchers in the area of separation technology. Membrane separation techniques used to separate two or more components or contaminants by passing through a semipermeable barrier (membrane). A thin sheet of synthetic or natural material that covers a surface and allows certain components of the solution to pass through is called a membrane. The primary technologies for membrane separation are electrodialysis, gas separation, pervaporation, reverse osmosis, ultrafiltration, and microfiltration [106,107]. Here we would like to emphasize the CDs based membranes for the above-mentioned separation techniques against various organic, inorganic, and microbial contaminants filtration. Usually, the commercial polymer membranes has certain drawbacks such as membrane fouling, longevity, limited selectivity, and limited flux [108,109]. Some of these problems could be overcome by adding the nanomaterials to the traditional membranes. It's due to nanomaterials' high mechanical strength, hydrophilicity, permeability, and antimicrobial activity. Hence, we are reviewing recent reports on CDs, CNTs, and graphene-related nanomaterials in membrane technology [110]. In this particular section, we are discussing the CDs based membranes. In order to eliminate organic solvents, sub-5 nm CDs with adjustable carbonation degrees, or surface groups, were easily produced as nanofillers by Yuan *et al*. Additionally, polyethyleneimine (PEI) was chosen as the polymer matrix because of its superior film-forming and solvent resistance. A layer of cross-linked PEI-CDs was applied to a hydrolyzed poly-acrylonitrile (PAN) substrate in order to create a thin, perfect composite membrane. Through the investigation of solvent uptake behavior, solvent flux, and solute rejection, the nanofiltration performances of membranes were assessed. This confirmed that the advantages of hybridizing small-sized CDs with PEI could effectively be created: the fully cross-linked PEI networks guaranteed superior solvent resistance and solute rejection ability, while CDs functioned as specific nano-accelerators for solvent transfer through their functional groups. The degree of carbonation influence the rejection of polar and non-polar solvents selectively due to the varying amount of surface functional groups and the PEI-CDs polarity [111]. By combining CDs with a poly-ether sulfone (PES) matrix, a unique mixed matrix nanofiltration membrane was created. The properties of pure water flux, antifouling, dye, and salt rejection were also investigated. A solution of bovine serum albumin (BSA) was filtered through the prepared nanocomposite membranes to assess their fouling resistance. The roughness of PES membrane can be effectively reduced by adding CDs, as seen by the estimated roughness values. Through stepwise increases in the dosage of CDs from 0.05 to 0.50 weight percent, the membrane permeability was enhanced to a maximum value of 76.5 kg/m^2 h, double that of bare PES. Significant antifouling characteristics were also demonstrated by the 0.50 wt% PES/CDs membrane compared to individual PES [112]. Developed a PVDF/ATP-CDs composite membrane with dual functionality of heavy metal ion adsorption and detection by reacting CDs with attapulgite

 doi:10.20944/preprints202510.0466.v1

(ATP) in the PVDF/ATP hybrid membrane. The PVDF/ATP-CDs membrane has shown excellent wettability followed by a permeability of about 110 L/m^2 h due to the additional features from ATP and CDs [113]. ZQDs-g-CA, an anti-fouling zwitterionic cellulose acetate (CA) membrane, was created by grafting CQDs onto the CA membrane's surface and then zwitterionizing CQDs (Figure 6C) by 1-ethyl-3-(3-dimethylaminopropyl)carbodiimide (EDC) and 1,4-butanesultone (1,4-BS). With a permeation flux of 426.1 ± 9.6 L m^{-2} h^{-1} bar^{-1} and an oil rejection of 99.4%, the modified CA membrane showed outstanding water flow (602.2 ± 30.2 L m^{-2} h^{-1} bar^{-1}) and oil/water emulsion separation performance. Furthermore, the anti-fouling tests showed excellent results, with good flux recovery. The findings demonstrated that, for various oil/water emulsions, the in-situ ZQDs on the CA membrane obtained grater than 96% rejection rate [114]. Similarly, another zwitterionic CD-CS-thermoplastic polyurethane (TPU) membrane was prepared for 100% Cu (II) removal and antifouling to *E.coli* [115]. The modified PSF membrane with CQDs demonstrates antibacterial activity against both Gram-positive and Gram-negative bacteria was seen in Figure 6D [116]. CD/Ag NPs-Polysulfone (PSF) membrane was fabricated and obtained improved results of tartrazine dye rejection with good water flux [117]. A low quantity of CDQs (1% w/w) was present, which increased the CA electrospun adsorbent's adsorption capability. The loaded membranes showed an increase in adsorption capacity of 160% for MB and 300% in the case of MV when compared to CA electrospun membranes without CQDs. Consequently, the adsorption of cationic dyes onto polymeric membranes was significantly improved by the addition of CQDs derived from sawdust [118]. Phase inversion was used to create PES, peracetic acid (PAA) membranes based on graphene oxide QDs (GQDs-Ms). The GQDs-Ms demonstrated a negative surface charge and a significant oxygen content. Superior suppression of *E. coli* cells was achieved as well as increased hydrophilicity, pore size, porosity, and flow after adding GQDs to the polymer matrix [119]. Developed thin-film nanocomposites (TFN) based on GOQDs and tannic acid (TA). The TA/GOQDs TFN membrane maintained high dye rejection to MB (97.6%) and Congo red (99.8%) while exhibiting a pure water flux of up to 23.33 L m^{-2} h^{-1} bar^{-1} (0.2 MPa) 1.5 times greater than that of the pristine TA TFC membrane. This was due to the loose active layer structure and the combination of Donnan exclusion and steric hindrance [120]. By creating a thin, selective layer on top of the modified MWCNT matrix membrane using an interfacial polymerization technique, N-GQDs membrane composites were created. Upon controlling the N-GQDs contents, the membranes' pore sizes could be freely adjusted. More than 96% of various charged dyes were rejected by the appropriate N-GQDs membrane [121]. Similarly, CDs are used to simultaneously control the surface charge and pore size of a nanofiltration membrane, improving the selective expulsion of salts from water. Several CDs based membranes also reported successfully to improve the capabilities of membrane filtration. The discussed membranes have improved polarity, roughness, hydrophilicity, and wettability followed by the permeability, and tunable membrane pore sizes by adding CDs are advantageous to further enhance the membrane technology [122–126].

3.2.3. Photocatalytic Degradation of Wastewater

Photocatalysis has emerged as a popular physical, chemical, and biological technology for water cleanup in current times due to its gentle and environmentally benign character, low byproduct generation, and good functional-group compatibility. Since TiO_2 was first used in photocatalysis, semiconductor photocatalysis has garnered widespread research interest. Nevertheless, the hybrid photocatalysts and certain traditional and usually used CDs (Zn/Se QDs, Ag_2S QDs, Pb/Se QDs, and Cd/Se QDs) are toxic, moderately active in the visible-NIR spectrum, costly, or need lengthy, multi-step fabrication procedures, which limits their practical use [127]. Hence, highly efficient, broad absorption, low toxic, and economic photocatalysis are wanted. Though other carbon nanomaterials such as CNTs, carbon nanofibers (CNF) are good adsorbents, they need dopants to be a good photocatalyst. But graphene and GO are considerable photocatalysts in their native form [76]. Certain appealing properties of CQDs include their strong visible-spectrum photoluminescence, tunable emission wavelength, broad and continuous excitation spectrum, very good water solubility and

 doi:10.20944/preprints202510.0466.v1

stability, biocompatibility, inert to photobleaching, ease of preparation, and affordability, make them a good photocatalysis [128]. Since electron-hole pairs are the main oxidizing species in photocatalytic reactions, CQDs have been found to function as independent photocatalysts in recent years. This is because they can absorb visible light. Because of their special qualities, CQDs are materials that show promise for photocatalytic applications, which will degrade a variety of environmental pollutants [129–132]. Das *et al*. demonstrated bare CQDs for MB degradation. Pear juice was used as the starting material for a simple, scalable, one-pot solvothermal technique that produced green-emissive CQDs. Because of their efficient light absorption, electron transfer, and separation of photogenerated charge carriers, the prepared CQDs have excellent photocatalytic activity under visible light irradiation, enabling ~99.5% destruction of MB in 130 min. Figure 6 (E-a) reveals that the MB is not sensitive to the visible light and CQDs in dark. Whereas The CQDs under illumination has given remarkable MB degradation within 130 min. Figure 6 (E-b) shows rate constant of the degradation was 0.03889 min^{-1}. Figure 6(E-c) is the photocatalysis reaction under light, where the CQDs generate the electrons and holes by charge separation, followed by the MB changes into color less is an indication of successful degradation. Figure 6(E-d) shows the exact reaction mechanism of electron-hole pair and radical species generation, and subsequent light-mediated degradation of MB dye. The CQDs also used for sensing the Fe (III) and ascorbic acid based on a turn-off and turn-on mechanism [133]. Nizam *et al*. prepared blue color CQDs from rubber seed shells for 90% removal of CR and MB dyes in the presence of sunlight [134]. Meena *et al*. created two CQDs with different molecular surfaces: C-CQDs (carboxylic-rich) and A-CQDs (amine-rich) from natural sources. Between these two, the A-CQDs have a low band gap and generate a larger amount of photo electrons. Rapid visible light-driven photolysis of H_2O_2 was made possible by A-CQDs, which also generated more •OH radicals to aid in the mineralization of petroleum waste, which includes genuine textile wastewater as well as benzene, ethylbenzene, toluene, and xylene. From this report, we can learn that different functionalization of CQDs can have different band gaps [135]. Zandipak *et al*. prepared N-S-CDs with covalent organic triazine framework polymer (COTF-P). Since the bandgap value of N-S-CQD/COTF-P heterojunction was smaller at 2.1 eV than that of 1.9 eV, and the photogenerated charges were better separated, it exhibited optimal activity for the photocatalytic oxidation of phenanthrene from water. After five cycles of reuse, the N-S-CQD/COTF-P heterojunction demonstrated satisfactory stability [136]. In Boyar *et al*. report, aspartic acid was pyrolyzed at 320 °C, approximately 25 nm-sized N-g-CDs with polymeric carbon nitride (PCN) embedded were produced. The surface area of PCN increased from 11.5 to 104.9 $m^2 g^{-1}$ due to the in-plane infiltration of nanosized N-g-CDs. When evaluated for photocatalytic chromium reduction, the N-g-CDs/PCN hybrid catalyst showed a rate that was around three times greater than PCN. Additionally, rhodamine B (RhB) dye and the antibiotic tetracycline (TC) both broke down quickly and with quicker degradation rates. The excellent separation of photo-excitons is governed by the electron acceptor features of N-g-CDs, and photoactivity augmentation is partly attributed to excellent surface area of N-g-CDs/PCN, which was confirmed by carrier dynamic and computational investigations [137]. The CDs were also combined with traditional semiconductor TiO_2 to extract the enhanced photodegradation of organic pollutants. Under solar flow mode, the photodegradation of two commonly used antibiotics in aquaculture, sulfadiazine (SDZ) and oxolinic acid (OXA), was examined both in the absence and in the presence of CQDs combined with TiO_2. The CQDs-TiO_2 have given satisfactory results against antibiotics and pathogen degradation [138]. Choi *et al*. created CQDs with ease by combining lemon juice and citric acid. The structural and optical properties were impacted by incorporation of CQDs with TiO_2. TC was efficiently decomposed by synthesized CQD using TiO_2 nanocomposites. 91.5% of the TC was eliminated after two hours at p^H 8 using visible light. The target compounds' active sites were also predicted by density functional theory (DFT) calculations [139]. It was discovered that GQDs can enhance the black titanium dioxide nanofibers (bTiO_2 NFs) photo degradation capability towards RhB dye. It was due to the enhanced charge carrier separation and formation of superoxide radical anions [140]. Similarly, TiO_2-Colloidal CQDs for effective visible light photocatalytic degradation of antibiotics [141], and a unique quaternary ammonium structure of CDs altered TiO_2 (CPC-CDs/TiO_2)

 doi:10.20944/preprints202510.0466.v1

were prepared. Excellent Cr(VI) reduction by CPC-CDs/TiO_2 is over a broad p^H range. Under natural sunlight, a considerable decrease of Cr(VI) is demonstrated by CPC-CDs/TiO_2. The bactericidal and recyclability of CPC-CDs/TiO_2 are exceptional [142]. Here, in all these studies, the CDs enhanced the photocatalytic property of the TiO_2 very efficiently. It was also claimed that chemical dyes, expired medications, and solar-mediated oil absorption/separation could be effectively removed by CQDs/ZnO, Fe-doped CDs, N-CQDs, multi-doped CDs, and CDs/polylactic acid nanofibrous membranes [142–145]. Overall, various kinds of photoactive CDs with high efficiency of pollutant eradication were observed.

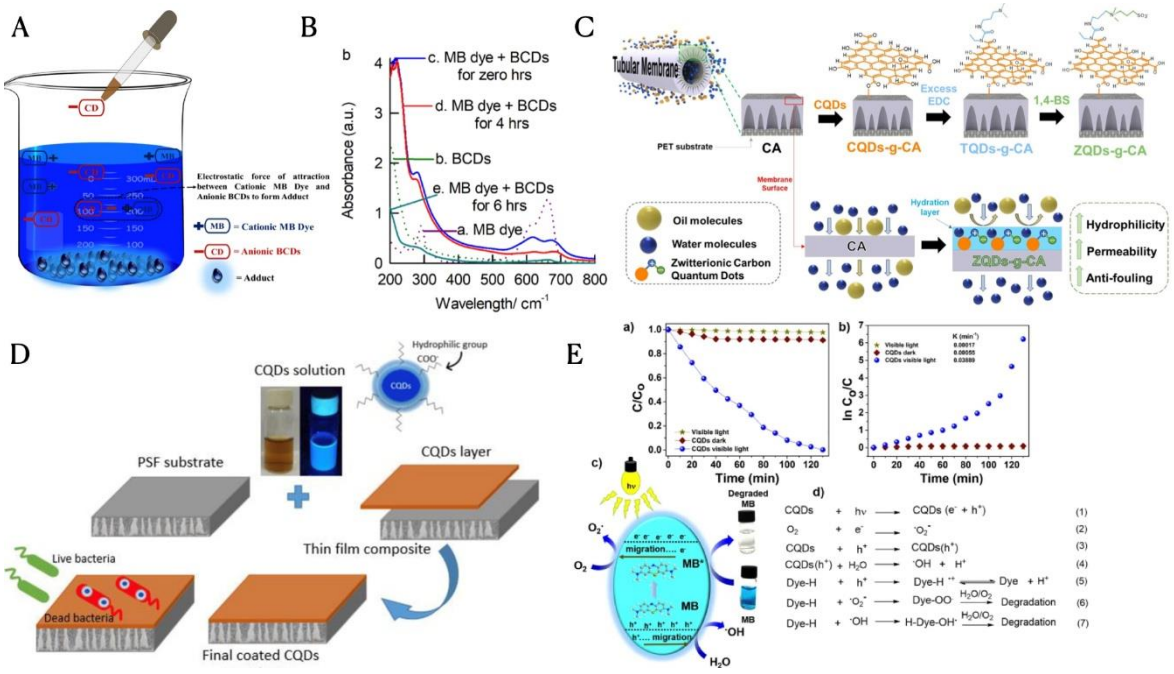

Figure 6. A. Adsorption mechanism of cationic MB dye on anionic BCDs. B. BCDs and MB dye's UV-Vis sensitivity under various testing scenarios. C. Zwitterionic CDs on CA tubular membrane surface for oil separation from water with increased hydrophilicity, permeability, and anti-fouling property. D. The CQDs modified PSF membrane with antifouling property against gram-positive and gram-negative bacteria. E. Photodegradation of MB caused by visible light. (a) Photodegradation of MB using CQDs at various conditions. (b) Plot of ln C_o/C; (c) Theoretical mechanism of MB degradation under vis-light illumination; (d) Proposed MB degradation mechanism. Reprinted/adapted with permission from Refs. [74,93,114,116]. Copyright 2024, Copyright SCI Reports, Copyright 2024, copyright Elsevier, Copyright 2019, Copyright SCI Reports, and Copyright 2020, copyright Elsevier.

3.3. Carbon Nanotubes for Water Treatment

One of the most significant carbon nano-allotropes is CNTs. A CNT is a cylindrical nanocarbon or one-dimensional tube. Iijima made the discovery in 1991. It is made up of a rolled graphene nanosheet with carbon atoms that are sp^2-bonded. CNTs can be categorized as single-walled (SWCNT), double-walled (DWCNT), or multi-walled (MWCNT) based on quantity of rolled overlapping cylinders [146,147]. Their remarkable qualities include great strength (about 37 GPa), thermal conductivity (approximately 3500 W/m/K), BET surface areas (50-300 m^2/g), optical adsorption, chemical stability, and ballistic electronic transfer. Crucially, their helical angle (χ), or the angle formed by the tube axis and the graphene lattice edge, determines whether they are metallic or semiconducting. A collection of indices, (n, m), corresponding to multiples of the graphene unit can be used to represent the structure of a SWCNT. Based on the helicity, the CNTs could be zigzag (m = 0) and armchair (n = m) structures. The CNTs have different properties based on the helicity. Due to these properties, CNTs have been used in different applications like electronics, energy, automobile,

 doi:10.20944/preprints202510.0466.v1

health, and environmental studies [148–150]. When it comes to water treatment applications, pristine CNTs are not very effective as they are not water soluble. It is due to the strong covalent network of carbon atoms. Ma *et al*. observed that CNTs lower their surface area due to their aggregation, which can be overcome by the alkali treatment of the CNTs. Such CNTs can remove the organic pollutants including dyes effectively [151]. However, the water solubility can be created and enhanced based on different functionalization. Such as defect creation and oxidation strategies by testing the CNTs by sting acids, acids, $KMnO_4$, and other strong oxidizing agents' treatment, metal doping, and functionalizing various water soluble polymers [152,153]. Figure 7A shows the systematic functionalization of CNTs with H_2SO_4 and HNO_3 followed by magnetization with Fe_2O_3 NPs, trimethoxysilylpropanethiol (MPTs), and hydrazine for adsorption studies [154].

3.3.1. Adsorption

Inorganic pollutants are very toxic to the environment and causes many adverse effects and great risk to health. Anitha *et al*. published the molecular dynamic study of +2 state heavy metal ions (Cu, Cd, Hg, Pb) adsorption on functionalized CNTs having $-COO^-$, OH^-, and $CONH_2$ functional groups. The simulation results reveal that the adsorption efficacy of functionalized SWCNTs was 150-230% higher than bare CNTs and increased along with higher concentrations of heavy metals. The order of adsorption was as follows: $Pb^{2+} > Cu^{2+} > Cd^{2+} > Hg^{2+}$ [155]. When MWCNTs are treated with acid, their adsorption capacity can be significantly enhanced. With 6 h acidified MWCNTs, the highest adsorption capacity achieves 85 mg/g at a starting Pb(II) concentration of 50 mg/L, p^H-2 at time 20 min, which is 20 times and 5 times higher than that of initial MWCNTs and activated carbon, respectively. The oxygen related functional groups on acidified MWCNTs can react with Pb (II) to create salt or complex deposited on the surface of MWCNTs, are primarily responsible for the increased adsorption of acidified MWCNTs [156]. The functionalization of CNTs is particularly important as the adsorption strength increases along with it. Selenophosphoryl functionalized MWCNTs revealed that the Pb (II) can be removed effectively [157]. Organic and inorganic acid functionalized CNTs were used for Cu (II) and Ni (II) eradiction [158]. Inanition to acid functionalization Oliveira *et al*. showed the application of CNTs in the elimination of Pb (II), Cu (II), Ni (II), and Zn (II) from aqueous solutions, with the help of CNT modification using surfactants such as anionic (SDBS), non-ionic (Pluronic F-127), and cationic (polyDADMAC MMW) [159]. The adsorbent separation is difficult by using CNTs alone, it need a filtration to separate the adsorbent. Hence the CNTs are additionally functionalized with iron nanomaterials to facile the magnetic adsorption. Wang *et al*. claimed a maximum adsorption of 215.05 mg/g using multiwall magnetic CNTs (60-MWCNTs@Fe_3O_4) for Pb (II) selective adsorption over Cu (II) and Cd (II) ions. This is significantly higher compared to the adsorption capacity of similar types of adsorbents currently in use. 60-MWCNTs@Fe_3O_4 that adsorbs metal ions can efficiently accomplish excellent separation from the solution in the presence of an external magnetic field. Figure 7B SQUID analysis reveals the magnetic nature of the Fe_3O_4 and the 60-MWCNTs@Fe_3O_4 composite and its magnetic separation behavior. Figure 7C is an adsorption isotherm to demonstrate the adsorption of different metal ions such as Pb(II), Cu(II), and Cd (II) [160]. Many other magnetic CNTs have been reported for the facile separation of adsorbents. In the very recent reports, Alkallis *et al*. reported MWCNTs-COO@Fe_3O_4 nanocomposite structure using a femtosecond laser ablation procedure, which will be utilized to remove Pb (II) and obtained 66.85 mg / g at p^H 6, starting concentration of 100 mg/L within 10 min [161]. Various functionalized CNTs have been well summarized in a recent review by systematic evaluation of various pollutants [162–166].

Toxic organic pollutants have a negative results on the environment and on public worldwide. CNTs one among other adsorbents which can effectively remove the organic contaminants from polluted water. Zare *et al*. have utilized untreated MWCNTs for the adsorptive capture of Congo red (CR). By analyzing the effects of batch variables including temperature, contact time, solution p^H, and starting initial dye concentration, the adsorbent's efficacy toward CR was examined. In an equilibrium period of 60 min, MWCNTs demonstrated a 92% clearance effectiveness of CR with 231

 doi:10.20944/preprints202510.0466.v1

mg/g efficacy [167]. Machado *et al*. did comparative research to determine how reactive blue 4 removed from single and MWCNTs made via catalytic chemical vapor deposition method. It was shown that at p^H 2.0, the greatest adsorption capacities of 487.6 and 442 mg/g, respectively, occurred. Because SWCNTs have a high surface area and total pore volume than MWCNTs, they have a higher capability for adsorbing reactive blue 4 [168]. In addition, the treated CNTs such as oxidized, magnetically and polymer functionalized CNTs have been used to achieve better adsorption results towards different conditions against diversified pollutants [169]. Indigo carmine dye was removed using CNTs and CNT-COOH and achieved 88.5 and 136 mg/g removal efficacy with an initial concentration of 100 mg/g, at room temperature, and 15 min of time [170]. 96 mg/g of methyl orange (MO) was removed by MWCNTs-NH_2 which was less efficient than the acid functionalized CNTs [171]. A poly-l-lysine (PLL)-functionalized magnetic Fe_3O_4-(GO-MWCNTs) hybrid composite with a large surface area and an abundance of hydroxyl and amino groups were prepared using a unique, efficient, and environmentally friendly technique. The hybrid combination comprising PLL, Fe_3O_4, and GO-MWCNTs showed exceptional adsorption capabilities in eliminating tartrazine, a dye, and Pb(II). The PLL-Fe_3O_4-(GO-MWCNTs) hybrid is particularly noteworthy for its high adsorption capacity, quick separation, and low time requirements. Under ideal circumstances, the equilibrium adsorption efficacies for Pb(II) and tartrazine were 1038.42 mg/g and 775.19 mg/g, respectively. The Langmuir adsorption model was shown to govern the removal of these two contaminants, and the pseudo-second-order kinetic model described the adsorption kinetics [172]. Utilizing the arc discharge technique and air heat treatment, SWCNTs loaded with magnetic Fe_2O_3 NPs (SWCNTs/Fe_xO_y) were prepared. The maximum adsorption capacity of the composite was found to be 117 mg/g when bisphenol A (BPA) was removed using SWCNTs/Fe_xO_y. When BPA content was below 0.05 mmol/L, the adsorption reached more than 90% in just 5 min of time [173]. Functionalized MWCNTs was used to create simple one-pot-Fe_3O_4/MWCNTs, which were then used to catalytically degrade 4-ntrophenol from an aqueous solution [174]. Similarly magnetized polymer CNT composite was reported for 11 mg/g removal of MB dye [175]. The maximum adsorptions of 15.82 mg/g for MB and 33.54 mg/g for RB were obtained by the composites of $FeSe_2$@Fe_3O_4@CNT-NH_2. The reported results are lower than the other magnetic CNTs composite was noticed [176]. Losartan and diclofenac were eliminated using CNTs functionalized with iron and coffee husk. Diclofenac absorbed more than losartan. Kinetic analysis, neural networking prediction, and machine learning methods were provided to know the adsorption mechanism of the pollutants on magnetic CNTs [177,178]. Apart from iron oxide, ZnO functionalized MWCNTs (AC-MWCNTs-ZnO) has been prepared to remove MB dye. ZnO NPs have excellent dispersion on carbon surfaces which makes the adsorption process easier. By adding ZnO NPs, the surface area increased between 269.48 and 1723.64 m^2g^{-1}. 89.5% of MB dye was removed by AC-MWCNTs composites containing 30 wt% ZnO NPs [179]. In the same way, hydrothermal green synthesis of CNTs/ZnO composite was prepared for BG dye removal. The sorption capability enhanced from 9.67 to 161.74 mg/g when the starting concentration of brilliant cationic green dye increased from 10 mg/L to 200 mg/L at 20 °C, p^H 6.6 ± 0.1 in 60 min [180]. Eskandarian *et al*. synthesized poly(propylene imine) dendrimer functionalized MWCNTs (CNT-Den) for Direct Blue 86 (DB86) and C.I. Direct Red 23 (DR23) eradication, and achieved 667 and 1000 mg/g, which is one of the highest in the literature reported. The possible mechanism was explained in two steps. The CNT-Den is initially submerged in an acidic solution (p^H-3), which protonates the NH_2 functional groups of the adsorbent and gives strong affinity for the simple and quick adsorption of the anionic dye molecules. The second phase involves the positively charged CNT-Den at p^H-3 electrostatically attracting the negatively charged dye molecules. A tiny amount of the synthesized adsorbent (0.1 g/L) could almost completely remove over 95% of the direct dyes (50 mg/L) after 60 min of contact time for the treatment of the simulated industrial colored effluents [181]. Radia *et al*. prepared hydrogel MWCNTs polymer nanocomposite for the removal of cationic CV dye from aqueous solutions. The better results of 84 mg/L CV adsorption were achieved at p^H-8, 200 mg/L of concentration, and 120 min contact time [182]. To eliminate ciprofloxacin (Cip), carbamazepine (Cbz), diclofenac (Dcf), benzo[a]pyrene (Bap), and anthracene (Ant) from different water samples, modified

 doi:10.20944/preprints202510.0466.v1

M-MWCNTs with immobilized laccase (L@M-MWCNTs) were employed. The L@M-MWCNTs was highly stable and removed > 90 % of pollutants than M-MWCNTs [183]. Among all the CNT composites discussed, the PLL-Fe_3O_4-(GO-MWCNTs) and CNT-Den have sown the highest removal efficacy of 775 mg/g and 1000 mg/g.

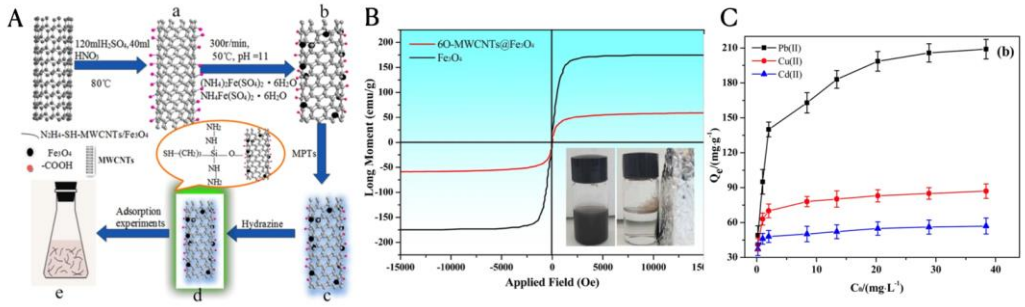

Figure 7. A. Acid treatment, magnetic and polymer functionalization of CNTs. B. SQUID results of 60-MWCNTs@Fe_2O_3 and Fe_2O_3. C. Adsorption isotherms of the 60-MWCNTs@Fe_2O_3 for Pb (II), Cu (II), and Cd (II). Reprinted/adapted with permission from Ref. [154,160]. Copyright 2016, Copyright Elsevier, and Copyright 2021, Copyright SCI Reports.

3.3.2. Membrane Filtration

Membrane filtration is one of the most reliable methods to refresh or purify contaminated water, wastewater, seawater, and brackish water. The membranes are usually made of ceramic, organic polymers, and hybrid materials, and their fabrication relies on the molecular weight cut off of the pollutants. Such is how the membranes and filtration names are given; membrane distillation (MD), reverse osmosis (RO), pervaporation (PV), nanofiltration (NF), ultrafiltration (UF), and microfiltration (MF) are frequently used in the purification of water [184]. Due to their outstanding mechanical strength and very good selectivity, polymeric membranes are typically employed in the purification and desalination of water. Conversely, the strong thermal and chemical stability of ceramic membranes, they are usually adopted for difficult water filtration procedures. Nonetheless, there is still room for advancement because each of these membrane types has certain limitations. In many water treatment applications, polymeric membranes show lower chemical stability and fouling resistance compared to ceramic membranes. Conversely, because of their excessive cost, ceramic membranes are usually only suggested for small-scale operations. Certain nanomaterials, such as metals, metal oxides, and carbon materials, have been used to improve the drawbacks involved in the existing membranes [185,186]. Because of their enhanced permeability, strength, disinfection, rejection, and antifouling activity, CNTs have shown to be excellent fillers in a variety of membranes [187]. The CNT membrane composites can be of three types. The very first one is vertically aligned CNT (VA-CNT) membranes, where the CNTs are aligned vertically, and the water flux is high with moderate mechanical strength. The second is mixed CNT membranes, where the CNTs are arranged randomly; hence, the water flux rate is low but shows great mechanical strength. The third one is Bucky paper CNT membranes, whose fabrication process is simple, moderate water flux and limited mechanical strength [186]. The schematic diagram for the three kinds of membrane can be seen in Figure 8A. There are commercial polymer membranes such as PES, PSF, TPU, CA, polyvinyl difluoride (PVDF), and some other polymers that have been functionalized with CNT, and evaluated for their properties, and used for water purification [188].

The VA-CNT functionalized polysulfone (PSf) has shown increased flux than commercial polymer has reported [189]. Arahman *et al*. investigated and reported the effects of CNTs and pluronic (PF) on the properties and stability of PVDF and PES membranes. The functionalized CNTs/PF-PES exhibit superior stability, including hydrophilicity, shape, chemical composition, and functional groups. While the CNTs/PF-PVDF water contact angle rises to 69.1°, the CNTs/PF-PES

 doi:10.20944/preprints202510.0466.v1

water contact angle raises from 59.4° to 64.7°. Additionally, the performance of CNTs/PF-PES demonstrates more consistent results, with a flow loss of just 1.31 L m^{-2} h^{-1}, whereas the flux decrease of CNTs/PF-PVDF can reach 16.31 L $m^{-2}h^{-1}$. Consequently, compared to PVDF, CNTs and PF modifications impart more stability to the PES membrane matrix [190]. Nagoma *et al*. examined the effect of CNT loading and pressure on PES membrane. The authors identified that increasing the CNT concentration and pressure are proportional to the flux rate. The PES/5 wt% CNT membrane outperformed the others, rejecting 89.6% Cu, 100% Fe, 90.5% Ni, 68.8% Zn, and 99.99% Cl at 300 KPa while maintaining a respectably high flow of 43.7 L m^{-2} h^{-1}. These outperforming results; increased rejection, thermal stability, membrane pore size, and surface area would result from the encapsulation of acid-functionalized CNTs in the membrane matrix. The outcomes demonstrated the potential application of functionalized CNTs implanted in PES membranes for industrial wastewater treatment [191]. A study by Zhao *et al*. offers a new block amphiphilic polymer called polyethersulfone-g-carboxymethyl chitosan@MWCNT (PES-g-CMC@MWCNT). This polymer created by grafting hydrophobic PES on hydrophilic CMC to enhance the penetration of water and antifounilg properties of PES. The resulting ultrafiltration membranes continue to reject bovine serum albumin (91.75%) with outstanding efficiency, displaying good water flow (198.10 L m^{-2} h^{-1}), appropriate hydrophilicity (64.77°), and increased antifouling characteristics (82.96%). Additionally, the cross-sectional shape of the membrane has improved, leading to increased porosity (84.60%) and more regular pore sizes (47.64 nm) [192].

PVDF based membranes were modified using a CNTs and 1-butyl-3-vinylimidazolium bromide ionic liquid (IL) grafting (PVDF-g-IL/CNTs). The grafted IL dramatically enhanced the hydrophilicity and pore structure of the modified PVDF membranes by producing hydrophilic groups on PVDF chains and working in tandem with the CNTs to cause the formation of hydrophilic β-crystalline phase of PVDF. PVDF-g-IL/CNTs membranes produced extremely hydrophilic/oleophobic, fouling-resistant, and with good separation efficiency. The ideal membrane's pure water flux reached 294.2 m^{-2} h^{-1} bar^{-1}, which was 5.2 times higher than the pure PVDF membranes. The membrane is good use for dye, and water-oil separation [193]. Prepared a nanocomposite membranes through the use of phase inversion technique to blend poly(vinylidene fluoride-co-hexafluoropropene) (PVDF-HFP) polymeric membranes with Ag NPs attached to poly(amidoamine) dendrimer (P)-functionalized MWCNTs. The physicochemical properties of measured water, consisting of turbidity, TSS, TDS, and carbonate hardness, were dramatically reduced by the nanocomposite membranes to 4 NTU, 7.0 mg/L, 7.7 mg/L, and 6.0 mg/L, respectively. Following membrane treatment, notable improvements were observed in the reduction of BOD (3.0 mg/L) and the microbiological load (0 CFU/mL). In addition, hazardous heavy metal concentrations of Ni, Cd, and Cr were noticeably lowered to 0.015, 0.0012, and 0.0138 mg/L, respectively from water samples. The outcomes unequivocally imply that treating surface water can be accomplished using the AgP-CNT/PVDF-HFP nanocomposite membrane [194]. Chitosan polysaccharide derivatives (CS-SDAEM) and tannic acid-coated carbon nanotubes (TA@CNTs) have been uniformly coated on PVDF membrane for increased antifouling character and oil-water pollutants separation with 95% flux recovery by creating the extra functional groups and hydrophilicity [195].

Self-assembled composite membranes have impressive selectivity, high operational efficacy, and environmental sustainability are becoming increasingly recognized for their promise in wastewater treatment. However, obstacles including high membrane fouling and insufficient removal efficacies for low molecular weight dyes limit their wider industrial use. A structurally stable composite membrane made of sodium lignosulfonate CNTs and alkalized MXene (SLS-CNT/alk-MXene) has been developed in response to these difficulties. This membrane uses a layer-by-layer self-assembly method to assemble homogenous nanoparticles on a PES substrate that has been pretreated with dopamine. With a permeation flux of 51.6 L m^{-2} h^{-1} bar^{-1}, it demonstrated a high degree of selective permeability, achieving 98% retention capability for MB and Congo Red. In just one hour, this membrane effectively broke down a number of organic dyes, including Rh B, MB, phthalic acid, and methyl orange through electrocatalysis [196]. In order to separate oil from oily wastewater, ZnO

 doi:10.20944/preprints202510.0466.v1

coated CNTs on polylactic acid membranes were prepared via electrospinning. The produced fibrous membranes have attained 73.2 g/g of oil absorption successfully [197]. Hybrid MWCNTs/UiO-66-NH_2 forward osmosis membrane was prepared and used for antifouling and microplastic removal. The MWCNTs/UiO-66-NH_2 incorporation increases the 44% hydrophilicity and 67% water flux due to its good water dispersibility and reduced agglomeration [198].

Yang *et al*. reported an ultra-strong, densified, flexible, free-standing papery all-CNT membrane with high antifouling and separation abilities. It is four times stronger than the virgin CNT membrane and an order of magnitude stronger than many of the membranes made by polymers. The chemically densified free-standing CNT membrane (D-CNT-M) has an extraordinary tensile strength of up to 330 MPa. Figure 8A shows the preparation strategy of the D-CNT-M from pristine CNT-M, P-CNT (purified CNT) via acid (H_2SO_4 and chlorosulfonic acid (CSA)) treatment. Figure 8B(a) reveals the densification process of the membranes. Figure 8B(b-d), the low and high magnification SEM clearly show that the CNTs densified after the acid treatment process. Figure 8B(e) is the cross-sectional image of the D-CNT-M, where one can see the free-standing well well-aligned CNTs, which can facilitate the high water flux and purification. Figure 8B(f) is the Raman spectra, which shows the highest I_D/I_G ratio of the D-CNT-M, which is the significance of the lower disorder of the CNTs in the membrane after densification. XPS in Figure 8B(g) indicates the decline of C/O due to the acid densification. Moreover, the acid treatment by CSA not only enhances the oxygen content, but it can also functionalize the sulfur on the CNTs was evidenced. After successful preparation and characterization of the membrane, the CNT membranes were demonstrated for their water purification ability.

As predicted, the membrane's flow dropped as the molecular weight of PEG increased (Figure 8C(a)) , indicating a size sieving separation mechanism. P-CNT-M and D-CNT-M have the same fluxes, which suggests that their mass transfer resistances are also similar. In contrast to CNT-M and P-CNT-M, the denser D-CNT-M membrane had noticeably greater PEG rejections (Figure 8C(b)). The membrane fouling is usually tested by using BSA, and the D-CNT-M has given the highest flow and rejection during the time of BSA filtration than CNT-M (Figure 8C(c)). Figure 8C(d) and (e) show the interesting flux variations towards RhB and acid orange (AO) and opposite removal efficiency towards these two dyes. The D-CNT-M can remove 90% of RhB and 10% of AO dye, which indicates the D-CNT-M is selective towards organic dyes. Out of these three CNT membranes, this finding suggests that D-CNT-M has the most antifouling performance. Even when two dyes have comparable molecular sizes, they can be effectively separated by the negatively charged surface of D-CNT membrane. Meanwhile, because of its reinforced hydration layer brought about by the hydrophilic functional groups that result from chemical densification, the densified CNT membrane demonstrates veery good antifouling nature during filtration of dyes, humic acid, and bovine serum albumin solutions, and oil-in-water emulsions. In the filtration of fluids containing foulants, the chemically D-CNT membrane exhibits better long-term stability and regeneration in addition to outstanding separation and antifouling performance. The filtration mechanism predicted from the XPS results (Figure 8C(f)) confirms the π–π and electrostatic attractions between the π electrons and oxygen functional groups in D-CNTs membranes [199]. Overall, reduced surface roughness and porosity, high tensile strength, large-scale manufacturing, excellent foldability, consistent water flux, increased surface functionality made the D-CNT-M was a good membrane for selective dye removal without membrane fouling.

In addition, GO-CNT membranes [200], MWCNTs, polyvinylidene fluoride (PVF), and TiO_2 (PVF-x%MWCs-x%TiO_2) nanocomposites [201] and conductive CNTs [202] were also reported for organic dye removal, photocatalytic dye degradation, and chlorine decontamination of wastewater.

 doi:10.20944/preprints202510.0466.v1

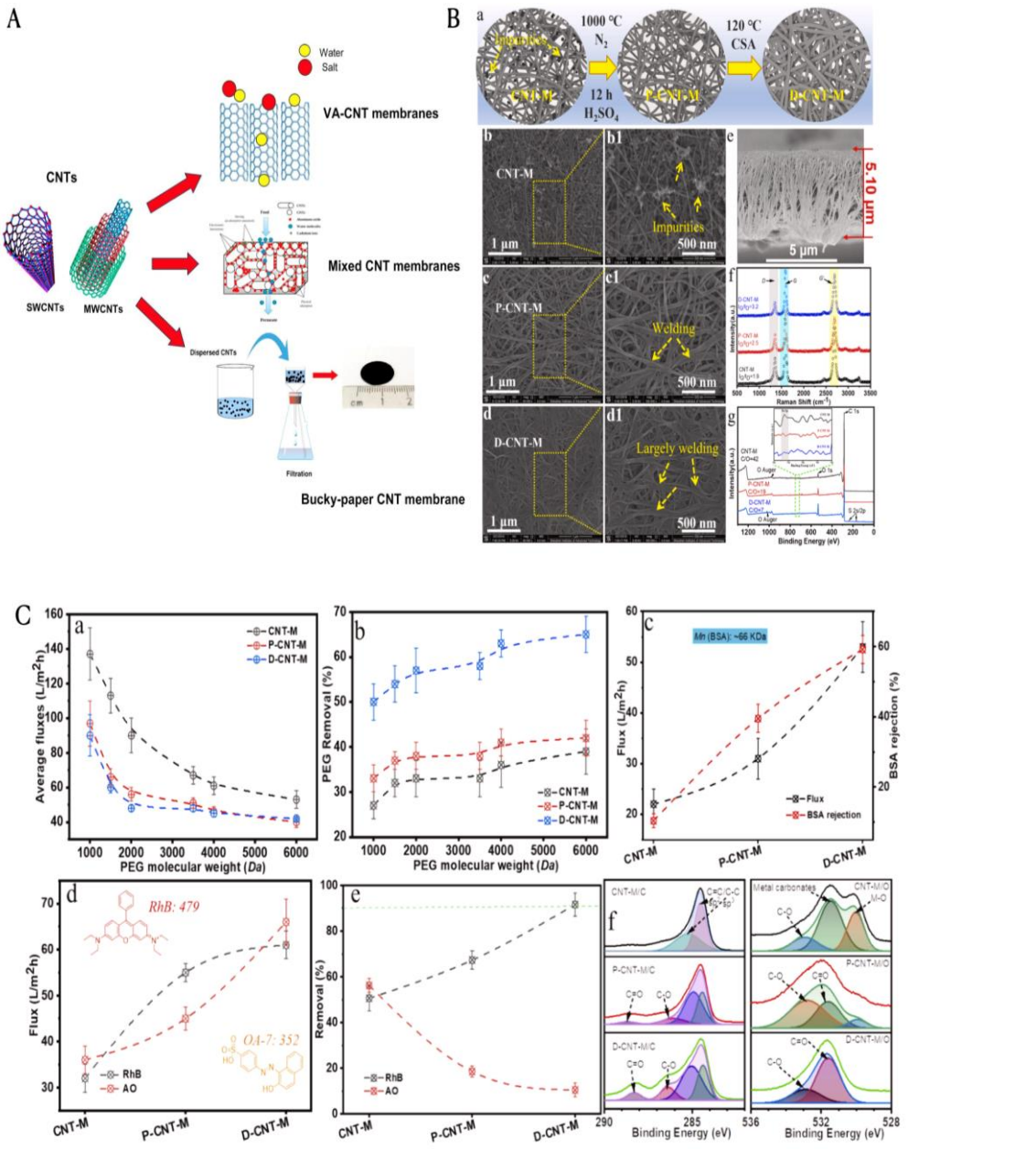

Figure 8. A. Types of CNT based membranes. B. (a) Preparation of D-CNT-M from pristine CNTs. The pristine CNTs contain metal impurities and need purification. Acid purification and oxidation of CNT-M followed by CSA treatment. B(b-e) SEM images, Raman, and XPS spectra of the prepared membranes. C. (a) the flux average and removal of, (b) PEG, (c) BSA, (d-e) RhB and AO. (f) The XPS of the CNT membrane after peak splitting. Reprinted/adapted with permission from Refs. [187,199]. Copyright 2019, Copyright Elsevier, and Copyright 2024, Copyright Elsevier.

3.3.3. Photocatalytic Degradation of Wastewater

CNTs are renowned for having very good electrical conductivity, a high specific surface area, and active sites on it. CNTs are acceptors of photogenerated electrons and can function as an efficient electron transport material. Thus, in the presence of ultraviolet/visible light, the photodegradation of the organic pollutants (dyes) on the CNT surface starts when the dye is adsorbed on the surface of the CNTs. The hydroxyl groups are oxidized by the holes (h^+) to form a (OH•), which can break down the organic pollutants like MB. The oxygen molecules adsorbed on the CNTs surface react with the photoelectrons and will form a highly reactive superoxide radical ions ($O^{\bullet -2}$) that oxidizes the organic dyes efficiently [203–207]. However, the action of photocatalysis is very promising with metallic

 doi:10.20944/preprints202510.0466.v1

semiconducting oxides such as ZnO, TiO_2, MgO, CeO_2, WO_3, CeO, SnO_2, ZrO_2, CuO, and AgO etc. [208]. During photocatalysis the semiconductor generate the h^+/e^- pair. The efficacy of the catalyst depends on the amount of e^-/h^+ generation and separation. However, there is a chance of recombination and hence charge separation is important. Due to the highly conductive nature of CNTs, these could facilitate the electron conduction through charge separation. Thereby by could achieve better photodegradation [203].

There are several reports presented on the synergistic effects of CNTs and metal oxide composites to photocatalytic degradation and conversion of organic and inorganic pollutants. Chen *et al*. prepared CNT/TiO_2 heterojunction photocatalyst through an in-situ method for RhB degradation. By creating a heterojunction and facilitating the flow of photoinduced free electrons from TiO_2 matrix to the CNT, the TiO_2 growth on CNT surface can boost the rate of photocatalytic oxidation by preventing e^-/h^+ recombination [209]. Shaban *et al*. synthesized TiO_2 nanoribbons/CNT composite (TiO_2NRs/CNT) through CVD method. The composite has shown red-shifted bandgap than TiO_2 NRs, and triggered 100% MB degradation under sunlight at 5 mg/L dye concentration and, 300 min of light exposure. The composite has shown 50% faster degradation than TiO_2 NRs with high catalytic stability [210]. The TiO_2/MCNT composites were made using a straightforward evaporation-drying procedure for the tetracycline (TC) contaminated wastewater. The results showed that, in comparison to TiO_2, the TiO_2/MWCNT composite exhibited improved photocatalytic activity from 86% to (95% TC removal [211]. BPA and carbamazepine (CBZ) were degraded by MWCNT-TiO_2-SiO_2, and the studies reveal that the production of nontoxic degradation products [212]. Akter *et al*. incorporated Ti^{3+} into the TiO_2/CNT composite. The obtained Ti^{3+}/TiO_2/CNT has particularly good visible light absorption and given a great photocatalytic performance towards various organic dyes such as MB, MO, phenol, Rh B, and Congo red. The photocatalyst has shown great stability and reusability up to five consecutive cycles [213]. It was also reported that the addition of Ag and TiO_2 to CNT increases the adsorption and photodegradation of MB than CNT alone [214]. Another work led by Eid M.S. *et al*. proved that the addition of AgNPs and cationic surfactant (C10) enhances surface area and dispersibility of TiO_2/CNTs composite. The prepared TiO_2@CNTs/AgNPs/C10 has given high MB degradation and great stability [218]. A ternary CAT (CNTs-Ag-TiO_2, CAT) composite was prepared by simple mechanical mixing and was tested for Congo red under visible light irradiation as well [216]. In a very recent report by Chen *et al*. given a new approach in the degradation of azo dyes that are extremely toxic, refractory, mutagenic, and carcinogenic using the intimately coupled photocatalysis and biodegradation (ICPB) method. This has shown excellent removal performance by combining the benefits of oxidation with the high mineralization rate of biodegradation. The ICPB was developed by adding the Rhodopseudomonas palustris and sodium alginate (SA) to the CAT to obtain (*R. palustris*/CAT@SA, R-CAT) [218]. A similar strategy (ICPB/ R-CAT) was also adopted by Liu et al. for the removal of CR dye [219]. Akhter *et al*. hydrothermally synthesized TiO_2, CNTs, and TiO_2-CNTs Photocatalysts. A systematic photocatalytic capability of TiO_2, CNTs, and TiO_2-CNTs was studied by using MB dye. Figure. 9A (a-c) reveal the SEM of TiO_2 nanoparticles with different magnification, which shows the rough surface with aggregations in high magnification. Figure. 9A (d-f) reveals the dense and tubular structure of CNTs.

 doi:10.20944/preprints202510.0466.v1

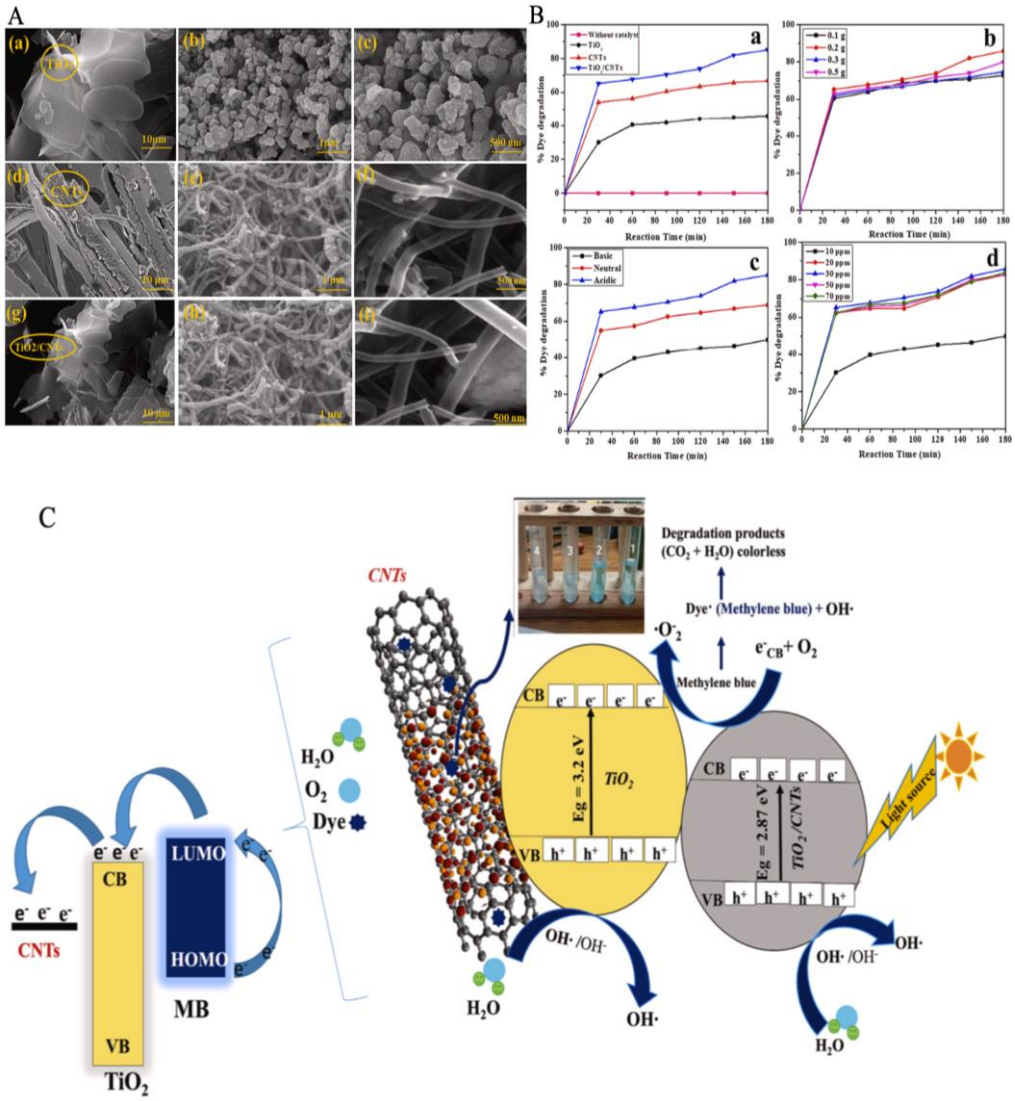

Figure 9. Photocatalysis of TiO_2, CNTs, and TiO_2-CNTs nanocomposite for MB degradation. A. SEM images of (a-c) TiO_2NPs, (d-f) CNTs, and (g-i) TiO_2-CNTs with increasing magnification. B. (a) Photocatalytic efficacy of TiO_2, CNTs, and TiO_2-CNTs under sunlight and without catalyst. (b) Impact of weight of photocatalyst, (c) p^H, and (d) various MB concentrations. Reprinted/adapted with permission from Refs. [219]. Copyright 2024, Copyright Elsevier.

Figure. 9A (g-i) confirms the functionalization of TiO_2 on top of CNTs and retention of the tubular structure of CNTs after functionalization. Based on the SEM and other characterizations reported the composite formation was successfully confirmed. After that the photocatalytic performance was assessed. Figure 9B (a) is the graphical representation of the MB degradation in absence and presence of the catalysts (TiO_2, CNTs, and TiO_2-CNTs). The graphical curves represents no degradation of MB without catalyst and ~90% of degradation using TiO_2-CNTs. Whereas the TiO_2 and CNTs given 40% and 60% under light. Figure 9B(b-d) are the effects of the amount of photocatalysts, pH and MB concentrations. At 0.2 g of TiO_2-CNTs, acidic pH, and 30 ppm of MB has given the maximum degradation in 180 min of reaction time was reported. Figure 9C depicts the photocatalytic mechanism mediated by TiO_2-CNT via light absorption, e^-/h^+ generation by the TiO_2, TiO_2-CNT. The reduced band gap of the composite facilitate the enhanced electron conduction there by MB conversion from blue to color less. Which is the indication of generated ROS mediated destruction of carbon skeleton of MB and results in CO_2 and H_2O as a degradation products [219]. Other catalysts like inexpensive aerogel TiO_2 -CNT for RhB and MB degradation about > 97% in 110 min under UV irradiation [220], chitosan-TiO_2@MWCNT for MB, MO and **ciprofloxacin (CIP)**

 doi:10.20944/preprints202510.0466.v1

removal [221], electro spun nanofibers mats TiO_2/ MWCNTs electro spun nanofibers mats for Cr (VI) reduction to Cr (III) were successfully discussed in the literature [222]. In addition to TiO_2-CNT composites, CNT-ZnO, N-Doped ZnO/SWCNTs, ZnO/CNT/Chitosan Ternary Composite, ZnO-$CoFe_2O_4$ - CNTs, CNT/MgO/$CuFe_2O_4$, $CoFe_2O_4$/CNT, Nb_2O_5/MWCNT, CNT-WO_3, PANI-MWCNTs, g-C_3N_4/$BiFeO_3$/CNTs, and Bi_2O_3/MWCNTs were well reported towards organic and inorganic pollutants oxidation and reductive elimination [223–231].

3.4. Graphene-Based Nanomaterials for Water Treatment

Graphene is the strongest carbon material with a two-dimensional honeycomb lattice structure with sp^2 hybridized carbons. It was treated as a component of graphite in 1940. Boehm and colleagues (1962) used heat and chemical reduction to separate the carbon flakes from the oxidized graphite (GO). However, Geim's use of specialized tape to repeatedly peel high-directional pyrolytic graphite did not result in the thermodynamic stability of monolayer graphene being discovered until 2004. Because of its layered structure, graphene has high electrical properties (electron mobility is 200000 $cm^2/(V{\cdot}s)$), exceptional thermodynamic properties (5300 W/(m·k)), mechanical properties (Young's modulus and breaking strength are 1100 GPa and 125 GPa, respectively), and a high specific surface area (2600 m^2/g). This groundbreaking finding has drawn the attention of researchers in the physical, chemical, biological, and environmental sciences [232–235].

Due to these astonishing features, graphene-based nanomaterials (GBNs) like GO, and RGO are ideal materials for water treatment technologies. The graphene, GO and RGO can be fabricated by top-down and bottom-up approaches [233]. Among several preparation methods, solution-based exfoliation is economical and attractive to produce on a gram scale. Figure 10A-H shows the chemical exfoliation of graphite into GO and RGO and their chemical structures and characterization by AFM, SEM, TEM, and XPS [236–239].

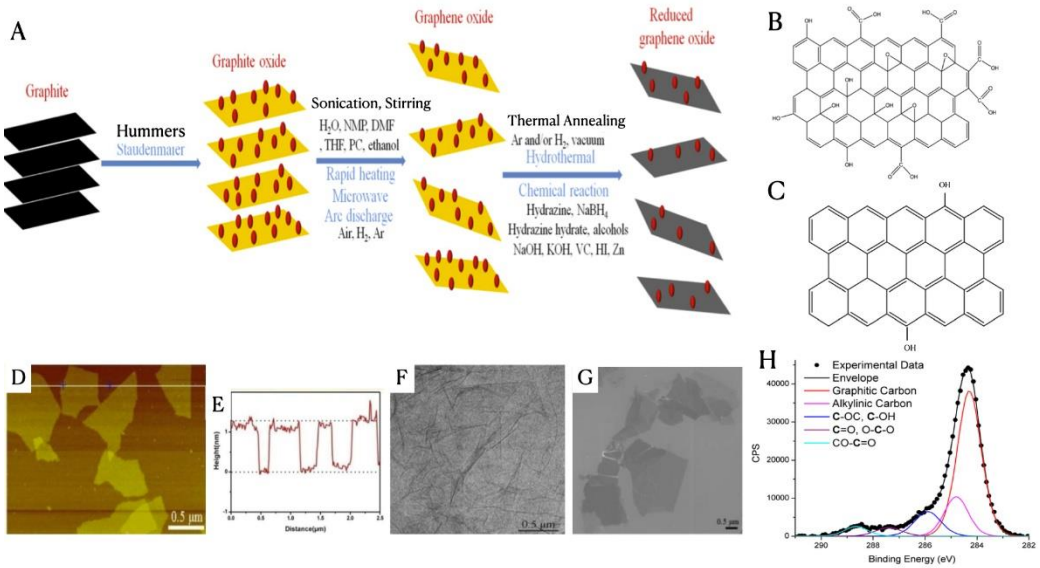

Figure 10. A. Schematic exfoliation of graphite into GO and its reduction into RGO using various reduction methods. B and C are chemical structures of GO with many oxygen functional groups and RGO with limited oxygen functional groups. D. and E AFM images of GO with their height profiles showing 1 nm thickness. F. TEM of GO with thin transparent layers. G. The 2D layered morphology of SEM which is same as AFM. H. XPS of GO confirming many surface oxygen functional groups. Reprinted/adapted with permission from Ref. [237, 238, 239, 240. Copyright 2017, Copyright Elsevier. Copyright 2019, Copyright ACS. Copyright 2011, Copyright IVYSPRING, Theranostics. Copyright 2013, Copyright ACS.

The unique dimensionality and high surface area, and tunable surface chemistry, these GBNs can be functionalized with different functional groups, such as organic linkers, ligands, metals, metal

 doi:10.20944/preprints202510.0466.v1

oxides, and polymers to enhance the pollutants' capability. In a basic form of pure graphene has only double bonds and pi electrons, hence its water treatment capability is low. However, after oxidative treatment it can generate the oxygen functional groups such as -OH, -O-, -C=O, -COOH. Hence, it can more favor the surface phenomenon of tracing the pollutants through electrostatic interactions along with π–π interactions [240–242]. Parallel to other family members like C60, CDs and CNTs, graphene/GO can be used as an adsorbent, membrane, photocatalyst and antimicrobial agent to purify the water by eradicating the inorganic and organic pollutants and pathogens [243].

3.4.1. Adsorption

GBNs have unique dimensionality, surface area, and rich surface functionality, which can favor adsorption of heavy metals and organic pollutants through π–π, electrostatic interactions and surface complexation on both sides of GBNs. Based on one of the review on GO for inorganic pollutants removal, a report by Peng *et al*. has shown the highest removal (1119 mg/g) of Pb (II) among other divalent metals: Cu (II), Cd (II), Zn (II) of 294, 345, 530 mg/g which is one of the highest reported in the literature. The removal efficacy of the GO was due to good water solubility, surface area and high oxygen functionality [236,244]. Apart from bare GO various functionalized GOs are also reported. Among them, chitosan/GO was used to remove Au (III) and Pb (II). The reported efficacy was 1077 and 217 mg/g at p^{H} 3-4 and T 323 K [245]. In another composite, Poly(N-vinyl carbazole) (PVK)/ GO has shown high removal of 888 mg/g of Pb (II) at pH 7.0, T 298K [246]. Poly(acrylamide) (PAM)/RGO has given 1000 mg/g of Pb (II) and 1530 mg/g of MB removal [247]. Between the bare GO and functionalized/RGO, the GO has shown better removal of Pb (II) than any another divalent heavy metal ions. Apart from these findings we would like to summarize the latest reports based on GBNs for inorganic/organic pollutants here.

Very recently Patel *et al*. reported GO, amino trimethylene phosphoric acid (ATMP) and zirconium (GO-ZrATMP) composite to improve the aggregation, and dispersibility of GO. The composite has shown monolayer adsorption of Pb (II), Cd (II), and Hg (II) effectively by removing 373, 320, and 281 mg/g [248]. However, Gou *et al*. made a GO-hydrogel composite using GO, diethylenetriaminepentaacetic acid, and carboxymethyl cellulose for high adsorption and stability towards selective removal of Pb (II). It was observed that the highest removal of 521.917 mg/g was observed, which is the highest towards Pb (II) removal at present [249]. GO/GONRs/CS nanocomposite was fabricated using chemical exfoliation and freeze drying by Jabbar *et al*. The composite was well characterized and used to remove the U (VI). Studying the effect of adsorbent dosage, time and p^{H} found to remove high amount about 1209 mg/g of U (VI). The outstanding performance of the composite is because of the high amount of oxygen functional groups on GO, GONR (GO nanoribbons) and amine functional groups from CS [250]. These functional groups interact with U (VI) with multiple interactions such as ionic, surface complexation, and coordination bonds. Hence, high removal was possible with good stability and specific surface area of adsorbent. The present report on GO/GONRs/CS has given the best adsorption towards U (VI) than any other graphene composites discussed here. Magnetic separation is one of the convenient and versatile adsorption method to remove pollutants. Ortiz-Quiñonez *et al*. claimed simple and economic method to synthesize GO-$NiFe_2O_4$ magnetic nanoadsorbent to eradicate Cr (III). Though the synthesis method is effective, the adsorption capacity was 17 mg/g only [251]. Bagbi *et al*. prepared a mesoporous SiO_2 ($MSiO_2$)-GO composite using ultrasonication method and used for Pb (II) removal. The results show that $MSiO_2$-GO composite has shown better removal (90% at 25 °C) than bare $MSiO_2$. It is due to the outstanding features of GO. However, the obtained Pb (II) removal was poor (14.7 mg/g at 25 °C) than other GO composites discussed [252]. Besides heavy metal cations removal, anions like iodide (I^-) and phosphates (PO_4^{3-}) are also removed by graphene composites. Pan *et al*. prepared RGO-Ag nanocomposite to eradicate radioactive waste containing I^-. The best adsorption capacity of 2.9 mmol/g was observed by varying the pH condition. The I^- was selectively adsorbed among other interfering anions like CO_3^{2-}, SO_4^{2-}, NO_3^-, and Cl^-. The adsorption mechanism was due to the AgI complexation on RGO surface [253].

 doi:10.20944/preprints202510.0466.v1

Graphene and GO composites are good adsorbents to remove toxic organic pollutants as well. Figure 11A shows the structure of GO which contain 2D structure where it contain several types of negative oxygen functional groups which can electrostatically bind the cationic organic and inorganic pollutants. The GO also contain rich π electrons which can physically interact and hold the pollutants with π–π interactions. Due to its high surface area, it can behold any kind of pollutants with warping nature and function as a vessel to hold a plethora of pollutants [254]. Hence, the GO and GBNs have a versatile applications in catalysis and water industries. In order to evaluate the adsorption capability Abd-Elhamid *et al*. fabricated GO-C, a nanocomposite contain GO and sodium citrate (C) linked by tertaethylene orthosilicate (TEOS) as seen in Figure 11B. The functionalization of citrate improved the additional oxygen functional groups on GO with negative charge. This feature can inevitably attract different cationic pollutants than anionic contaminants. The adsorption experiments in Figure 11C(a) reveals that 90% removal of MB (cationic organic dye methylene blue), CV (cationic organic dye crystal violet), Cu^{2+}, and Co^{2+}. The Langmuir isotherm in Figure 11C(b). GO-C has given the adsorption of ~222, 270, 163, and 145 mg/g towards MB, CV, Cu^{2+}, and Co^{2+} respectively. The R^2 value of 0.999 was obtained for CV than other pollutants. Figure 11D reveals the color change and declining the adsorption of dyes after with GO-C composites. Here the researchers mixed the anionic dye (MO) along with cationic dyes (MB, CV) to investigate the selectivity and confirm the anionic and cations interactions between GO-C and dyes. Unlike MB and CV, the UV-Vis results shows that there is no change in the adsorption of anionic dye MO, it's due to the negative charge-negative charge repulsions. The GO-C was also assessed to treat factory real samples (FD) and after treatment (TFD) . Figure 11E reveals the decrease in the adsorption and change in the color of the GO-C treated sample. These results provided the confidence that GO-C can remove the pollutants from real water samples. Based on the recycling experiments, the GO-C could be used for 5 cycles with ~90% efficacy. The article also made a comparative table towards various adsorbents, and the GO-C was stood one of the best among all [255].

Ghadim *et al*. prepared GO using Hummer's method to remove TC an antibiotic used for variety of bacterial infections. When the GO was added to the TC containing water, the equilibrium reached within 15 min, and obtained 323 mg/g removal efficiency at 298 K. The adsorption mechanism was interpreted to be π–π and cationic and π interactions between GO and TC [256]. Kyzas *et al*. decontaminated the pharmaceutical wastewater containing dorzolamide using GO/CSA composite prepared using GO, polyacrylic acid containing chitosan. The TC was removed about 334 mg/g at optimum p^H, which is higher than the GO and CSA (175 and 229 mg/g). It was claimed that the amine functional groups on the TC interacts with the well available acid functional groups on the composite [257]. Acridine orange (AO) is one of the water contaminant and known to be a DNA and RNA disrupter was eliminated using in situ reduced GO by sodium hydrosulfite. The GO could be able to remove a very high amount about 2158 mg/g of AO [258]. The Hummer method was used to create the GO, and FTIR, SEM, and XRD were used to characterize it. As model dyes, basic red 18 (BR18), basic blue 41 (BB41), and basic red 46 (BR46) were utilized. The Langmuir isotherm and pseudo-second-order kinetics were observed to be followed by the dye adsorption on GO. GO has the ability to eliminate BB41, BR18, and BR46 at concentrations of 1429, 1250, and 476 mg/g, in that order. According to the findings, colored wastewater containing cationic dyes can be effectively adsorbed onto GO [259]. Apart from these reports many other research reports based on organic dye removal were well reviewed by Takur *et al*. [237]. Recent report by Leao *et al*. stated the effect of dimensionality and degree of oxidation against atenolol a pharmaceutical drug adsorption. The authors considered 1D CNTs with and without oxidation, 2D RGO, 3D GO and RGO. Based on the adsorption studies, the authors found that degree of oxidation and increasing in the dimensionality enhances the adsorption rate of atenolol. It is due to the increased high surface area, pores and functionality of 3DGO. Moreover, the adsorbent has shown excellent recyclability performance. Hence it could be used in water treatment technologies for various drug related pollutants [260]. The broad class of industrially produced organic compounds known as per- and polyfluoroalkyl substances (PFAS) is of great concern because of its harmful impact on ecosystems and human health. Adsorption is still

 doi:10.20944/preprints202510.0466.v1

a practical and efficient way to remove PFAS, even with the availability of other technologies. As a result, the work examined the effectiveness of a novel type of GO-based adsorbent in eradicating PFAS from water. With an almost 100% removal rate for all eleven PFAS evaluated, a GO-CTAC, GO modified by the cationic surfactant cetyltrimethylammonium chloride (CTAC) was determined to be the best of the eight adsorbents tested [261]

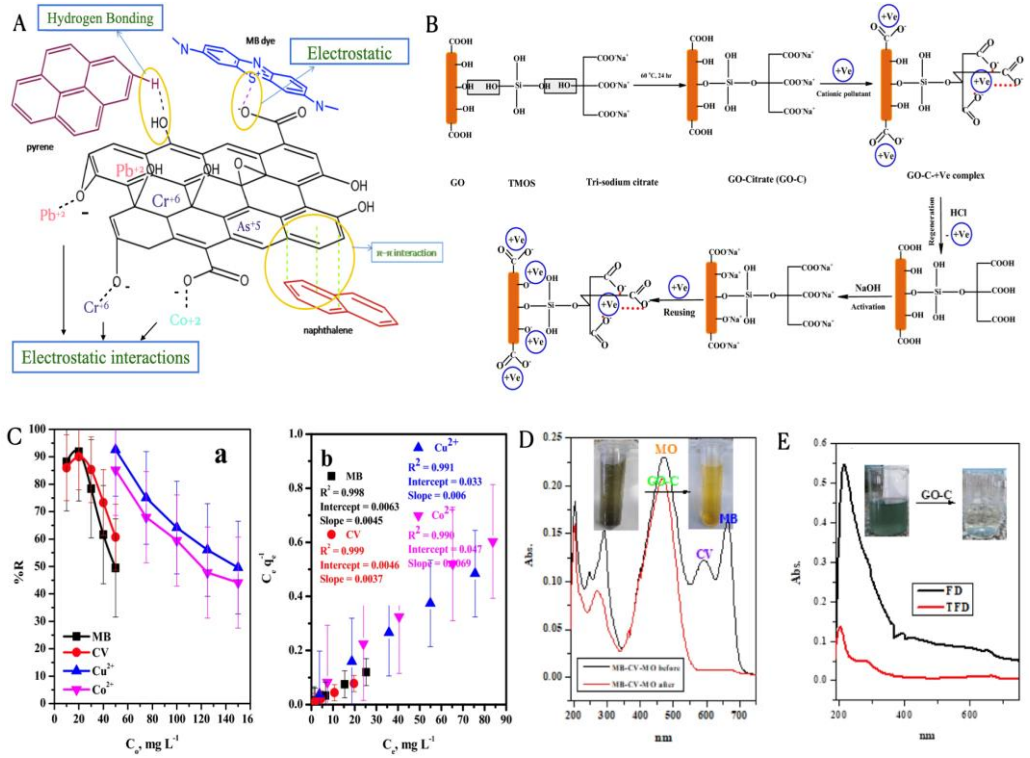

Figure 11. A. GO and its interactions with organic and inorganic pollutants such as MB, naphthalene, pyrene, Pb^{2+}, Cr^{6+}, Co^{2+}, As^{5+}. B. Synthesis streps involved in preparation of GO-C. C. (a) Percentage removal of MB, CV, Cu^{2+}, Co^{2+} at different concentrations, (b) Langmuir adsorption isotherm. D. MB–CV–MO mixture containing system before and after treatment with GO-C and their UV-Vis spectral. E. Realtime factory sample analysis using GO-C (before (FD) and after treatment (TFD)). F. Recycling experimental results with GO-C and pollutants. Reprinted/adapted with permission from Ref. [254,255]. Copyright 2019, Copyright ACS and Copyright 2022, Copyright SCI.

Pramanik *et al*. fabricated FGO a 2D fluorinated GO and 3D porous system based on FGO-polyethylenimine (PEI) to eradicate pharma related hazards, polyfluoroalkyl substances (PFAS) and microbial pathogens from water. With a 99% removal rate for both short and long-chain perfluorononanoic acid (PFNA), the FGO-PEI has an adsorption capability (q_m) of ~219 mg/g. This suggests that hydrophobic, electrostatic, and fluorophilic interactions are significant for the removal of PFAS. With an estimated q_m of ~299 mg/g, reported data showed that the FGO-PEI based nanoplatform can remove 100% of moxifloxacin antibiotics. Moreover, the nanoplatform may completely eradicate Salmonella and Escherichia coli from water since its pores are far smaller than those of pathogens. Furthermore, documented results reveal that the nanoplatform can remove viruses, pharmaceutical poisons, and PFAS from spiked river, lake, and tap water samples with a simultaneous effectiveness of about 96% [262]. Another 3D Graphene - sugar derived carbon aerogel (G-SCA) was fabricated toeliminate different types of hydrophilic pollutants such as nitroarenes, phoskill, ciprofloxacin, and pyridine, and hydrophobic contaminants like crude oil, waste oil and organic solvents. The G-SCA has outstanding recyclability up to 10 cycles. Hence, it could be a one of the good adsorbent to use in real time industrial applications [263]. One more 3D composite, TiVCTx MXene/graphene aerogels (TiVCTx/GAs) are fabricated by hydrothermal method followed

 doi:10.20944/preprints202510.0466.v1

by freeze-drying. With adsorption capacities of 319.7, 304, 230, 218, and 283 mg/g for MB, Rh B, CR, MO, and tetracycline hydrochloride, respectively, TiVCTx/GAs show excellent adsorption of a variety of dyes and medications. This is another effective adsorbent which worked for variety of organic pollutants [264]. Similarly, graphene/polydopamine aerogels (G-PDAG) was prepared to remove malachite green (MG) and MO. Where the hydrogel eliminates cationic MG by about 769 mg/g than MO. The high efficiency was explained due to the π–π and electrostatic attractions between G-PDAG and MG [265]. The discharge of highly poisonous substances like nile blue (NB) dye into sewage poses a substantial risk to both human health and the environment. GO, rGO, and Ag-g-rGO are prepared and used for NB adsorption. The Ag-rGO has shown better efficacy than rest [266]. Green synthesis is one of the attractive method to prepare green graphene or RGO. GO reduced by jute leaf extract was prepared and assessed to eliminate greater than 97% of tetracycline (TEC), oxytetracycline (OTC), and chlortetracycline (CTC) [267]. Among all the adsorbents, GO and graphene based aerogels are more attractive than its similar. Besides, the theoretical experiments DFT-D have also been done towards 112 emerging aromatic organic contaminants (AOCs) to interpret the adsorption mechanism. Different machine learning (ML) models are made based on quantum molecular descriptions. In the adsorption of most AOCs on graphene, the global interpretation identified that the molecular-volume-generated van der Waals interactions, including π–π stacking, are prominent, while the rest of the interactions such as hydrogen and electrostatic are less relevant. Furthermore, local interpretation revealed that hydrogen bonding and induced dipole interactions with surrounding water were significantly explaining factors in the adsorption of AOCs with sulfur and carbonyl functional groups. As a result, for theoretical and experimental investigations, the DFT-D-based ML models generated may serve as a reference model [268]. Overall, we have discussed the practical and theoretical experiments on adsorption of graphene on organic pollutants.

3.4.2. Membrane Filtration

Graphene's atomic thickness ensures great fluid permeability (higher than most commercial nanofiltration, NF, membranes) and hence energy/cost efficiency when it comes to water separation. Furthermore, there is a considerable chance of size-selective transport via 2D nanochannels between neighboring piled graphene sheets or through nanopores of a strong graphene layer. The membranes can also be made by using GO and RGO [269]. Figure 12A reveals the single and multilayered graphene with selective pores which can allow the water and reject the salts and pollutants based on size exclusion principle [270]. However, Making high-density, adjustable sub nanometer holes on two-dimensional membranes with robust mechanical properties is one of the main obstacles. Reported a straightforward method for fabricating high-density nanopores on bilayer graphene membranes by utilizing dual-side oxygen plasma treatment. The bilayer dual sided stable nonporous graphene is 78 % selective which is comparable to the mono layered graphene [271]. In addition to graphene, GO membranes are effective due to their hydrophilicity, antimicrobial activity originated from surface functionality. Multilayered GO membranes have given promising results in desalination. However, its swelling nature in water was a serious concern in practical usage. Reddy *et al*. studied a Na^+ and Mg^{2+} intercalated lamellar and nonlamellar multilayered GO's stability, water permeance, rejections of salts in RO process. The lamellar GO shows a fantastic water permeability and the nonlamellar GO has shown excellent salt rejection due to their well-defined and complex structural arrangement. It was observed the Mg^{2+} retained more time than K^+ hence the Mg^{2+} laminates are more stable in aqueous media without swelling [272]. Lv *et al*. demonstrated how to precisely customize monovalent cation sieving technique to improve water flow by intercalating GO membranes with certain crown ethers. A crucial interlayer gap (~11.04 Å) is found to enhance water flux (53.4 mol m^{-2} h^{-1} bar^{-1}) without compromising ion selectivity by adjusting the lamellar spacing of GO. Improved water permeance is thus provided by the meticulously increased interlayer spacing. At the same time, it has also shown selectivity towards various cations [273]. Wang *et al*. reported organic cations intercalated GO membrane layers. The cationic toluidine blue O intercalated GO

 doi:10.20944/preprints202510.0466.v1

layers have shown a rejection towards plethora of salts and neutral contaminants at various concentrations in a real time. This is due to the tuning of the interlayer spacing and creating the appropriate diffusion barrier [274]. Gong *et al*. fabricated both organic cation and anion intercalated GO layers. Obtained 0.71 nm size of channels, which can reject 100 % of NaCl and good range of water flux. Used pervaporation method for separation. Theoretical studies demonstrate that the organic ions function as vapor traps to shorten the vapor diffusion distance and subsequently as water pumps to significantly increase the water permeability, In addition to strongly influencing the 2D channel size of GO through cation/anion–π and π–π interactions [275]. The current problem of GO/RGO membranes monovalent ions poor rejection of monovalent ions was addressed by Zhang *et al*. To inhibit anion-cation co-transport and break the connection between anions and cations, they suggested a method of electrostatically induced ion-confined partitioning in a RGO membrane. This significantly improved the desalination capability. The membrane surpass the reported RGO membranes in terms of salt rejection, showing a rejection of 95.5% for NaCl and a water permeance of 48.6 L $m^{-2} h^{-1} bar^{-1}$. It also shows a salt rejection of 99.7% and a water flux of 47.0 $m^{-2} h^{-1} bar^{-1}$ under osmosis-driven conditions [276]. Figure 12 B(a) shows the structure of sodium polystyrenesulfonate (PSSNa) anionic dye and its intercalation between arginine cross linked rGO membrane layers for monovalent ion rejection. Figure 12 B(b) is a schematic synthesis of rGO by hydrazine reduction and vacuum deposition on PVDF substrate to obtain rGO membrane, followed by PSSNa deposition can get ArGO-PSSNa membrane. The photos of both membranes can be seen in Figure 12C(a) SEM cross-sectional images reveal the thickness of the membranes 37 nm (rGO) and 63 nm (ArGO-PSSNa) respectively in Figure 12C(b-c). The water and salt flux efficacy were explained in Figure 12D(a). The ArGO-PSSNa has shown high water flux of 47.0 L $m^{-2} h^{-1} bar^{-1}$ and low 3.8 L $m^{-2} h^{-1} bar^{-1}$ of NaCl flux. The results are in contrast to the GO membrane. Figure 12D(b) discloses that high salt rejection is about 99.7% with ArGO-PSSNa higher than GO. In addition, the saltwater ratios are decreased from GO to ArGO-PSSNa due to the selectivity of water and salt of the membrane. Overall, an anionic functionalized rGO was prepared and well demonstrated for desalination of water through forward osmosis method.

Oil separation is one of the big concern in the water industry. Hence, hydrophilic stable GO membrane are needed. To fabricate the needy, the GO was intercalated by hydrophilic halloysite (H) nanotubes which provide the required hydrophilicity and interlayer spacing. The GO/H has an improved permeance from 50.0 to 1150.7 $Lm^{-2} h^{-1} bar^{-1}$. In addition, the composite has good wettability and self-cleaning ability. The composite was reported to withstand at various concentrations and pressures (1000-5000 ppm and 0.5-3.0 bar) [277]. Wu *et al*. played with the surface charges and potentials of the GO by treating with KOH and HCl. The obtained GO has some defects which act as a microchannel, high surface potential and negative charged due to the oxygen functional groups facilitating the interlayer pores and trigger the ion rejection and high water flux [278]. Chen *et al*. fabricated a self Na^+ rejection of thin GO membranes which can operate at 1 bar pressure. The process of separation is multistage; it was 10 times effective than RO and consumes just 10% of energy in it [279].

Membranes based on sustainable green materials are attractive due to the safety concerns. In this perspective, the lignin originated green GO (bGO) and bamboo biomass derived reduced (brGO) laminar channels were prepared for nanofiltration. The bGO has a pore size of 1.15 nm and brGO has a 0.03 nm. The respective water pathway lengths are 65 and 49 nm. The brGO membrane has shown 52-60 fold enhancement in water permeance and rejection towards MB, direct red 81, and Na_2SO_4 than bGO due to its small pores and narrow water channels. In the ultrasound swelling test the brGO withstands for 2h without swelling in the experimental conditions [280]. Arginine, an amino acid functionalized GO membrane (Arg/GO) with various thickness was prepared by Soomro *et al*. The salt and dyes are separated using Arg@GO membrane composites of varying thicknesses. With good water permeance, the 900-nm-thick Arg@GO composite membrane exhibits rejection rrate of 98% for NaCl and 99.8% for $MgCl_2$, $Ni(NO_3)_2$, and $Pb(NO_3)_2$. Besides, this membrane has a remarkable separation efficiency (100%) for the dyes Evans blue, RhB, and MB. Meanwhile, up to 2100 ± 10 L m^{-}

 doi:10.20944/preprints202510.0466.v1

^{2} h^{-1} bar^{-1} may be found in the ultrathin Arg@GO composite membrane (220 ± 10 nm) demonstrating strong water permeance. Moreover, the 900 nm thick Arg@GO composite membrane swells much less after 40 days in an aqueous environment [281]. Another green, economic, simple, and ultra efficient lignin based GO membranes (GOLB) are fabricated with various thickness and unique laminated structure. The thickness of the membrane can be varied with different concentrations of GOLB used. A high concentration of GOLB could possess a plethora of oxygen functional groups which is also a reason for thickness. At 240 nm of thickness the GOLB shows exceptionally high water permeance of 1380 L m^{-2} h^{-1} bar^{-1}. According to Ali *et al*. GOLB has best permeance than other GO membranes reported. The membrane's ability to reject various salts, dyes, proteins, and biomolecules is also examined. It demonstrates good separation ability (> 99%) for a number of probe colors and biomolecules, and less than 10% rejection for Na_2SO_4 salt. In addition, they do not break down for 37 days in water compared to pristine GO membranes (pGOMs) [282]. MXene-Intercalated GO membranes for salt and dye rejection with anti-swelling properties [283], tunable interlayer distance of RGO membrane by intercalating the xylene isomers [285], reusable graphene-based water filters for the home to eliminate heavy metals [285], several graphene based membranes have been proposed for desalination and wastewater treatment [286]. Besides water purification Tian *et al*. worked on membrane biofouling of GO based on diversified microstructure on the GO's surface. The biofouling was assessed in relevance to surface water purification for about 110 days of continuous operation. Here in this experiment, the scientists prepared GO/Fe, GO/Fe(OH)$_3$, and GO/(OH)$_3$Fe-H. Among all the GO/Fe(OH)$_3$ shows high consistent waste flux and extremely low biofouling due to the relatively smooth surface and hydrophilicity than other composites [287,288].

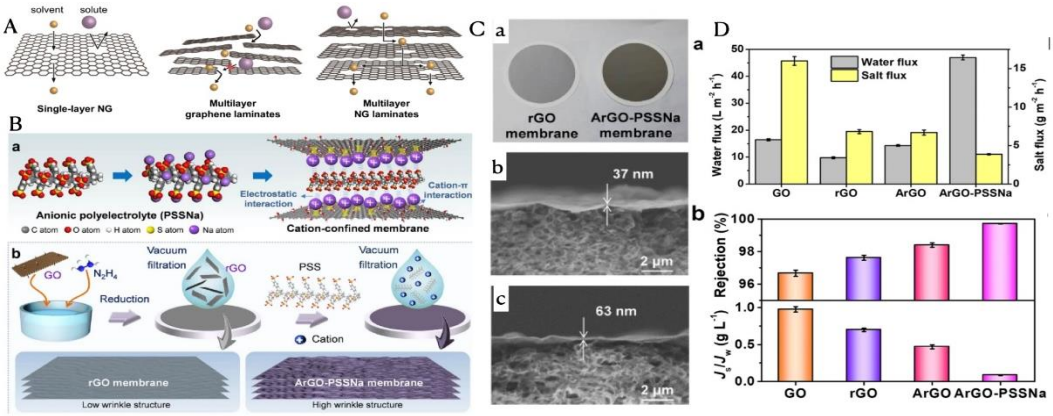

Figure 12. A. Mono layered graphene separation. B(a). Diagram showing the ArGO-PSSNa membrane's structure. b. Systamatic illustrations showing rGO and ArGO-PSSNa membrane wrinkle architectures as well as the preparation process. Ca. Digital images of the membranes ArGO-PSSNa and rGO. b-c. SEM photos of the respective membrane cross sections. Da. Aqueous and NaCl permeation fluxes in membranes made of GO, rGO, ArGO, and ArGO-PSSNa. The draw and feed solutions used in the studies were DI water and 0.5 M NaCl, respectively, and they were carried out at room temperature in the FO (the active layer facing the feed solution) mode. Db. The Js/Jw and rejection rates of salts by GO, rGO, ArGO, and ArGO-PSSNa membranes are presented. Reprinted/adapted with permission from Ref. [270,276]. Copyright 2021, Copyright MDPI, and Copyright 2024, Copyright Nature Communications.

3.4.3. Photocatalytic Degradation of Wastewater

The superior properties of graphene highlited in the introductory section such as excellent conductivity, chemical and thermal stability, surface area, tunable band gaps, and high adsorption capacity of metals and organic pollutants made graphene related materials such as RGO, GO, and their composites as good scaffolds for photocatalytic applications. Specifically in water technology, the graphene composites can degrade organic pollutants and inorganic pollutants through electrochemical reactions [289]. The band gap between 1.5-3.0 eV is the required to degrade most of

 doi:10.20944/preprints202510.0466.v1

the organic pollutants in visible region. The graphene has a zero band gap, RGO with 0.1-2 eV and GO with 1.5-3.0 eV, and the band gap could be altered by selective oxidation and tuning the conjugated π electrons [289]. The typical photoactive semiconductors like TiO_2 and ZnO has band gaps between 3.0-3.5 eV and are active in UV light and need modifications to active in visible - NIR range. To be effective, the respective catalyst has to be modified to achieve the best performance in visible region [290,291].

For the first time RGO-P25 (TiO_2) catalyst was prepared by simple in situ hydrothermal method to degrade MB dye. Compared to P25, the RGO-P25 has shown improved photocatalytic degradation in visible light [292]. GO-Graphene TiO_2 nanoarray photocatalyst was prepared to effectively degrade six anticancer drugs [293]. Another well-known photocatalyst ZnO was also functionalized with graphene and found to raise in their RhB degradation than bare ZnO [294]. Thereafter several improvements have been reported and been tried to seek various types of graphene and other photocatalytic combinations [295–297]. However, the recent report reveals that GO alone could work as an efficient photocatalyst. Very recently, GO and RGO were prepared with and without $NaNO_3$ and $CaCl_2$ for MB reduction. The GO prepared with $NaNO_3$ has given 60-90% of MB degradation in UV-Visible light [298]. In the latest report by Thakur *et al*. presented synthesis of GO-I, GO-II, and GO-III with tunable band gapes (2.51 to 2.76 eV) by modified Hummer's method to serve as an adsorbent as well as a visible light photocatalyst. The modified controlled (different acid concentrations) synthesis permitted the tailored optical property, structural arrangement, and surface functionality, which helps the enhanced adsorption and photocatalysis of water containing organic pollutants. Among the GOs tested, the GO-II has a better adsorption (454.54 mg/g) and photocatalysis (99%) to MB, due to high surface area, pore volume, bandgap, and optimum oxygen functional groups obtained via optimum oxidation conditions than GO-I and GO-III. Furthermore, the study emphasizes how GO's self-cleaning properties under natural sunshine contribute to its sustainable solar light-induced green chemistry, making it a great recyclable adsorbent with significant potential for environmentally friendly and useful applications [299]. The study presents GO as a nanophotocatalyst as well as an effective stand-alone nanoadsorbent without any other metal or metal oxide. In addition, the graphene based materials are well proven to be antimicrobial agents. Hence, they can remove the waterborne bacteria and fungus along with organic and inorganic contaminants [300].

4. Antibacterial Activity of Carbon-Based Nanomaterials

The nanoallotropes of carbon such as fullerenes, CDs, CNTs, GO, RGO, and graphene have been an attractive antimicrobial agents against broad spectrum of pathogens, such as bacteria, fungi, and. Figure 13 reveals the simultaneous sensing and killing of water containing pathogens [301]. The outstanding performance of these CBNs originated due to the surface functionality, rough surface area, dimensionality, needle or blade-like action, warping nature, and small size, which helps to hold and penetrate inside the cell. The discussed nanometer purifiers trigger the physical destruction of the cell wall and generate ROS after internalization into the cells. The rich π electrons and high conductivity of these nanomaterials could also interfere with respiratory system of the microbe and inhibit the cell metabolism. Additionally, these CBNs create nutritional starvation in their presence. Hence, they are hungry and swallow the nanomaterials, which function as trojans to distract the cellular components like proteins, DNA, RNA, mitochondria, and cytoplasm [302,303]. Besides, the fluorescence of the CDs and fluorescent dye functionalized GO, RGO, and CNTs could help to detect pathogens in the contaminated water visually [304]. Hence, the CBNs could serve as adsorbents, membranes, photocatalysts, and antimicrobial agents to fulfill the needs of water treatment systems to filter and destroy the organic, inorganic pollutants, and microbial fouling. These common features can reduce the cost and increase the purification performance.

 doi:10.20944/preprints202510.0466.v1

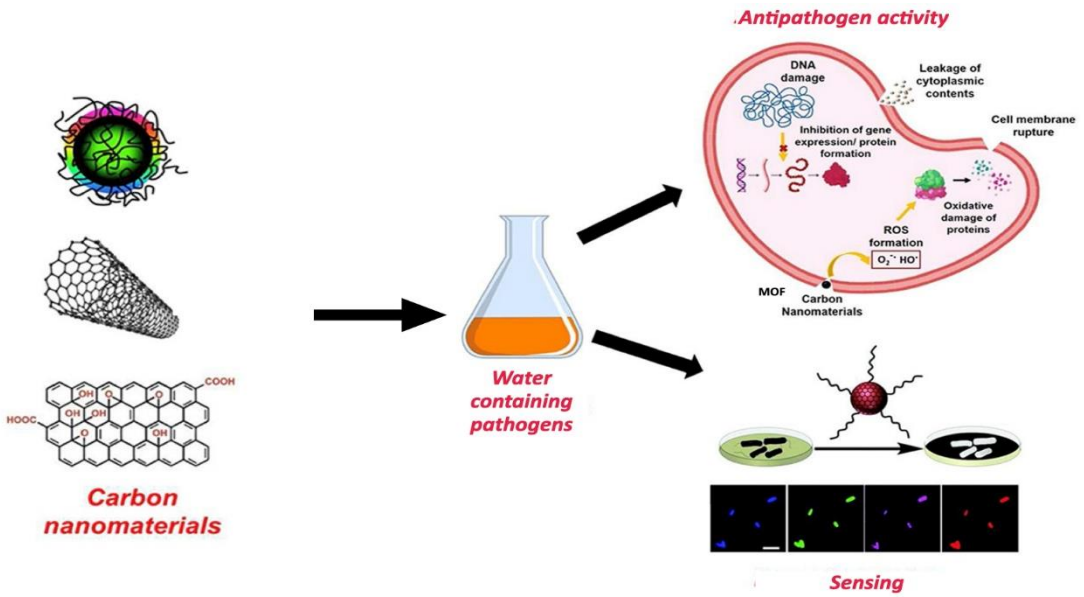

Figure 13. CDs, CNTs, and GO/RGO for water containing pathogenic killing and sensing. The image was modified and reprinted/adapted with permission from Ref. [301]. Copyright 2023, Copyright Elsevier.

5. Comparison of Various CBNs Targeted for Wastewater Treatment

Over the decades, nanomaterials usage in wastewater treatment has been increasing overwhelmingly due to the valuable results they impart in this field. However, the nanomaterials related toxicity towards animal, humans, and aquatic life has been a debate. Due to their small size, the nanomaterials can enter into the human body and into the cells, and there they may cause health disorders [305]. For CBNs, similar environmental implications such as bioaccumulation and food chain effects, toxicity to aquatic organisms, impact on soil microbial ecosystems, adsorption of other pollutants, residual presence, release during handling and processing, mixture toxicity due to combined effects of CBNs with other pollutants present in wastewater leading to additive, synergistic, or antagonistic toxic effects on organisms all add to CBNs complex environmental interactions and public concern.

Though a lot of advancement has been happening in waste technology industries, the role of several nanomaterials is consistently experimented with to fulfill the existing gaps. The challenges in wastewater technology are the cost and hazards of chemicals used, energy consumption, dealing with sludge, skills for operation, accountability, and competence are some of the notable challenges. Among the challenges, the toxicity and cost related problems could be solved using cost-effective nanomaterials with high and ideal specifications related to water treatment. Though outstanding performance has been seen by the CNTs, still some of the problems has to be solved. In case of C60, aggregation, solubility, and toxicity have to be resolved including economic fabrication methods. Though CDs have good water dispersibility and tunable fluorescence, their low surface area and controllability in synthesis are challenges. The CNTs and graphene have aggregation issues due to hydrophobicity and need sophistication to synthesize in high purity. High cost and toxicity are other challenges for these two materials. However, the GOs and RGO can provide good water solubility and high-scale economic synthesis. However, its long-term stability in the water environment remains challenging.

The measures put in place to supply clean water have faced significant challenges in recent decades as the demand for clean water sources has decreased dramatically. The expense and effectiveness of providing clean water are the primary motivations for the regulations imposed to provide it. Due to their high raw material capabilities, reduced manufacturing costs, and increased efficiency, a wide range of CBNs are available as listed in Table 1. These CBNs have already been applied to the treatment of water on a lab scale, with positive results. The primary obstacle at hand

 doi:10.20944/preprints202510.0466.v1

pertains to implementing this laboratory-scale idea in the actual world of industry, given the significant variations in CBNs suitability for commercialization. To determine the effectiveness and suitability of these CBNs for the eradication of contaminants from water, they should first be assessed in real-world environments using wastewater from industry as well as more realistic conditions. Prior to now, more CBNs should have been used in lab-scale research, and the research duration should have been longer. The long-term performance of CBNs in the wastewater treatment is addressed by this. Therefore, a comparison of the short and long-term applications of CBNs will yield more definitive results. Table 1 summarizes the commonly used CBNs for wastewater treatment along with their target pollutants, key benifits, and main limitations.

Table 1. Comparison of various CBNs types targeted for wastewater treatment.

CBN Type	Target Pollutants	Key Advantages	Main Limitations
Activated Carbon	Organic dyes, heavy metals, VOCs	High surface area, low cost, widely available	Poor regeneration, limited selectivity [306].
Fullerenes (C60, etc.)	Pharmaceuticals, pathogens	Good redox properties, antiviral and antibacterial activity	Expensive, limited water dispersion
CNTs	Heavy metals, organic pollutants, pathogens	High mechanical strength, effective adsorbent and antimicrobial	High cost, toxicity, separation issues
CQDs	Dyes, pharmaceuticals, sensors	Photocatalytic activity, low toxicity, useful in sensing	Lower adsorption capacity than GO/CNTs
GO	Heavy metals, dyes, antibiotics	Tunable surface chemistry, strong adsorption, antimicrobial	Potential toxicity, costly synthesis [307].
RGO	Organic micropollutants, heavy metals	Conductive, good electron transfer (useful in Advanced Oxidation Process)	Agglomeration in water, harder to disperse

Furthermore, the CBNs can also be physically integrated into various configuration to meet targeted application at certain scenario as listed in Table 2.

 doi:10.20944/preprints202510.0466.v1

Table 2. Comparison of various CBNs integrations targeted for wastewater treatment.

Integration	Application Mode	Key Advantages	Main Challenges
Magnetic composites (e.g., GO-Fe_3O_4)	Recovery & reuse	Easy separation with magnets	Reduced surface area, synthesis issues
Embedded in composites	Continuous flow reactors	Enhanced selectivity, easier handling	Material compatibility, cost
Coated on membranes	Filtration + adsorption	Reduced fouling, reusable	Membrane fabrication complexity
Dispersed in batch systems	Adsorption, disinfection	Simple setup, direct contact	Difficult to recover CBNs

6. Sustainable Practices

6.1. Concerns about CBNs Targeted for Wastewater Treatment

Barceló *et al*. early studied on ecotoxicity assessment of engineered CBNs focusing on fullerenes and CNTs in the aquatic environment. Special attention was paid to their surface properties, which are indespinsiable for their aggregation in water, mobility in aquatic systems, interactions with aquatic organisms, with natural organic matter , and probable entry into the food chain [308]. Kang *et al*. study in the same year evaluates the cytotoxicity SWNTs, MWNTs, aqueous phase C60 nanoparticles, and colloidal graphite in gram negative and gram positive bacteria. These CBNs potential impacts on microorganisms in natural and engineered aquatic systems are also evaluated. SWNTs inactivate the highest percentage of cells in monocultures of four studied bacteria as well as in the diverse microbial communities of river water and wastewater effluvium. The authors concluded that CBN toxicity in bacterial monocultures was ineffective for microbial inactivation in chemically and biologically complex environmental samples [309].

Zaytseva and Neumann reviewed the major production techniques and important trends of fullerenes, CNTs, and graphene on plant growth and development for agricultural and environmental applications. The agricultural applications of CBNs include plant growth stimulators and fertilizers, nanoencapsulation and smart delivery systems, antifungal and antibacterial agents, as well as sensing systems and precision agriculture. The CBNs impacts on plants are discussed separately during the germination, plant cell culture, as well as plant growth and development stages. The authors concluded that an inclusive survey of the key factors is promonent for interactions of the various CBNs with living organisms and the environment will be indispensable for both risk assessment and the characterization of potential applications will be a main challenge for the future [310]. Freixa et al. review literature on CBNs toxic effects in aquatic organisms as well as through other micropollutants. The results indicated that environmental concentrations of CBNs do not cause harm to aquatic organisms by themselves. The identified CBNs concentrations in aquatic environments are in ngL^{-1} or even much lesser. Toxic effects have been mainly observed in short-term experiments at high concentrations, and toxicity principally depends on the type of organisms, exposure time, and CBNs fabrication methods. CBNs play a role either as carriers or sorbents, thereby changing the original toxicity of the pollutants. However, there is a need to study the interactive

 doi:10.20944/preprints202510.0466.v1

effects of CBNs with other micro-pollutants at environmentally relevant concentrations to know the long-term effects on biological communities [311]. Pikula *et al*. recently worked on reviewing both toxicity and interaction of CBNs with other pollutants in water environments based on the analysis of 53 publications focusing on the joint toxicity and interaction of CBNs. The work highlights the impressive extension of CBNs fabrication and application (including wastewater treatment) [312].

6.2. Systematic Thinking and Precautionary Principle

Systematic thinking is essential when dealing with CBNs for wastewater treatment. The following is a breakdown of the crucial approaches: (1) Acknowledging Complexity of Interactions: Multiple pathways and potential transformations are present between CBNs and biological systems and environment [313]. (2) Identifying Potential Hazards: Take a comprehensive evaluation of the CBNs entire lifecycle from synthesis to disposal. This includes identifying potential hazards at each stage, such as inhalation during manufacturing, release into water systems, or accumulation in organisms. (3) Understanding Exposure Pathways: Trace and investigate how CBNs might enter the human body and the environment, which is important for evaluating risks and developing mitigation strategies. (4) Considering Long-Term Effects: Look beyond immediate impacts and consider potential long-term consequences, such as chronic toxicity, bioaccumulation in food chains, and persistent environmental contamination. (5) Developing Comprehensive Risk Assessments: Integrate information from various disciplines, including toxicology, environmental science, materials science, and analytical science for more thorough risk assessments. (6) Designing Safer Materials and Processes: By understanding the aforementioned factors that contribute to potential risks, apply systematic thinking to guide the design of inherently safer CBNs and treatment processes. This includes modifying their properties to reduce toxicity or prevent environmental release.

Precautionary principle is essential too when dealing with CBNs for wastewater treatment. The following is a breakdown of the crucial factor: (1) Scientific Uncertainty: The precautionary principle advises taking preventative action even when scientific evidence of CBNs potential long-term health and environmental effects is not yet conclusive but there are plausible risks of serious or irreversible harm [314]. (2) Irreversible Harm Potential: Some aforementioned potential effects such as widespread environmental contamination or genetic damage could be irreversible. Actions need to be taken to avoid such outcomes. (3) Early Intervention: Some aforementioned potential harm needs early action to prevent, rather than waiting for conclusive evidence of damage. As early intervention might be more effective and less costly in the long run [315]. (4) Shifting the Burden of Proof: The burden of proof regarding the safety of a new CBN or application should lie with those who introduce it, rather than requiring regulators to prove harm [316]. (5) Promoting Responsible Innovation: The precautionary principle can guide innovation in CBNs nanotechnology towards safer and more sustainable pathways by encouraging a cautious approach. (6) International Consensus: The precautionary principle is recognized in numerous international environmental agreements and is increasingly considered in the regulation of emerging technologies like nanotechnology [317].

In brief, systematic thinking provides the framework for understanding the complex interactions and potential pathways of CBNs. The precautionary principle provides the guiding principle for decision-making in case of the uncertainties identified through systematic thinking, erring on the side of caution to protect human health and the environment. By combining these two approaches, we can strive for responsible innovation and minimize the possible risks associated with the growing use CBNs of while still harnessing their beneficial properties.

7. Future Perspective and Conclusions

The measures put in place to supply clean water have faced significant challenges in recent decades as the demand for clean water sources has decreased dramatically. The expense and effectiveness of providing clean water are the primary motivations for the regulations imposed to provide it. Due to their high raw material capabilities, reduced manufacturing costs, and increased efficiency, a wide range of carbon materials like RGO appear to be one of the most promising

 doi:10.20944/preprints202510.0466.v1

candidates to remove any kind of impurities from the water source. These CBNs have already been applied to the treatment of water on a lab-scale, with positive results. The primary obstacle at hand pertains to implementing this lab-scale idea in the actual world of industry, given the significant variations in CBNs' suitability for commercialization. To determine the effectiveness and suitability of these CBNs for the eradication of contaminants from wastewater, they should first be assessed in real-world environments using wastewater from industry as well as more realistic conditions. Prior to now, more CBNs should have been used in lab-scale research, and the research duration should have been longer. The long-term performance of CBNs in the treatment of wastewater is addressed by this. Therefore, a comparison of the short and long-term applications of CBNs will yield more definitive results regarding the use of CBNs in wastewater treatment. To improve their effectiveness in the treatment process, these CBNs can be further altered by applying an acidic or alkaline treatment or by coating. Therefore, to lower the effective cost of the water treatment process, researchers should focus more on using readily available raw materials, such as agricultural and biomass waste, to produce CBNs. To satisfy the need for clean water, target-specific adsorbents with high surface area, porosity, tunable charge, functionality, and shape are warranted. In the case of membrane technology, the CBNs could enhance the water flux and contaminant rejection even at high pressures. In addition, if the CBNs have a good capability of adsorbing visible light and lead a photocatalytic degradation and antimicrobial activity towards a variety of pollutants and microbes are highly desired in the future.

This review discussed CBNs for wastewater treatment. We have systematically examined the sources of wastewater, types of contaminants, and their treatment methods. We highlight the fullerenes, CDs, CNTs, graphene, GO, RGO, and their composites, for OD, ID, 2D, and 3D materials. In the case of CNTs, the 2D and 3D composites have improved performance due to their specific surface area, porosity, and surface functionality, optical and electrical properties, and antimicrobial activity, though the composition of all carbon materials is the same. We discussed adsorption, membrane separation, and photocatalysis to evaluate their water purifying capacity. We have observed from the vast literature that researchers are trying to give the best solutions for the existing problems concerning treatment methods by using nanomaterials. Most studies have found that carbon nanocomposites outperform bare nanomaterials in terms of results and performance. However, the best CNB with simple, green production, with a cost-effective method, high performance, stability, antifouling nature, and high biocompatibility, has to be reported in a single experiment to completely understand its fate in real time. Sustainable practices pay attention to concerns about CBNs targeted for wastewater treatment as well as systematic thinking and precautionary principle are indispensable considerations.

This review discussed carbon nanomaterials for wastewater treatment. We have systematically examined the sources of wastewater, types of contaminants, and their treatment methods. We highlight the fullerenes, CDs, CNTs, graphene, GO, RGO, and their composites, for OD, ID, 2D, and 3D materials. In the case of CNTs, the 2D and 3D composites have improved performance due to their specific surface area, porosity, and surface functionality, optical and electrical properties, and antimicrobial activity, though the composition of all carbon materials is the same. We discussed adsorption, membrane separation, and photocatalysis to evaluate the water purifying capacity of CNTs. We have observed from the vast literature that researchers are trying to give the best solutions for the existing problems concerning treatment methods by using nanomaterials. Most studies have found that carbon nanocomposites outperform bare nanomaterials in terms of results and performance. However, the best nanomaterial with simple, green production, cost-effective, high performance, stability, antifouling nature, and high biocompatibility, has to be reported in a single experiment to completely understand its fate in real time. Sustainable practices pay attention to concerns about CBNs targeted for wastewater treatment as well as systematic thinking and precautionary principle are indispensable considerations.

 doi:10.20944/preprints202510.0466.v1

Author Contributions: All authors conceptualized the outline and agreed on the content of the manuscript. G.G. prepared the manuscript. Y.-C.L. revised the manuscript. All authors have read and agreed to the published version of the manuscript.

Funding: This research received no external funding.

Institutional Review Board Statement: Not applicable.

Informed Consent Statement: Not applicable.

Data Availability Statement: Not applicable.

Conflicts of Interest: The authors declare no conflict of interest.

References

1. Barman, S.R.; Gavit, P.; Chowdhury, S.; Chatterjee, K.; and Nain, A. Wastewater Treatment. JACS Au. 2023, 3(11), 2930-2947.
2. UNWWDR. United Nations World Water Development Report 2020. Available online: https://www.unwater.org/publications/un-world-water-development-report-2020 (accessed 2025-04-11).
3. World Health Organization, Guidelines for Drinking-Water Quality: Incorporating the First and Second Addenda. World Health Organization, 2022. https://www.who.int/publications/i/item/ 9789241549950 (accessed 2025-04-11).
4. Sen, T.K. Agricultural Solid Wastes Based Adsorbent Materials in the Remediation of Heavy Metal Ions from Water and Wastewater by Adsorption: A Review. Molecules 2023, 28(14), 5575.
5. Silva, J.A. Treatment and Reuse for Sustainable Water Resources Management: A Systematic Literature Review. Sustainability 2023, 15(14), 10940.
6. Rashid, R.; Shafiq, I.; Akhter, P.; Iqbal, M.J.; Hussain, M. A state-of-the-art review on wastewater treatment techniques: the effectiveness of adsorption method. Environ. Sci. Pollut. Res. Int. 2021, 28, 9050-9066.
7. Singh, B. J.; Chakraborty, A.; Sehgal, R. A systematic review of industrial wastewater management: Evaluating challenges and enablers. J. Environ. Manag. 2023, 348, 119230.
8. Jassby, D.; Tzahi Y. Cath, T.Y.; Buisson, H. The role of nanotechnology in industrial water treatment. Nat. Nanotechnol. 2018, 13, 670-672.
9. Jain,K.; Patel,A.S.; Vishwas P. Pardhi,V.P.; Flora,S.J.S. Nanotechnology in Wastewater Management: A New Paradigm Towards Wastewater Treatment. Molecules 2021, 26(6), 1797.
10. Devi, M.K.; Yashika, P.R.; Kumar, P.S.; Manikandan, S.; Oviyapriya, M.; V. Varshikaa, V.; Rangasamy, G. Recent advances in carbon-based nanomaterials for the treatment of toxic inorganic pollutants in wastewater. New J. Chem. 2023, 47, 7655-7667.
11. Abbo, H.S.; Gupta, K.C.; Khaligh, N.G.; Titinchi, S.J.J. Carbon Nanomaterials for Wastewater Treatment. ChemBioEng Rev 2021, 8(5), 1-28.
12. Liu, Y.; Phillips, B.; Li, W.; Zhang, Z.; Fang, L.; Jingjing Qiu, J.; Wang, S. Fullerene-Tailored Graphene Oxide Interlayer Spacing for Energy-Efficient Water Desalination. *ACS Applied Nano Materials* 2018, 1(11), 6168-6175.
13. Mishra, S.; Sundaram, B. Efficacy and challenges of carbon nanotube in wastewater and water treatment, Environ. Nanotechnol. Monit. Manag. 2023, 19, 100764.
14. Tabish, T.A.; Memon, F.A.; Gomez, D.E.; David W. Horsell, D.W.; Zhang, S. A facile synthesis of porous graphene for efficient water and wastewater treatment, Sci. Rep. 2018, 1817.

 doi:10.20944/preprints202510.0466.v1

15. Asghar, F.; Shakoor, B.; Fatima, S.; Munir, S.; Razzaq, H.; Shazia Naheeda, S.; Butler, I.S. Fabrication and prospective applications of graphene oxide-modified nanocomposites for wastewater remediation, *RSC Adv*., 2022,12, 11750-11768.
16. Kaur, H.; Devi, N.; Siwal, S.S.; Alsanie, W.F.; Thakur, M.K.; Thakur, V.K. Metal–Organic Framework-Based Materials for Wastewater Treatment: Superior Adsorbent Materials for the Removal of Hazardous Pollutants. ACS Omega 2023, 8, 9004-9030.
17. Kesari, K.K.; Soni, R.; Jamal, Q.M.S.; Tripathi, P.; Lal, J.A.; Jha, N.K.*et al*. Wastewater Treatment and Reuse: a Review of its Applications and Health Implications. Water Air Soil Pollut 2031, 232, 208. https://doi.org/10.1007/s11270-021-05154-8.
18. Naseem, T.; Durrani, T. The role of some important metal oxide nanoparticles for wastewater and antibacterial applications: A review, J. Environ. Chem. Ecotoxicol. 2021, 3. 59-75.
19. Silva, J.A. Wastewater Treatment and Reuse for Sustainable Water Resources Management: A Systematic Literature Review, Sustainability 2023, 15, 10940. https://doi.org/10.3390/su151410940.
20. Wastewater Treatment Overview, avengtraining, https://arvengtraining.com/en/waste-water-treatment-overview/ (accessed 2025-04-11).
21. Lee, J.D. (1996) Concise Inorganic Chemistry. 5th Edition, Chapman and Hall Ltd., London, 619-621.
22. Gollavelli, G.; Ghule, A.V.; Ling, Y.-C. Multimodal Imaging and Phototherapy of Cancer and Bacterial Infection by Graphene and Related Nanocomposites. Molecules 2022, 27, 5588. https://doi.org/10.3390/molecules27175588.
23. Gollavelli, G.; Gedda, G.; Mohan, R.; Ling, Y.-C. Status Quo on Graphene Electrode Catalysts for Improved Oxygen Reduction and Evolution Reactions in Li-Air Batteries. Molecules 2022, 27, 7851. https://doi.org/10.3390/molecules27227851.
24. Çeçen, F.; Aktaş, Ö. (2011). Water and Wastewater Treatment: Historical Perspective of Activated Carbon Adsorption and its Integration with Biological Processes. In Activated Carbon for Water and Wastewater Treatment (eds F. Çeçen and Ö. Aktaş).
25. Kroto, H.; Heath, J.; O'Brien, S.; Curl, R.F.; Smalley, R,E. C60: Buckminsterfullerene. Nature 1985, 318, 162-163 . https://doi.org/10.1038/318162a0.
26. Discovery of Fullerenes, National Historic Chemical Landmark, Designated October 11, 2010, at the Richard E. Smalley Institute for Nanoscale Science and Technology at Rice University in Houston, Texas.
27. Boo, W.O.J. An Introduction to Fullerene Structures Geometry and Symmetry, Journal of Chemical Education, J. Chem. Educ. 1992, 69(8), 605, https://doi.org/10.1021/ed069p605.
28. Poulomi, B.; Bhavna, B. Fullerene and its applications: A review. J INDIAN ACAD ORAL M. 2020, 32(2), 159-163. DOI: 10.4103/jiaomr.jiaomr_191_19.
29. Kumar, P.A.; Namboodiri, V.V.; Joshi, G.; Mehta, K.P. Fabrication and applications of fullerene-based metal nanocomposites: A review. J. Mater. Res. 2021, 36, 114-128. https://doi.org/10.1557/s43578-020-00094-1.
30. Dubey, R.; Dutta, D.; Sarkar, A.; Chattopadhyay, P. Functionalized carbon nanotubes: synthesis, properties and applications in water purification, drug delivery, and material and biomedical sciences, Nanoscale Adv., 2021, 3, 5722-5744, https://doi.org/10.1039/D1NA00293G.
31. Gacem, M.; Modi, S.; Yadav, K.V.; Islam, S.; Patel. A.; Dawane. V.; Jameel. M.; Inwati, K. G.; Piplode, S.; Solanki, S. V.; Basnet, A. Recent Advances in Methods for Synthesis of Carbon Nanotubes and Carbon Nanocomposite and their Emerging Applications: A Descriptive Review. J. Nanomater. 2022(1), 7238602. https://onlinelibrary.wiley.com/doi/10.1155/2022/7238602.

 doi:10.20944/preprints202510.0466.v1

32. Balkanloo, P.G.; Sharifi, K.M.; Marjani, A.P. Graphene quantum dots: synthesis, characterization, and application in wastewater treatment: a review. Mater. Adv., 2023, 4, 4272-4293, https://doi.org/10.1039/D3MA00372H.
33. Deepa, C.; Rajeshkumar, L.; Ramesh, M. Preparation, synthesis, properties and characterization of graphene-based 2D nano-materials for biosensors and bioelectronics. J Mater Res Technol, 2022, 19, 2657-2694, https://doi.org/10.1016/j.jmrt.2022.06.023.
34. Cheng, X.; Kan, A.T.; Tomson, M.B. Uptake and Sequestration of Naphthalene and 1,2-Dichlorobenzene by C60. J Nanopart Res 2005, 7, 555-567. https://doi.org/10.1007/s11051-005-5674-z.
35. Ballesteros, E.; Gallego, M.; Valcárcel, M. Analytical potential of fullerene as adsorbent for organic and organometallic compounds from aqueous solutions, J. Chromatogr. A 2000, 869, 101-110. https://doi.org/10.1016/S0021-9673(99)01050-X.
36. Alekseeva, O.V.; Bagrovskaya, N.A.; Noskov, A.V., Sorption of heavy metal ions by fullerene and polystyrene/fullerene film composite. Prot Met Phys Chem Surf 2016, 52(3), 443-447. https://doi.org/10.1134/S2070205116030035.
37. Samonin, V.; Nikonova, V.; Podvyaznikov, M. Sorption properties of activated carbon with respect to metal ions. Protection of Metals 2014, 44, 190-192. https://doi.org/10.1134/S0033173208020148.
38. Samonin, V.; Nikonova, V.; Podvyaznikov, M, 2014. Carbon adsorbents on the basis of the hydrolytic lignin modified with fullerenes in producing. Russ. J. Appl. Chem. 2014, 87(2), 190-193. https://doi.org/10.1134/S1070427214020116.
39. Stylianakis, M.M. Distinguished Contributions in the Fields of Biomedical and Environmental Applications Incorporating Nanostructured Materials and Composites. Molecules 2021, 26, 2112. https://doi.org/10.3390/molecules26082112.
40. Sudareva, N.; Penkova, A.; Kostereva, T.; Polotskii, A.; Polotskaya, G. Properties of casting solutions and ultrafiltration membranes based on fullerene-polyamide nanocomposites. Express Polym. Lett. 2012, 6, 178-188. DOI: 10.3144/expresspolymlett.2012.20.
41. Semenov, K.N.; Andrusenko, E.V.; Charykov, N.A.; Litasova, E.V.; Panova, G.G.; Penkova, A.V.; Murin, I.V.; Piotrovskiy, L.B. Carboxylated fullerenes: Physico-chemical properties and potential applications. Prog. Solid State Chem. 2017, 47-48, 19-36. https://doi.org/10.1016/j.progsolidstchem.2017.09.001.
42. Yan, L.; Zhao, F.; Li, S.; Hu, Z.; Zhao, Y. Low-toxic and safe nanomaterials by surface-chemical design, carbon nanotubes, fullerenes, metallofullerenes, and graphenes. *Nanoscale* 2011, 3, 362-382. https://doi.org/10.1039/C0NR00647E.
43. Brunet, L.; Lyon, D.Y.; Hotze, E.M.; Alvarez, P.J.J.; Wiesner, M.R. Comparative Photoactivity and Antibacterial Properties of C60 Fullerenes and Titanium Dioxide Nanoparticles. Environ. Sci. Technol. 2009, 43(12), 4355-4360.
44. Zhang, B.-T.; Zheng, X.; Li, H.-F.; Lin, J.-M. Application of carbon-based nanomaterials in sample preparation: A review. Anal. Chim. Acta 2013, 784, 1-17. https://doi.org/10.1016/j.aca.2013.03.054.
45. Burakov, A.E.; Galunin, E.V.; Burakova, I.V.; Kucherova, A.E.; Agarwal, S.; Tkachev, A.G.; Gupta, V.K. Adsorption of heavy metals on conventional and nanostructured materials for wastewater treatment purposes: A review. Ecotoxicol. Environ. Saf. 2018, 148, 702-712. https://doi.org/10.1016/j.ecoenv.2017.11.034.
46. Yashas, S.R.; Shahmoradi, B.; Wantala, K.; Shivaraju, H.P. Potentiality of polymer nanocomposites for sustainable environmental applications: A review of recent advances. Polymer 2021, 233, 124184. https://doi.org/10.1016/j.polymer.2021.124184.

 doi:10.20944/preprints202510.0466.v1

47. Shen, Q.; Xu, S.J.; Xu, Z.L.; Zhang, H.Z.; Dong, Z.Q. Novel thin-film nanocomposite membrane with water-soluble polyhydroxylated fullerene for the separation of Mg^{2+}/Li^{+} aqueous solution. J. Appl. Polym. Sci. 2019, 136, 48029. https://doi.org/10.1002/app.48029.
48. Li, Y.; He, G.; Wang, S.; Yu, S.; Pan, F.; Wu, H.; Jiang, Z. Recent advances in the fabrication of advanced composite membranes. J. Mater. Chem. A 2013, 1, 10058-10077. https://doi.org/10.1039/C3TA01652H.
49. Tan, X.F.; Liu, Y.G.; Gu, Y.L.; Xu, Y.; Zeng, G.M.; Hu, X.J.; Liu, S.B.; Wang, X.; Liu, S.M.; Li, J. Biochar-based nano-composites for the decontamination of wastewater: A review. Bioresour. Technol. 2016, 212, 318-333. https://doi.org/10.1016/j.biortech.2016.04.093.
50. Plisko, T.V.; Liubimova, A.S.; Bildyukevich, A.V.; Penkova, A.V.; Dmitrenko, M.E.; Mikhailovskii, V.Y.; Melnikova, G.B.; Semenov, K.N.; Doroshkevich, N.V.; Kuzminova, A.I. Fabrication and characterization of polyamide-fullerenol thin film nanocomposite hollow fiber membranes with enhanced antifouling performance. J. Memb. Sci. 2018, 551, 20-36. https://doi.org/10.1016/j.memsci.2018.01.015.
51. Dmitrenko, M.; Penkova, A.; Kuzminova, A.; Atta, R.; Zolotarev, A.; Mazur, A.; Vezo, O.; Lahderanta, E.; Markelov, D.; Ermakov, S. Development and investigation of novel polyphenylene isophthalamide pervaporation membranes modified with various fullerene derivatives. Sep. Purif. Technol. 2019, 226, 241-251. https://doi.org/10.1016/j.seppur.2019.05.092.
52. Kausar, A.; Ahmad, I.; Maaza, M.; Eisa, M.H. State-of-the-Art of Polymer/Fullerene C60 Nanocomposite Membranes for Water Treatment: Conceptions, Structural Diversity and Topographies. Membranes 2023, 13, 27. https://doi.org/10.3390/membranes13010027.
53. Penkova, A.V.; Dmitrenko, M.E.; Sokolova, M.P.; Chen, B.; Plisko, T.V.; Markelov, D.A.; Ermakov, S.S. Impact of fullerene loading on the structure and transport properties of polysulfone mixed-matrix membranes. J. Mater. Sci. 2016, 51, 7652-7659. DOI 10.1007/s10853-016-0047-9.
54. Ranjbar, T.; Akbarzadeh, H.; Esmat Mehrjouei, E.; Abbaspour, M.; Salemi, S.; Yaghoubi, H. Molecular insight into C60-grafted graphene oxide as a novel reverse osmosis membrane with low energy consumption for seawater desalination. Desalination 2022, 542, 116062. https://doi.org/10.1016/j.desal.2022.116062.
55. Liu, Y.; Phillips, B.; Li, Wei.; Zhang, Z.; Fang, L.; Qiu, J.; Wang, S. Fullerene-Tailored Graphene Oxide Interlayer Spacing for Energy-Efficient Water Desalination, ACS Appl. Nano Mater. 2018, 1(11), 6168-6175, https://doi.org/10.1021/acsanm.8b01375.
56. Liu, Q.; Guo, C.; Yang, Z.; Yao, H.; Hu, J.; Liu, G.; Jin, W. Enabling efficient water desalination and mitigating membrane fouling by the novel two-dimensional fullerene with unlocking its electrostatic forces. J. Memb. Sci. 22023, 687, 122074, https://doi.org/10.1016/j.memsci.2023.122074.
57. Jani, M.; Arcos-Pareja, J.A.; Ni, M. Engineered Zero-Dimensional Fullerene/Carbon Dots-Polymer Based Nanocomposite Membranes for Wastewater Treatment. Molecules 2020, 25, 4934. https://doi.org/10.3390/molecules25214934.
58. Rabenau, T.; Simon, A.; Kremer, R.K.; Sohmen, E. The energy gaps of fullerene C60 and C70 determined from the temperature dependent microwave conductivity. Z. Phys. B:Condens. Matter. 1993, 90, 69-72. https://doi.org/10.1007/BF01321034.
59. Pan, Y.; Liu, X.; Zhang, W.; Liu, Z.; Zeng, G.; Shao, B.; Liang, Q.; He, Q.; Yuan, X.; Huang, D.; Chen, M. Advances in photocatalysis based on fullerene C60 and its derivatives: Properties, mechanism, synthesis, and applications. Appl. Catal. B: Environ. 2020, 265, 118579, https://doi.org/10.1016/j.apcatb.2019.118579.
60. Peng, B. Monolayer Fullerene Networks as Photocatalysts for Overall Water Splitting, J. Am. Chem. Soc. 2022, 144(43), 19921-9931. https://doi.org/10.1021/jacs.2c08054.

 doi:10.20944/preprints202510.0466.v1

61. Krishnan, A.; Swarnalal, A.; Das, D.; Krishnan, M.; Saji, V.S.; Shibli, S.M.A. A review on transition metal oxides based photocatalysts for degradation of synthetic organic pollutants. J. Environ. Sci. 2024, 139, 389-417. https://doi.org/10.1016/j.jes.2023.02.051.
62. Yao, S.; Yuan, X.; Jiang, L.; Xiong, T.; Zhang, J. Recent Progress on Fullerene-Based Materials: Synthesis, Properties, Modifications, and Photocatalytic Applications. Materials 2020, 13(13), 2924. https://doi.org/10.3390/ma13132924.
63. Chronopoulos, D.D.; Otyepka, M.; Kokotos, C.G. Photochemical Carbocatalysis: Fullerene-, Carbon Nanotube- or Graphene-Based Metal-Free Photocatalysts for Organic Transformations. ChemCatChem 2024, 16(14), e202400042. https://doi.org/10.1002/cctc.202400042.
64. Othman, Z.; Sinopoli, A.; Mackey, HR.; Mahmoud, K.A. Efficient Photocatalytic Degradation of Organic Dyes by AgNPs/TiO_2/$Ti_3C_2T_x$ MXene Composites under UV and Solar Light. ACS Omega 2021, 6(49), 33325-33338, https://doi.org/10.1021/acsomega.1c03189.
65. Lee, S.Y.; Kang, D.; Jeong, S.; Do, H.T.; Kim, J.H. Photocatalytic Degradation of Rhodamine B Dye by TiO_2 and Gold Nanoparticles Supported on a Floating Porous Polydimethylsiloxane Sponge under Ultraviolet and Visible Light Irradiation, ACS Omega 2020, 5(8), 4233-4241. https://doi.org/10.1021/acsomega.9b04127.
66. Zhang, X.; Wang, Q.; Zou, L-H.; You, Z-W. Facile fabrication of titanium dioxide/fullerene nanocomposite and its enhanced visible photocatalytic activity, J. Colloid Interface Sci. 2016, 466, 56-61, https://doi.org/10.1016/j.jcis.2015.12.013.
67. Lim, J.; Monllor-Satoca, D.; Jang, J.S.; Lee, S.; Choi, W. Visible light photocatalysis of fullerol-complexed TiO_2 enhanced by Nb doping. Appl. Catal. B 2014(152-153), 233-240. https://doi.org/10.1016/j.apcatb.2014.01.026.
68. Krishna, V.; Noguchi, N.; Koopman, B.; Moudgil, B. Enhancement of titanium dioxide photocatalysis by water-soluble fullerenes. J. Colloid Interface Sci. 2006, 304(1), 166-171. https://doi.org/10.1016/j.jcis.2006.08.041.
69. Youssef, Z.; Colombeau, L.; Yesmurzayeva, N.; Baros, F.; Vanderesse, R.; Hamieh, T.; Toufaily, J.; Frochot, C.; Roques-Carmes, T.; Acherar, S. Dye-sensitized nanoparticles for heterogeneous photocatalysis: Cases studies with TiO_2, ZnO, fullerene and graphene for water purification, Dyes and Pigments, 2018, 159, 49-71. https://doi.org/10.1016/j.dyepig.2018.06.002.
70. Fu,H.; Xu,T.; Zhu,S.;†Zhu,Y. Photocorrosion Inhibition and Enhancement of Photocatalytic Activity for ZnO via Hybridization with C60, Environ. Sci. Technol. 2008, 42(21), 8064-8069. https://doi.org/10.1021/es801484x.
71. Behera, A.; Mansingh, S.; Das, K.K.; Parida, K. Synergistic $ZnFe_2O_4$-carbon allotropes nanocomposite photocatalyst for norfloxacin degradation and Cr (VI) reduction. J. Colloid Interface Sci. 2019, 544, 96-111. https://doi.org/10.1016/j.jcis.2019.02.056.
72. Tahir, M.B.; Nabi, G.; Rafique, M.; Khalid, NR. Role of fullerene to improve the WO_3 performance for photocatalytic applications and hydrogen evolution. Int J Energy Res. 2018, 42(15), 4783-4789. https://doi.org/10.1002/er.4231.
73. Parambil, A.M.; Rajan, S.; Huang, P.-C.; Shashikumar, U.; Tsai, P.-C.; Rajamani, P.; Lin, Y.-C.; Ponnusamy, V.K. Carbon and Graphene Quantum Dots Based Architectonics for Efficient Aqueous Decontamination by Adsorption Chromatography Technique - Current State and Prospects. Environ. Res. 2024, 251(Part 1), 118541. https://doi.org/10.1016/j.envres.2024.118541.
74. Das, G.S.; Shim, J.P.; Bhatnagar, A.; Tripathi, K.M.; Kim, T.Y. Biomass-Derived Carbon Quantum Dots for Visible-Light-Induced Photocatalysis and Label-Free Detection of Fe(III) and Ascorbic Acid. Sci. Rep. 2019, 9, 15084. https://doi.org/10.1038/s41598-019-49266-y.

 doi:10.20944/preprints202510.0466.v1

75. Gorle, G.; Gollavelli, G.; Nelli, G.; Ling, Y.-C. Green Synthesis of Blue-Emitting Graphene Oxide Quantum Dots for In Vitro CT26 and In Vivo Zebrafish Nano-Imaging as Diagnostic Probes. Pharmaceutics 2023, 15(2), 632. https://doi.org/10.3390/pharmaceutics15020632.
76. Zulfajri, M.; Gedda, G.; Ulla, H.; Habibati.; Gollavelli, G.; Huang, G.G. A review on the chemical and biological sensing applications of silver/carbon dots nanocomposites with their interaction mechanisms. Advances in Colloid and Interface Science, 2024, 325, 103115. https://doi.org/10.1016/j.cis.2024.103115.
77. Bhattacharjee, T.; Konwar, A.; Boruah, J.S.; Chowdhury, D.; Majumdar, G. A sustainable approach for heavy metal remediation from water using carbon dot based composites: A review, J HAZARD MATER ADV, 2023, 10, 100295. https://doi.org/10.1016/j.hazadv.2023.100295.
78. Hussen, N.H. Hasan, H.; Khedr, Y,M.F.; Bogoyavlenskiy, A.; Bhat, A.R,; Jamalis, J. Carbon Dot Based Carbon Nanoparticles as Potent Antimicrobial, Antiviral, and Anticancer Agents, ACS Omega 2024, 9(9), 9849-9864. https://doi.org/10.1021/acsomega.3c05537.
79. Sabet, M.; Mahdavi, K. Green synthesis of high photoluminescence nitrogen-doped carbon quantum dots from grass via a simple hydrothermal method for removing organic and inorganic water pollutions, Appl. Surf. Sci. 2019, 463, 283-291. https://doi.org/10.1016/j.apsusc.2018.08.223.
80. Rani, U.A.; Ng, L.Y.; Ng, C.Y.; Mahmoudi, E. A review of carbon quantum dots and their applications in wastewater treatment, Adv. Colloid and Interface Sci. 2020, 278, 102124. https://doi.org/10.1016/j.cis.2020.102124.
81. Mahmoud, M.E.; Fekry, N.A.; Abdelfattah, A.M. Removal of uranium (VI) from water by the action of microwave-rapid green synthesized carbon quantum dots from starch-water system and supported onto polymeric matrix, J. Hazard. Mater. 2020, 397, 122770. https://doi.org/10.1016/j.jhazmat.2020.122770.
82. Meng, Y.; Xiao, L.; Muslim, A. Hojiahmat, M. Improving the adsorption of poly(o-phenylenediamine) to heavy metal ions in aqueous solution through its composite with carbon dots. J Polym Res 2021, 28, 404. https://doi.org/10.1007/s10965-021-02739-z.
83. Perumal, S.; Atchudan, R.; Thirukumaran, P.; Dong Ho Yoon, D.H.; Yong Rok Lee, Y.R. In Woo Cheong, Simultaneous removal of heavy metal ions using carbon dots-doped hydrogel particles, Chemosphere 2022, 286, 131760. https://doi.org/10.1016/j.chemosphere.2021.131760.
84. Li, J.; Wang, L.; Jiang, G.; Wan, Y.; Wang, J.; Li, Y.; Pi, F. Luminescent carbon dots-rooted polysaccharide crosslinked hydrogel adsorbent for sensitive determination and efficient removal of Cu^{2+}. Food Chemistry, 447, 2024, 138977. https://doi.org/10.1016/j.foodchem.2024.138977.
85. Li, M.; Zhang, P.; Mao, J .; Li, J.; Zhang, Y.; Xu, B.; Zhou, J.; Cao, Q.; Xiao, H. Construction of cellulose-based hybrid hydrogel beads containing carbon dots and their high performance in the adsorption and detection of mercury ions in water. J. Environ. Manage. 2024, 359, 121076. https://doi.org/10.1016/j.jenvman..121076.
86. Wei, T.; Ni, H.; Ren, X.; Zhou, W.; Gao, H.; Hu, S. Fabrication of nitrogen-doped carbon dots biomass composite hydrogel for adsorption of Cu (II) in wastewater or soil and DFT simulation for adsorption mechanism. Chemosphere 2024, 361, 142432. https://doi.org/10.1016/j.
87. You, X-Y.; Yin, W-M.; Wang, Y.; Wang, C.; Zheng, W-X.; Guo, Y -R.; Li, S.; Pan, Q-J. Enrichment and immobilization of heavy metal ions from wastewater by nanocellulose/carbon dots-derived composite. Int. J. Bio. Macromol. 2024, 255, 128274. https://doi.org/10.1016/j.ijbiomac.2023.128274.
88. Thakur, A.; Kumar, A.; Ambrish Singh, A. Adsorptive removal of heavy metals, dyes, and pharmaceuticals: Carbon-based nanomaterials in focus. Carbon, 2024, 217, 118621. https://doi.org/10.1016/j.carbon.2023.118621.

 doi:10.20944/preprints202510.0466.v1

89. Mahmoud, M.E.; Fekry, N.A.; Abdelfattah, A.M. Engineering nanocomposite of graphene quantum dots/carbon foam/alginate/zinc oxide beads for efficacious removal of lead and methylene, J. Ind. Eng. Chem. 2022, 115, 365-377. https://doi.org/10.1016/j.jiec.2022.08.020.
90. Parambil, A.M.; Rajan, S.; Huang, P-C.; Shashikumar, U.; Tsai, P-C.; Rajamani, P.; Lin, Y-C.; Ponnusamy, V.K.; Carbon and graphene quantum dots based architectonics for efficient aqueous decontamination by adsorption chromatography technique - Current state and prospects, Environ. Res. 2024, 251(Part 1), 118541. https://doi.org/10.1016/j.envres.2024.118541.
91. Fiorentini, E.F.; Rodríguez,E.M.V.; Bonilla-Petriciolet, A.; Escudero, L.B. Carbon Dots in Organic Pollutant Removal, Carbon Dots: Recent Developments and Future Perspectives, Chapter 12, pp 259-275. ACS Symposium Series Vol. 1465, eISBN: 9780841296992, DOI: 10.1021/bk-2024-1465.ch012.
92. Manikandan, V.; Lee, N.Y. Green synthesis of carbon quantum dots and their environmental applications, Environ Res. 2022, 212(Pt B), 113283. https://doi.org/10.1016/j.envres.2022.113283.
93. Waseem, B,Z.; Muniraj, S.; Kumar, A.S. Neem biomass derived carbon quantum dots synthesized via one step ultrasonification method for ecofriendly methylene blue dye removal. Sci Rep 2024, 14, 9706. https://doi.org/10.1038/s41598-024-59483-9.
94. Lu, S.; Yuan, G.; Zhu, Y.; Yu, S. Carbon dots crosslinked chitosan/cellulose sponge capture of methyl blue by an adsorption process, Luminescence 2021, 36(6), 1459. https://doi.org/10.1002/bio.4089.
95. Hashemzadeh, F.; Khoshmardan, M.E.; Sanaei, D.; Ghalhari, M.R.; Sharifan, H.; Inglezakis, V.J.; Arcibar-Orozco, J.A.; Shaikh, W.A.; Khan, E.; Biswas, J.K. Adsorptive removal of anthracene from water by biochar derived amphiphilic carbon dots decorated with chitosan, Chemosphere 352, 2024, 141248. https://doi.org/10.1016/j.
96. Yu, S.; S. Lu, S.; Zheng, G. Reusable flexible poly(vinyl alcohol)/chitosan-based polymer carbon dots composite film for acid blue 93 dye adsorption, Luminescence 2023, 38(9), 1552. https://doi.org/10.1002/bio.4543.
97. Teymoorian, T.; Hashemi, N.; Mousazadeh, M.H. Entezarian, Z. N. S doped carbon quantum dots inside mesoporous silica for effective adsorption of methylene blue dye. SN Appl. Sci. 2021, 3, 305. https://doi.org/10.1007/s42452-021-04287-z.
98. Gallareta-Olivares, G.; Rivas-Sanchez, A.; Cruz-Cruz, A.; Hussain, S.M.; González-González, R.B.; Cárdenas-Alcaide, M.F.; Iqbal, H.M.N.; Parra-Saldívar, R. Metal-doped carbon dots as robust nanomaterials for the monitoring and degradation of water pollutants. Chemosphere 2023, 312(Part 1), 137190. https://doi.org/10.1016/j.chemosphere.2022.137190.
99. Parambil, A.M.; Priyadarshini, E.; Goutam, R.; Tsai, P-C.; Huang, P-C.; Rajamani, P.; Lin, Y-C.; Ponnusamy, V.K. Self-assembled mesoporous silica decorated with biogenic carbon dot nanospheres hybrid nanomaterial for efficient removal of aqueous Methoxy-DDT via a Short-Bed Adsorption column technique. Environ Res. 2024, 260, 119653. https://doi.org/10.1016/j.envres.2024.119653.
100. Huang, T-Y.; Lin, Y-F.; Hu, S-R.; Huang, C-C.; Huang, Y-F. Chang H-T. Carbon-dot liposome–based synthesis of gold nanocatalysts for efficient reduction of 4-nitrophenol in wastewater. SUSTAIN MATER TECHNO. 2024, 40, e00896, https://doi.org/10.1016/j.susmat.2024.e00896.
101. Nguyen, M.B.; Doan, H.V.; Tan, D.L.H.; Lam, T .D. Advanced g-C_3N_4 and bimetallic FeNi-BTC integration with carbon quantum dots for removal of microplastics and antibiotics in aqueous environments. J. Environ. Chem. Eng. 2024, 12, 112965, https://doi.org/10.1016/j.jece.2024.112965.
102. Wang, W-R.; Chen, P-Y.; Deng, J.; Chen, Y.; Liu, H-J. Carbon-dot hydrogels as superior carbonaceous adsorbents for removing perfluorooctane sulfonate from water, J. Chem. Eng. 2022, 435, Part 2, 13502. https://doi.org/10.1016/j.cej.2022.135021.

 doi:10.20944/preprints202510.0466.v1

103. Hellal, A.; Abdelsalam, H.; Tawfik, W. Ibrahim. M.A. Removal of Atrazine from contaminated water by functionalized graphene quantum dots. Opt Quant Electron 2024, 56, 374. https://doi.org/10.1007/s11082-023-05909-z.
104. Kausar, A.; Ahmad, I. Graphene quantum dots—Nascent adsorbent nanomaterials for water treatment, Environ Nanotechnol Monit Manag 2024, 21, 100943, https://doi.org/10.1016/j.enmm.2024.100943.
105. Oves, M.; Ansari, M.O.; Iqbal M.I.; Ismail. Graphene quantum dot application in water purification, Editor(s): Mohammad Oves, Khalid Umar, Iqbal M.I. Ismail, Mohamad Nasir Mohamad Ibrahim, In Woodhead Publishing Series in Electronic and Optical Materials, Graphene Quantum Dots, Woodhead Publishing, 2023, 113-132, https://doi.org/10.1016/B978-0-323-85721-5.00012-1.
106. Wee, S. . -h.; Tye, C. -T., T.; Bhatia, S. Membrane separation process—Pervaporation through zeolite membrane, Sep. Purif. Technol. 2008, 63(3), 500-516. https://doi.org/10.1016/j.seppur.2008.07.010.
107. Ezugbe, E.O.; Rathilal, S. Membrane Technologies in Wastewater Treatment: A Review. *Membranes* 2020, *10*(5), 89. https://doi: 10.3390/membranes10050089.
108. Khraisheh, M.; Elhenawy, S.; AlMomani, F.; Al-Ghouti, M.; Hassan, MK.; Hameed, BH. Recent Progress on Nanomaterial-Based Membranes for Water Treatment. Membranes 2021, 11(12), 995; https://doi.org/10.3390/membranes11120995
109. Petukhov, D.I.; Johnson, D.J. Membrane modification with carbon nanomaterials for fouling mitigation: A review. Adv. Colloid Interface Sci. 2024, 327, 103140, https://doi.org/10.1016/j.cis.2024.103140.
110. Chadha, U.; Selvaraj, S.K.; Thanu, S.V.; Cholapadath, V.; Abraham, A.M.; Zaiyan M,M.; Manoharan, M.; Paramsivam, V. A review of the function of using carbon nanomaterials in membrane filtration for contaminant removal from wastewater. Mater. Res. Express 2022, 9, 012003 https://doi.org/10.1088/2053-1591/ac48b8.
111. Yuan, Z.; Wu, X.; Jiang, Y.; Li, Y.; Huang, J.; Hao, L.; Zhang,J .; Wang, J. Carbon dots-incorporated composite membrane towards enhanced organic solvent nanofiltration performance. J. Membr. Sci. 2018, 549, 1-11. https://doi.org/10.1016/j.memsci.2017.11.051.
112. Koulivand, H.; Shahbazi, A.; Vatanpour, V.; Rahmandoust, M. Development of carbon dot-modified polyethersulfone membranes for enhancement of nanofiltration, permeation and antifouling performance. Sep. Purif. Technol. 2020, 230, 115895. https://doi.org/10.1016/j.seppur.2019.115895.
113. Zhao, H.; Zhang, D.; Sun, H.; Zhao, Y.; Xie, M. Adsorption and detection of heavy metals from aqueous water by PVDF/ATP-CDs composite membrane. Colloids Surf. A: Physicochem. Eng. Asp. 2022, 641, 128573. https://doi.org/10.1016/j.colsurfa.2022.128573.
114. Carballo, G.V.; Hsu, Y.X.; Yang, H.L.; Lin, H.Y.; Huang, C. C.; Li, C.L.; Leron, R.B.; Tsai, H. A.; Lee, K.R. Novel in-situ zwitterionization of carbon quantum dots on membrane surface for oil/water separation. Sep. Purif. Technol. 2024, 348, 127757. https://doi.org/10.1016/j.seppur.2024.127757.
115. Yang, H.L.; Huang, C.T.; Lin, H.Y.; Chen, Y.H.; Tsai, H.A.; Lee, K.R. Zwitterionic carbon quantum dots incorporated ultrafiltration membrane for efficient removal of copper ion. Sep. Purif. Technol. 2024, 331, 125709. https://doi.org/10.1016/j.seppur.2023.125709.
116. Mahat, N.A.; Shamsudin, S.A.; Jullok, N.; Ma'Radzi, A.H. Carbon quantum dots embedded polysulfone membranes for antibacterial performance in the process of forward osmosis, Desalination 2020, 493, 114618, https://doi.org/10.1016/j.desal.2020.114618.
117. Gan, J.Y.; Chong, W.C.; Sim, L.C.; Koo, C.H.; Pang, Y.L.; Mahmoudi, E.; Mohammad, A.W. Novel Carbon Quantum Dots/Silver Blended Polysulfone Membrane with Improved Properties and Enhanced Performance in Tartrazine Dye Removal. Membranes 2020, 10, 175. https://doi.org/10.3390/membranes10080175.

 doi:10.20944/preprints202510.0466.v1

118. Viscusi, G.; Mottola, S.; Tohamy, HA.S.; Gorrasi, G.; De Marco, I. Design of Cellulose Acetate Electrospun Membranes Loaded with N-doped Carbon Quantum Dots for Water Remediation. In: Mannina, G., Ng, H.Y. (eds) Frontiers in Membrane Technology. IWA-RMTC 2024. Lecture Notes in Civil Engineering, vol 525. Springer, Cham. https://doi.org/10.1007/978-3-031-63357-7_22.
119. Tshangana, C.; Muleja, A. Graphene oxide quantum dots membrane: a hybrid filtration-advanced technology system to enhance process of wastewater reclamation. Chem. Pap. 78, 2024, 1317-1333. https://doi.org/10.1007/s11696-023-03187-3.
120. Zhang, C.; Wei, K.; Zhang, W.; Bai, Y.; Sun, Y.; Gu. J. Graphene Oxide Quantum Dots Incorporated into a Thin Film Nanocomposite Membrane with High Flux and Antifouling Properties for Low-Pressure Nanofiltration. *ACS Appl. Mater. Interfaces* 2017, 9(12), 11082–11094. https://pubs.acs.org/doi/abs/10.1021/acsami.6b12826.
121. Li, J.; Gong, J.L.; Si Qun Tang, S.Q.; Zhou, H.Y.; Liang Xiu Tang, L.X.; Zhao, J. Efficient decolorization performance of graphene quantum dots modulated nanofiltration membranes with tunable pore size for precise molecular sieving, Desalination 2024, 583, 117666, https://doi.org/10.1016/j.desal.2024.117666.
122. Yi-Fang, M.; Yi-Han, H.; Shu-Heng, H.; Ma, R.; Yi-Ding, M.; Zhi-Hai ,C. Simultaneous regulation of pore size and surface charge of nanofiltration membrane using carbon quantum dots for improved selective separation. Sep. Purif. Technol. 2023, 317, 123870. https://doi.org/10.1016/j.seppur.2023.123870.
123. Zahmatkesh, S.; Bing-Jie, Ni.; Klemeš, J.J.; Bokhari, A.; Hajiaghaei-Keshteli, M. Carbon quantum dots-Ag nanoparticle membrane for preventing emerging contaminants in oil produced water. J. Water Process Eng. 2022, 50, 103309, https://doi.org/10.1016/j.jwpe.2022.103309.
124. Jani, M.; Arcos-Pareja, J.A.; Ni, M. Engineered Zero-Dimensional Fullerene/Carbon Dots-Polymer Based Nanocomposite Membranes for Wastewater Treatment. Molecules 2020, 25, 4934. https://doi.org/10.3390/molecules25214934.
125. Anand, A.; Unnikrishnan, B.; Ju-Yi Mao, Chin-Jung, Lin.; Jui-Yang, Lai.; Chih-Ching ,H,. Carbon-based low-pressure filtration membrane for the dynamic disruption of bacteria from contaminated water. Water Res. 2022, 212, 118121. https://doi.org/10.1016/j.watres.2022.118121.
126. Ge, J.; Lian, L.; Wang, X.; Cao, X.; Gao, W.; Lou, D. Coating layered double hydroxides with carbon dots for highly efficient removal of multiple dyes. J. Hazard. Mater. 2022, 424, 127613, https://doi.org/10.1016/j.jhazmat.2021.127613.
127. Saini, D.; Garg, A.K.; Dalal, C.; Anand, S.R.; Sonkar, S.K.; Sonker, A.K.; Westman, G. Visible-Light-Promoted Photocatalytic Applications of Carbon Dots: A Review. ACS Appl. Nano Mater. 2022, 5, 3087-3109. https://doi.org/10.1021/acsanm.1c04142.
128. Ikram, Z.; Azmat, E.; Perviaz, M. Degradation Efficiency of Organic Dyes on CQDs As Photocatalysts: A Review, ACS Omega. ACS Omega. 2024, 9(9), 10017-10029. https://doi.org/10.1021/acsomega.3c09547.
129. Saputra, M.A.; Piliang, A.F.R.; Dellyansyah.; Marpongahtun.; Andriayani.; Goei, R.; Ramadhan H.T.S. R.; Gea, S. Synthesis, properties, and utilization of carbon quantum dots as photocatalysts on degradation of organic dyes: A mini review. Catal. Commun. 2024, 187, 106914. https://doi.org/10.1016/j.catcom.2024.106914.
130. Sbacchi, M.; Mamone, M.; Morbiato,L.; Gobbo, P.; Filippini,G.; Prato, M. Shining Light on Carbon Dots: New Opportunities in Photocatalysis, ChemCatChem 2023, 15, e202300667.
131. Tripti, T.; Singh, P.; Rani, N. *et al*. Carbon dots as potential candidate for photocatalytic treatment of dye wastewater. Environ Sci Pollut Res Int. 2024, 31, 6738-6765. https://doi.org/10.1007/s11356-023-31437-0.

 doi:10.20944/preprints202510.0466.v1

132. Zhao, F.; Li, X.; Zuo, M.; Liang, Y.; Qin, P.; Wang, H.; Wu ,Z.; Luo, L.; Liu, C.; Leng, L. Preparation of photocatalysts decorated by carbon quantum dots (CQDs) and their applications: A review. J. Environ. Chem. Eng. 2023, 11(2), 109487. https://doi.org/10.1016/j.jece.2023.109487.
133. Nizam, N.U.M.; Hanafiah, M.M.; Mahmoudi, E. et al. Synthesis of highly fluorescent carbon quantum dots from rubber seed shells for the adsorption and photocatalytic degradation of dyes. Sci Rep 2023, 13, 12777. https://doi.org/10.1038/s41598-023-40069-w.
134. Meena, S.; Sethi, M.; Saini, S.; Kumar,K.; Saini, P.; Meena, S.; Kashyap, S.; Yadav, M.; Meena, M.L.; Dandia, A.; Nirmal, N.K.; Parewa, V. Molecular surface-dependent light harvesting and photo charge separation in plant-derived carbon quantum dots for visible-light-driven OH radical generation for remediation of aromatic hydrocarbon pollutants and real wastewater. J. Colloid Interface Sci. . 2024, 660, 756-770, https://doi.org/10.1016/j.jcis.2024.01.079.
135. Zandipak, R.; Bahramifar, N.; Younesi, H.; Zolfigol, M.A. Electro-photocatalyst effect of N-S-doped carbon dots and covalent organic triazine framework heterostructures for boosting photocatalytic degradation of phenanthrene in water. Chemosphere 2024, 364, 142980. https://doi.org/10.1016/j.chemosphere.2024.142980.
136. Bhoyar, T.; Saraswat, N.; Jyothirmai, M.V.; Gupta, A.; Malla, S.K.; Park, J.; Vidyasagar, D.; Umare, S.S. Nitrogen-Doped Graphitic Carbon Dots Embedded in Carbon Nitride Scaffolds for Water Decontaminatio.. ACS Appl. Nano Mater. 2023, 6(5). 3484-3496. https://doi.org/10.1021/acsanm.2c05239.
137. Silva, V.; Louros, V.L.; Silva, C.P.; Tacão, M.; Otero, M.; Calisto, V.; Lima, D.L.D. A solar flow photo-reactor for antibiotic removal from aquaculture effluents using TiO_2/carbon quantum dots. Chemosphere 2024, 348, 140723, https://doi.org/10.1016/j.chemosphere.2023.140723.
138. Choi, N.; Tang, C.; Park, Y.; Du, A.; Ayoko, G.A.; Hwang, Y.; Chae, S. Visible-light-driven photocatalytic degradation of tetracycline using citric acid and lemon juice-derived carbon quantum dots incorporated TiO_2 nanocomposites. Sep. Purif. Technol. 2024, 350, 127836. https://doi.org/10.1016/j.seppur.2024.127836.
139. Shafiee, A.; Andrew J.; Carrier, A.J.; Nganou, C.; Ehsan, M.F.; Aibaghi, B.; Oakes, K.D.; Zhang, X. Mechanistic insight into the enhanced photodegradation by black titanium dioxide nanofiber-graphene quantum dot composites. Appl. Surf. Sci. 2023, 636, 157836. https://doi.org/10.1016/j.apsusc.2023.157836.
140. Shiwei. Xu.; S.. Zhang.; M. Guo.; B. Liu.; Y. Zhang. Electrostatic Attraction Enables Strong Interaction between TiO_2 and Colloidal Carbon Quantum Dots for Efficient Visible Light Photocatalytic Degradation of Antibiotics. http://dx.doi.org/10.2139/ssrn.4855268.
141. Xu, Z.; Ma, R.; Zhang, C.; Chen, J .; Fan, J.; Shi, Q. A novel quaternary ammonium structure of carbon dots modified TiO_2 for fast reduction of Cr(VI) over a wide pH range under sunlight. J. Chem. Eng. 2024, 489, 151363. https://doi.org/10.1016/j.cej.2024.151363.
142. Shalini, S.; Sasikala, T.; Tharani, D.; Venkatesh, R.; Muthulingam, S. Novel green CQDs/ZnO binary photocatalyst synthesis for efficient visible light irradiation of organic dye degradation for environmental remediation. J. Mol. Liq. 2024, 410, 125525. https://doi.org/10.1016/j.molliq.2024.125525.
143. Kamel, G.N.; El-Shaheny, R.; Shabana, R.A.; Hassan, A.H.E. Inherent photocatalytic activity of luminescent multi-doped carbon dots manufactured from expired medicine and its application for efficient water remediation and nanosensing. Microchem J. 2024, 201, 110576. https://doi.org/10.1016/j.microc.2024.110576.
144. Rani, U.A.; Ng, L.Y.; Ng, C.Y.; Mahmoudi, E.; Yee-Sern, Ng.; Mohammad, A.W. Sustainable production of nitrogen-doped carbon quantum dots for photocatalytic degradation of methylene blue and malachite green. J. Water Process Eng. 2021, 40, 101816. https://doi.org/10.1016/j.jwpe.2020.101816.

 doi:10.20944/preprints202510.0466.v1

145. Torsello. M.; Ben-Zichri. S.; Pesenti. L.; *et al*. Carbon Dot/Polylactic Acid Nanofibrous Membranes for Solar-Mediated Oil Absorption/Separation: Performance, Environmental Sustainability, Ecotoxicity and Reusability. Heliyon 2024, 10(4), , e25417. https://doi.org/10.1016/j.heliyon.2024.e25417.
146. Kausar, A. Carbonaceous nanofillers in polymer matrix, Editor(s): Kausar, A. In Woodhead Publishing Series in Composites Science and Engineering, Polymeric Nanocomposites with Carbonaceous Nanofillers for Aerospace Applications, Woodhead Publishing, 2023, 23-53, https://doi.org/10.1016/B978-0-323-99657-0.00009-0.
147. Mishra, Y.; Mishra, V.; Chattaraj, A.; Aljabali, A.A.A.; El-Tanani, M.; Farani, M.R.; Huh, Y.S.; Serrano-Aroca, A.; Murtaza , M.; Tambuwala. Carbon nanotube-wastewater treatment nexus: Where are we heading to? Environ. Res. 2023, 238, 117088. https://doi.org/10.1016/j.envres.2023.117088.
148. Yu, F.; Wu, Y.; Li, X.; Ma ,J. Kinetic and thermodynamic studies of toluene, ethylbenzene, and m-xylene adsorption from aqueous solutions onto KOH-activated multiwalled carbon nanotubes, J. Agric. Food Chem. 2012, 60, 12245-12253. https://doi.org/10.1021/jf304104z.
149. Baby , R.; Saifullah ,B.; Hussein ,MZ. Carbon Nanomaterials for the Treatment of Heavy Metal-Contaminated Water and Environmental Remediation. Nanoscale Res Lett. 2019, 14(1), 341. doi: 10.1186/s11671-019-3167-8.
150. Ogunsola, S.S.; Oladipo, M.E.; Oladoye, P.O.; Kadhom, M. Carbon nanotubes for sustainable environmental remediation: A critical and comprehensive review. Nano-Structures & Nano-Objects 2024, 37, 101099. https://doi.org/10.1016/j.nanoso.2024.101099.
151. Ma, J.; Yu, F.; Zhou, L.; Jin, L.; Yang, M.; Luan, J.; Tang, Y.; Fan, H.; Yuan, Z.; Chen, J. Enhanced adsorptive removal of methyl orange and methylene blue from aqueous solution by alkali-activated multiwalled carbon nanotubes. ACS Appl. Mater. Interfaces 2012, 4, 5749-5760. https://doi.org/10.1021/am301053m.
152. Rao, R.; Pint C, L.; Islam. A, E.; Weatherup, R.S.; Hofmann, S.; et al. Carbon Nanotubes and Related Nanomaterials: Critical Advances and Challenges for Synthesis toward Mainstream Commercial Applications. ACS Nano 2018, 12(12), 11756-11784. https://doi.org/10.1021/acsnano.8b06511.
153. Krishna, R.H.; Chandraprabha, M.N.; Samrat, K.; Murthy, T.P.K.; Manjunatha, C.; Kumar, S.G. Carbon nanotubes and graphene-based materials for adsorptive removal of metal ions – A review on surface functionalization and related adsorption mechanism. Appl. Surf. Sci. Adv. 2023, 16, 100431, https://doi.org/10.1016/j.apsadv.
154. Jiang, L.; Li, S.; Yu, H.; Zou, Z.; Hou, X.; Shen, F.; Li, C.; Yao, X. Amino and thiol modified magnetic multi-walled carbon nanotubes for the simultaneous removal of lead, zinc, and phenol from aqueous solutions. Appl. Surf. Sci. 2016, 369, 398-413, https://doi.org/10.1016/j.apsusc.2016.02.067.
155. Anitha, K.; Namsani, S.; Singh, J.K. Removal of Heavy Metal Ions Using a Functionalized Single-Walled Carbon Nanotube: A Molecular Dynamics Study. J. Phys. Chem. A 2015, 119(30) , 8349-8358. https://doi.org/10.1021/acs.jpca.5b03352.
156. Wang, H. J.; Zhou, A.L.; Peng, F.; Yu, H.; L.F. Chen. Adsorption characteristic of acidified carbon nanotubes for heavy metal Pb(II) in aqueous solution. Mater. Sci. Eng. A. 2007, 466, 201-206. doi:10.1016/j.msea.2007.02.097.
157. Kończy, k, J.; Żarska, S.; Ciesielski, W. Adsorptive removal of Pb(II) ions from aqueous solutions by multi-walled carbon nanotubes functionalised by selenophosphoryl groups: Kinetic, mechanism, and thermodynamic studies. Colloids Surf. A: Physicochem. Eng. Asp. 2019, 575, 271-282, https://doi.org/10.1016/j.colsurfa.2019.04.058.

 doi:10.20944/preprints202510.0466.v1

158. Gull, M., Hussain, S., Tariq, A. Khalid, Z.; Bibi, F.; Waseem, M. Organic and inorganic acids-functionalized CNTs for the adsorption of Cu^{2+} and Ni^{2+} ions from aqueous solution. Chem. Pap. 2023, 77, 6519-6531. https://doi.org/10.1007/s11696-023-02955-5.
159. Oliveira, A.R.; Correia, A.A.; Rasteiro, M.G. Heavy Metals Removal from Aqueous Solutions by Multiwall Carbon Nanotubes: Effect of MWCNTs Dispersion. Nanomaterials 2021, 11(8), 2082. https://doi: 10.3390/nano11082082.
160. Wang, Z.; Xu, W.; Jie, F. Zhao, Z.; Zhou, K.; Liu, H. The selective adsorption performance and mechanism of multiwall magnetic carbon nanotubes for heavy metals in wastewater. Sci Rep 2021, 11, 16878. https://doi.org/10.1038/s41598-021-96465-7.
161. Alkallas, F.H.; Alghamdi, S.M.; Alsubhe, E.; Albeydani, O.; Elsharkawy, W.B.; Mwafy, E.A. et al. Evaluation of synthesized MWCNTs-COO@Fe_3O_4 nanocomposite based on laser-assisted method for highly-efficient clean water. Mater. Chem. Phys. 2024, 316, 129093. https://doi.org/10.1016/j.matchemphys.2024.129093.
162. Tijani, J.O.; Abdulkareem, A.S.; Mustapha, S.; Ndamitso, M.M.; Bada, S.O.; Sagadevan, S. Polyethyleneglycol-polyhydroxylbutyrate functionalized carbon nanotubes for industrial electroplating wastewater treatment. Sep. Purif. Technol. 2024, 332, 125736. https://doi.org/10.1016/j.seppur.2023.125736.
163. Hoang, A.T.; Nižetić, S.; Cheng, C.K.; Luque, R.; Thomas, S.; Banh, T.L.; Pham, V.V.; Nguyen, X.P. Heavy metal removal by biomass-derived carbon nanotubes as a greener environmental remediation: A comprehensive review. Chemosphere, 287, 2022, 131959. https://doi.org/10.1016/j.chemosphere.2021.131959.
164. Al-Amrani, W.A.; Onaizi, S.A. Adsorptive removal of heavy metals from wastewater using emerging nanostructured materials: A state-of-the-art review. Sep. Purif. Technol. 2024, 343, 127018. https://doi.org/10.1016/j.seppur.2024.127018.
165. Bhasin, C.P.; Pathan, A.; Patel, R.V. An Evaluation of Carbon Nanotube-based and Activated Carbon-based Nanocomposites for Fluoride and Other Pollutant Removal from Water: A Review. Current Nanomaterials 2023, 9, 16-40. DOI:10.2174/2405461508666230221143138.
166. Sharma, M.; Dandautiya, R. Advancements in Nanotechnology for Heavy Metal Remediation in Wastewater Treatment: Challenges and Opportunities. e3s web of conferences 2024, 39, 01015. https://doi.org/10.1051/e3sconf/202450901015.
167. Zare, K.; Sadegh, H.; Shahryari-ghoshekandi, R.; Maazinejad, B.; Ali, V.; Tyagi, I. et al. Enhanced removal of toxic Congo red dye using multi walled carbon nano- tubes: kinetic, equilibrium studies and its comparison with other adsorbents. J Mol Liq 2015, 212, 266-271. https://doi.org/10.1016/j.molliq.2015.09.027.
168. Machado, F.M.; Bergmann, C.P.; Lima, E.C.; Royer, B.; de Souza, F. E.; Jauris, I. M. et al. Adsorption of reactive blue 4 dye from water solutions by carbon nanotubes: experiment and theory. Phys. Chem. Chem. Phys., 2012, 14, 11139-11153. https://doi. org/10.1039/c2cp41475a.
169. Mashkoor, F.; Nasar, A.; Inamuddin. Carbon nanotube-based adsorbents for the removal of dyes from waters: A review. Environ Chem Lett 2020, 18, 605-629. https://doi.org/10.1007/s10311-020-00970-6.
170. Dastgerdi, Z.H.; Meshkat, S.S.; Esrafili, M.D. Enhanced adsorptive removal of Indigo carmine dye performance by functionalized carbon nanotubes based adsorbents from aqueous solution: equilibrium, kinetic, and DFT study. J Nanostruct Chem 2019, 9, 323-334. https://doi.org/10.1007/s40097-019-00321-0.
171. Sadegh, H.; Ali, G.A.M.; Agarwal, S. Gupta, V.K. Surface Modification of MWCNTs with Carboxylic-to-Amine and Their Superb Adsorption Performance. Int J Environ Res 2019, 13, 523-531. https://doi.org/10.1007/s41742-019-00193-w.

 doi:10.20944/preprints202510.0466.v1

172. Hu, D.; Wan, X.; Li, X.; Liu, J.; Zhou, C. Synthesis of water-dispersible poly-l-lysine-functionalized magnetic Fe_3O_4-(GO-MWCNTs) nanocomposite hybrid with a large surface area for high-efficiency removal of tartrazine and Pb(II). Int. J. Biol. Macromol. 2017, 105, 1611-1621. https://doi.org/10.1016/j.ijbiomac.2017.03.010.
173. Chen, L.; Jiang, J.; Sheng, L. Removal of Bisphenol A from Water by Single-Walled Carbon Nanotubes Loaded with Iron Oxide Nanoparticles. Appl. Sci. 2024, 14, 3943. https://doi.org/10.3390/app14093943.
174. Alkallas, F. H.; Alghamdi, S. M.; Rashed, E. A.; Trabelsi, A.B.G.; Nafee, S.S.; Elsharkawy, W.B.; Alsubhe, E.; Alshreef, S.H.; Mostafa, A.M. Nanocomposite Fe_3O_4-MWCNTs based on femtosecond pulsed laser ablation for catalytic degradation, Diamond and Related Materials. 2023, 140, 110445. https://doi.org/10.1016/j.diamond.2023.110445.
175. Sayana, K.V.; Prajwal, K.; Deeksha, K.J.; Vishalakshi, B.; Vishwanath, T. Magnetized CNTs incorporated MBA cross-linked guar gum nano-composite for methylene blue dye removal. J. Appl. Polym. Sci. 2024, 141, e54868. https://doi.org/10.1002/app.54868.
176. Xiang, K.; Lu, W.; Wang, J.; Ma, P.; Xu, L. Aminated multi-walled carbon nanotubes doped magnetic flower-like $FeSe_2$ nanosheets towards efficient adsorption in acidic wastewater. J. Mol. Struct. 2024,1305, 137816. https://doi.org/10.1016/j.molstruc.2024.137816.
177. Costa, H.P.S.; Duarte, E.D.V.; da Silva, F.V.; da Silva, M.G.C.; Vieira, M.G.A. Green synthesis of carbon nanotubes functionalized with iron nanoparticles and coffee husk biomass for efficient removal of losartan and diclofenac: Adsorption kinetics and ANN modeling studies. Environ. Res. 2024, 251, 118733. https://doi.org/10.1016/j.envres.2024.118733.
178. Heloisa Pereira de Sá Costa.; Emanuele Dutra Valente Duarte.; Meuris Gurgel Carlos da Silva.; Melissa Gurgel Adeodato Vieira. Adsorption of diclofenac and losartan using multi-walled carbon nanotubes functionalized with iron nanoparticles via the green route: Equilibrium, thermodynamics, and machine learning studies. J. Water Process Eng. 2024, 58, 104923. https://doi.org/10.1016/j.jwpe.2024.104923.
179. Licona-Aguilar, A, I.; Torres-Huerta, A.M.; Domínguez-Crespo, M.A.; Negrete-Rodríguez, M.L.X.; Conde-Barajas, E. et al. Valorization of agroindustrial orange peel waste during the optimization of activated carbon–multiwalled carbon nanotubes–zinc oxide composites used in the removal of methylene blue in wastewater. J. Chem. Eng. 2024, 492, 152102. https://doi.org/10.1016/j.cej.2024.152102.
180. Aljeboree, A.M.; Hussein, S.A.; Jawad, M.A.; Alkaim, A.F. Hydrothermal synthesis of eco-friendly ZnO/CNT nanocomposite and efficient removal of Brilliant Green cationic dye. Results Chem. 2024, 7, 101364. https://doi.org/10.1016/j.rechem.2024.101364.
181. Eskandarian, L.; Arami, M.; Pajootan, E. Evaluation of Adsorption Characteristics of Multiwalled Carbon Nanotubes Modified by a Poly(propylene imine) Dendrimer in Single and Multiple Dye Solutions: Isotherms, Kinetics, and Thermodynamics, J. Chem. Eng. Data 2014, 59, 444-454, dx.doi.org/10.1021/je400913z. |
182. Radia, N.D.; Aljeboree, A.M.; Mhammed, A.A. Enhanced removal of crystal violet from aqueous solution using carrageenan hydrogel nanocomposite/MWCNTs. Inorg. Chem. Commun. 2024, 112803. https://doi.org/10.1016/j.inoche.2024.112803.
183. Grmasha, R.A.; Al-sareji, O.J.; Meiczinger, M.; Stenger-Kovács, C.; Al-Juboori, R.A.; Jakab, M. et al.K.S. A sustainable nano-hybrid system of laccase@M-MWCNTs for multifunctional PAHs and PhACs removal from water, wastewater, and lake water. Environ. Res. 2024, 246, 118097. https://doi.org/10.1016/j.envres.2024.118097.
184. Ezugbe, E,O.; Rathilal, S. Membrane Technologies in Wastewater Treatment: A Review. Membranes 2020, 10(5), 89. https://doi.org/10.3390/membranes10050089.

 doi:10.20944/preprints202510.0466.v1

185. Othman, N.H.; Alias, N.H.; Fuzil, N.S.; Marpani, F.; Shahruddin, M.Z.; Chew, C.M. et al. A Review on the Use of Membrane Technology Systems in Developing Countries. Membranes 2022, 12(1), 30. https://doi.org/10.3390/membranes12010030.
186. Barrejón, M.; Prato, M. Carbon Nanotube Membranes in Water Treatment Applications. Adv. Mater. Interfaces 2022, 9, 2101260. https://doi.org/10.1002/admi.202101260.
187. Ihsanullah, Carbon nanotube membranes for water purification: Developments, challenges, and prospects for the future. Sep. Purif. Technol. 2019, 209, 307-337. https://doi.org/10.1016/j.seppur.2018.07.043.
188. Membrane Preparation, Editor(s): Ian D. Wilson, Encyclopedia of Separation Science, Academic Press, 2000, Pages 1755-1764, https://doi.org/10.1016/B0-12-226770-2/05241-8.
189. Lee, B.; Baek, Y.; Lee, M.; Jeong, D.H., Yoon, J. *et al*. A carbon nanotube wall membrane for water treatment. Nat. Commun. 2015, 6, 7109. https://doi.org/10.1038/ncomms8109.
190. Arahman, N.; Rosnelly, C.M.; Aulia, M.P.; Haikal, R.D.; Yusni.; Ambarita, A.C. et al. Exploring the effect of CNTs and pluronic on characteristics and stability of polyethersulfone (PES) and polyvinylidene fluoride (PVDF) membranes. Case Stud. Chem. Environ. Eng. 2024, 10, 100777. https://doi.org/10.1016/j.cscee.2024.100777.
191. Ngoma, M.M.; Mathaba, M.; Moothi, K. Effect of carbon nanotubes loading and pressure on the performance of a polyethersulfone (PES)/carbon nanotubes (CNT) membrane. Sci Rep 2021, 11, 23805. https://doi.org/10.1038/s41598-021-03042-z.
192. Zhao, J.; Zeng, D.; Wang, Q.; Lin, Z.; Vogel, F.; Li, W.; Zhang, P. Effects of a dual functional filler, polyethersulfone-g-carboxymethyl chitosan@MWCNT, for enhanced antifouling and penetration performance of PES composite membranes. J. Environ. Manag. 2024, 365, 121611. https://doi.org/10.1016/j.jenvman.2024.121611.
193. Wang, Ruijia.; Liu, Hongxu.; Wang, Zicheng.; Zhao, Jingxuan.; Lv, Ziwei.; Qi, Yuchao. et al. Synergistic Interaction of Ionic Liquid Grafted Poly(vinylidene Fluoride) and Carbon Nanotubes to Construct Water Treatment Membranes with Multiple Separation Properties. Langmuir 2024, 40(23), 11903-11913. https://doi.org/10.1021/acs.langmuir.3c03913.
194. Macevele, L.E.; Moganedi, K.L.M.; Magadzu, T. Effects of Poly(Vinylidene Fluoride-co-Hexafluoropropylene) Nanocomposite Membrane on Reduction in Microbial Load and Heavy Metals in Surface Water Samples. J. Compos. Sci. 2024, 8, 119. https://doi.org/10.3390/jcs8040119.
195. Zhao, J.; Liu, H.; Zhao, Y.; Qi, Y.; Wang, R. et al. Construction of CS-SDAEM long-chain polysaccharide derivative on TA@CNTs coated PVDF membrane with effective oil-water emulsion purification and low contamination rate. Int. J. Biol. Macromol. 2024, 275, 134230. https://doi.org/10.1016/j.ijbiomac.2024.134230.
196. Zhang, Z.; Li, W.; Zhao, B.; Yang, X.; Zhao, C.; Wang, W. et al. Novel CNT/MXene composite membranes with superior electrocatalytic efficiency and durability for sustainable wastewater treatment. J. Chem. Eng. 2024, 495, 153605. https://doi.org/10.1016/j.cej.2024.153605.
197. Chen, J.; Liu, X.; Hong, S.; Mo, J.; Peng, J.; Su, T. et al. Polylactic acid/ zinc oxide decorated multi-wall carbon nanotubes fibrous membranes and their applications in oil-water separation. Colloids Surf. A: Physicochem. Eng. Asp. 2024, 692, 133837. https://doi.org/10.1016/j.colsurfa.2024.133837.
198. Golgoli, M.; Farahbakhsh, J.; Najafi, M.; Khiadani, M.; Johns, M.L.; Zargar, M. Resilient forward osmosis membranes against microplastics fouling enhanced by MWCNTs/UiO-66-NH2 hybrid nanoparticles. Chemosphere 2024, 359, 142180. https://doi.org/10.1016/j.chemosphere.2024.142180.
199. Yang, Y.; Cheng, Y.; Ling, S.; Wan, Y.; Xiong, Z.; Li, C. et al. Scalable, flexible, ultra-strong, free-standing papery all carbon nanotube membrane with excellent separation and antifouling properties. J. Chem. Eng. 2024, 490, 151750. https://doi.org/10.1016/j.cej.2024.151750.

 doi:10.20944/preprints202510.0466.v1

200. Jasim, H.K.; Al-Ridah, Z.A.; Naje, A.S. Graphene oxide–carbon nanotube composite membrane for enhanced removal of organic pollutants by forward osmosis. Desalin. Water Treat. 2024, 318, 100363. https://doi.org/10.1016/j.dwt.2024.100363.
201. Abumelha, H.M.; Pashameah, R.; Sari, A.A.A.; Bin-Ibrahim, S.F.; Alanazi, M.A.A.; Shah, R. et al. Remarkable photocatalytic activity of MWCs supported on PVF in recycling, solar and photodegradation processes for commercial dyes and real industrial wastewater. Opt. Mater. 2024, 150, 115319. https://doi.org/10.1016/j.optmat.2024.115319.
202. Hye-Jin, L.; Zhang, N.; Ganzoury. M.A.; Wu, Y.; de Lannoy, C-F. Simultaneous Dechlorination and Advanced Oxidation Using Electrically Conductive Carbon Nanotube Membranes. ACS Appl. Mater. Interfaces 2021, 13(29), 34084-34092. DOI: 10.1021/acsami.1c06137
203. Zhang, J.; Dai, M.; Zhang, S.; Dai, M.; Zhang, P.; Wang, S.; He, Z. (2022), Recent Progress on Carbon-Nanotube-Based Materials for Photocatalytic Applications: A Review. Sol. RRL, 6: 2200243. https://doi.org/10.1002/solr.202200243
204. Osorio-Aguilar, D.-M.; Saldarriaga-Noreña, H.-A.; Murillo-Tovar, M.-A.; Vergara-Sánchez, J.; Ramírez-Aparicio, J.; Magallón-Cacho, L.; García-Betancourt, M.-L. Adsorption and Photocatalytic Degradation of Methylene Blue in Carbon Nanotubes: A Review with Bibliometric Analysis. Catalysts 2023, 13, 1480. https://doi.org/10.3390/catal13121480
205. Mohapatra ,L.; Cheon, D.; Yoo ,SH. Carbon-Based Nanomaterials for Catalytic Wastewater Treatment: A Review. Molecules 2023, 28(4), 1805. https://doi.org/10.3390/molecules28041805.
206. Verma, P.; Ubaid, J.; Varadarajan, K.M.; Wardle, B.L.; Kumar, S. Synthesis and Characterization of Carbon Nanotube-Doped Thermoplastic Nanocomposites for the Additive Manufacturing of Self-Sensing Piezoresistive Materials. ACS Appl. Mater. Interfaces 2022, 14(6), 8361-8372. https://doi.org/10.1021/acsami.1c20491.
207. Hughes, K.J.; Iyer, K.A.; Bird, R.E.; Ivanov, J.; Banerjee, S.; Georges, Gilles.; Zhou, Q. A. Review of Carbon Nanotube Research and Development: Materials and Emerging Applications, ACS Appl. Nano Mater. 2024, 7(16), 18695-18173, https://doi.org/10.1021/acsanm.4c02721.
208. Karthikeyan, C.; Arunachalam ,P.; Ramachandran, K.; Al-Mayouf, A.M.; Karuppuchamy, S. Recent advances in semiconductor metal oxides with enhanced methods for solar photocatalytic applications. J. Alloys Compd. 2020, 828, 154281, https://doi.org/10.1016/j.jallcom.2020.154281.
209. Chen, Y.; Qian, J.; Wang, N.; Xing, J.; Liu, L. In-situ synthesis of CNT/TiO_2 heterojunction nanocomposite and its efficient photocatalytic degradation of Rhodamine B dye. Inorg. Chem. Commun. 2020, 119, 108071, https://doi.org/10.1016/j.inoche.2020.108071.
210. Shaban, M.; Ashraf, A.M.; Abukhadra, M.R. TiO_2 Nanoribbons/Carbon Nanotubes Composite with Enhanced Photocatalytic Activity; Fabrication, Characterization, and Application. Sci Rep 2018, 8, 781. https://doi.org/10.1038/s41598-018-19172-w.
211. Pete, KY.; Kabuba, J.; Otieno, B.; Ochieng, A. Modeling adsorption and photocatalytic treatment of recalcitrant contaminant on multi-walled carbon/TiO_2 nanocomposite. Environ Sci Pollut Res Int. 2023 , 30(41), 94154-94165. doi: 10.1007/s11356-023-28852-8.
212. Czech ,B.; Buda, W. Photocatalytic treatment of pharmaceutical wastewater using new multiwall-carbon nanotubes/TiO_2/SiO_2 nanocomposites. Environ Res. 2015, 137, 176-84. doi: 10.1016/j.envres.2014.12.006.
213. Akter, J.; Hanif, M.A.; Islam, M.A. et al. Selective growth of Ti^{3+}/TiO_2/CNT and Ti^{3+}/TiO_2/C nanocomposite for enhanced visible-light utilization to degrade organic pollutants by lowering TiO_2-bandgap. Sci Rep 2021, 11, 9490. https://doi.org/10.1038/s41598-021-89026-5

 doi:10.20944/preprints202510.0466.v1

214. Koo, Y.; Littlejohn, G.; Collins, B.; Yun, Y.; Shanov, V.N.; Schulz, M.; Pai, D.; Sankar, J. Synthesis and characterization of Ag–TiO_2–CNT nanoparticle composites with high photocatalytic activity under artificial light, Compos. B Eng. 2014, 57, 105-111, https://doi.org/10.1016/j.compositesb.2013.09.004.
215. Azzam, E.M.S.; Fathy, N.A.; El-Khouly, S.M.; Sami, R.M. Enhancement the photocatalytic degradation of methylene blue dye using fabricated CNTs/TiO_2/AgNPs/Surfactant nanocomposites, J WATER PROCESS ENG. 2019, 28, 311-321. https://doi.org/10.1016/j.jwpe.2019.02.016.
216. Yang ,Y.; Liu, K.; Sun, F.; Liu ,Y.; Chen ,J. Enhanced performance of photocatalytic treatment of Congo red wastewater by CNTs-Ag-modified TiO_2 under visible light. Environ Sci Pollut Res Int. 2022, 29(11), 15516-15525. doi: 10.1007/s11356-021-16734-w.
217. Chen, J.; Liu, K.; Liu, Y. Synergistic Molecular Mechanism of Degradation in Dye Wastewater by Rhodopseudomonas palustris Intimately Coupled Carbon Nanotube–Silver Modified Titanium Dioxide Photocatalytic Composite with Sodium Alginate. J. Environ. Manag. 2024, 351, 119913. https://doi.org/10.1016/j.jenvman.2023.119913.
218. Liu ,K.; Yang ,Y.; Sun, F.; Liu, Y.; Tang, M.; Chen, J. Rapid degradation of Congo red wastewater by Rhodopseudomonas palustris intimately coupled carbon nanotube - Silver modified titanium dioxide photocatalytic composite with sodium alginate. Chemosphere. 2022 Jul;299:134417. doi: 10.1016/j.chemosphere.2022.134417.
219. Akhter,P.; Ali,F.; Ali,A.; Hussain,M. TiO2 decorated CNTs nanocomposite for efficient photocatalytic degradation of methylene blue, Diamond and Related Materials, 141, 2024, 110702, https://doi.org/10.1016/j.diamond.2023.110702.
220. Gallegos-Cerda, S.D.; Hernández-Varela, J.D.; Chanona Pérez, J.J.; Huerta-Aguilar, C.A.; Victoriano, L .G.; Arredondo-Tamayo, B.; Hernández, O.R. Development of a low-cost photocatalytic aerogel based on cellulose, carbon nanotubes, and TiO2 nanoparticles for the degradation of organic dyes, Carbohydrate Polymers, 324, 2024, 121476, https://doi.org/10.1016/j.carbpol.2023.121476.
221. Rostami, M.S.; Khodaei, M.M.; Benassi, E. Surface modified of chitosan by TiO_2@MWCNT nanohybrid for the efficient removal of organic dyes and antibiotics. Int. J. Biol. Macromol. 2024, 274(Part 1), 133382. https://doi.org/10.1016/j.ijbiomac.2024.133382.
222. Su-Bin Kim.; Seul-Yi Lee.; Soo-Jin Park. TiO_2 / multi-walled carbon nanotube electro spun nanofibers mats for enhanced Cr (VI) photoreduction. Journal of Cleaner Production 2024, 448,141611. https://doi.org/10.1016/j.jclepro.2024.141611.
223. Hor-Yan ,Phin.; Yit-Thai, Ong.; Jin-Chung, Sin. Effect of carbon nanotubes loading on the photocatalytic activity of zinc oxide/carbon nanotubes photocatalyst synthesized via a modified sol-gel method, J. Environ. Chem. Eng., 2020, 8, 103222, https://doi.org/10.1016/j.jece.2019.103222.
224. Hanif,Md.A.; Young-Soon KimJeasmin AkterHong Gun KimLee Ku Kwac, Fabrication of Robust and Stable N-Doped ZnO/Single-Walled Carbon Nanotubes: Characterization, Photocatalytic Application, Kinetics, Degradation Products, and Toxicity Analysis, ACS Omega, ACS Omega 2023, 8(18), 16174–16185, https://doi.org/10.1021/acsomega.3c00370.
225. Humayoun ,UB.; Mehmood ,F.; Hassan ,Y.; Rasheed ,A.; Dastgeer ,G.; Anwar ,A.; Sarwar ,N.; Yoon, D. Harnessing Bio-Immobilized ZnO/CNT/Chitosan Ternary Composite Fabric for Enhanced Photodegradation of a Commercial Reactive Dye. Molecules 2023, 28(18), 6461. https://doi.org/10.3390/molecules28186461.
226. Foroutan,R.; Peighambardoust,S.J.; Esvandi,Z.; Khatooni,H.; Ramavandi,B. Evaluation of two cationic dyes removal from aqueous environments using CNT/MgO/$CuFe_2O_4$ magnetic composite powder: A comparative study, J. Environ. Chem. Eng. 2021, 9, 104752, https://doi.org/10.1016/j.jece.2020.104752.

 doi:10.20944/preprints202510.0466.v1

227. Rui-Jie Pan.; Jing Wu.; Jin Qu.; Tingting Zhang.; Fan-Zhen Jiao.; Mang Zhao.; Meng-Yan Han.; Xiaofeng L.; Zhong-Zhen Yu. Peak-like three-dimensional $CoFe_2O_4$/carbon nanotube decorated bamboo fabrics for simultaneous solar-thermal evaporation of water and photocatalytic degradation of bisphenol A. J. Mater. Sci. Technol. 2024, 179, 40-49. https://doi.org/10.1016/j.jmst.2023.08.045.
228. Fidelis, M.Z.; dos Santos, A.S.G.G.; de Paula ,E.T.; Lenzi, G.G.; Soares, O.S.G.P.; Andreo, O.A.B. Nb_2O_5/MWCNT nanocomposites for the degradation of ibuprofen via photocatalysis and catalytic ozonation. Catal. Commun. 2024, 187, 106853. https://doi.org/10.1016/j.catcom.2024.106853.
229. Isari, AA.; Mehregan, M.; Mehregan, S.; Hayati, F.; Kalantary, R.R.; Kakavandi, B. Sono-photocatalytic degradation of tetracycline and pharmaceutical wastewater using WO_3/CNT heterojunction nanocomposite under US and visible light irradiations: A novel hybrid system. J Hazard Mater. 2020, 15(39), 122050. doi: 10.1016/j.jhazmat.2020.122050.
230. Huo ,H.; Hu, X.; Wang ,H.; Li ,J.; Xie, G.; Tan ,X.; Jin, Q.; Zhou, D.; Li, C.; Qiu ,G.; Liu ,Y. Synergy of Photocatalysis and Adsorption for Simultaneous Removal of Hexavalent Chromium and Methylene Blue by g-C_3N_4/$BiFeO_3$/Carbon Nanotubes Ternary Composites. Int J Environ Res Public Health. 2019, 16(17), 3219. doi: 10.3390/ijerph16173219.
231. Mestre ,AS.; Carvalho ,AP. Photocatalytic Degradation of Pharmaceuticals Carbamazepine, Diclofenac, and Sulfamethoxazole by Semiconductor and Carbon Materials: A Review. Molecules 2019, 24(20), 3702. https://doi.org/10.3390/molecules24203702.
232. Novoselov, K.S.; Geim, A.K.; Morozov, S.V.; Jiang, D.; Zhang, Y.; Dubonos, S.V.; Grigorieva, I.V. Electric field effect in atomically thin carbon films. Science 2004, 306, 666-669.
233. Gollavelli, G.; Ling, Y.C. Chapter 21 Ultrathin graphene structure, fabrication and characterization for clinical diagnosis applications. In Smart Nanodevices for Point-of-Care Applications; Kanchi, S., Chokkareddy, R., Rezakazemi, M., Eds.; CRC Press: Boca Raton, FL, USA, 2022; pp. 263-280.
234. Gollavelli, G.; Chang, C.-C.; Ling, Y.-C. Facile Synthesis of Smart Magnetic Graphene for Safe Drinking Water: Heavy Metal Removal and Disinfection Control. ACS Sustainable Chem. Eng. 2013, 1, 462-472. https://doi.org/10.1021/sc300112z.
235. Liu, Y. Application of graphene oxide in water treatment 2017 IOP Conf. Ser.: Earth Environ. Sci. 2017, 94, 012060. DOI 10.1088/1755-1315/94/1/012060.
236. Peng, W.; Li, H.; Liu, Y.; Song, S. A review on heavy metal ions adsorption from water by graphene oxide and its composites. J. Mol. Liq. 2017, 230, 496-504, http://dx.doi.org/10.1016/j.molliq.2017.01.064.
237. Thakur, K.; and Kandasubramanian, B. Graphene and Graphene Oxide-Based Composites for Removal of Organic Pollutants: A ReviewJ. Chem. Eng. Data 2019,64, 833-867, DOI: 10.1021/acs.jced.8b01057.
238. Huang, P.; Xu, C.; Lin, J.; Wang, C.; Wang, X.; Zhang, C.; Zhou, X.; Guo, S.; Cui, D. Folic Acid-conjugated Graphene Oxide loaded with Photosensitizers for Targeting Photodynamic Therapy. Theranostics 2011, 1,240-250. doi:10.7150/thno/v01p0240. https://www.thno.org/v01p0240.htm .
239. Patel, M. A.; Yang, H.; Chiu, P. L.; Mastrogiovanni, D. D. T.; Flach, C. R.; Savaram, K.; Gomez, L.; Hemnarine, A.; Mendelsohn, R.; Garfunkel, E.; Jiang, H.; He, H. Direct Production of Graphene Nanosheets for Near Infrared Photoacoustic Imaging. ACS Nano 2013, 7, 8147-8157. DOI: 10.1021/nn403429v.
240. Mahmood, F.; Ashraf, S.; Shahzad, M.; Li, B.; Asghar, F.; Amjad, W.; Omar, M. M. Graphene Synthesis from Organic Substrates: A Review. Ind. Eng. Chem. Res. 2023, 62, 17314-17327. DOI: 10.1021/acs.iecr.3c01715.
241. Verma, G.; Mondal, K.; Islam, M.; Gupta, A. Recent Advances in Advanced Micro and Nanomanufacturing for Wastewater Purification. ACS Appl. Eng. Mater. 2024, 262-285. DOI: 10.1021/acsaenm.3c00071.

 doi:10.20944/preprints202510.0466.v1

242. Yuan, S.-J.; Wang, J.-J.; Dong, B.; Dai, X.-H. Biomass-Derived Carbonaceous Materials with Graphene/Graphene-Like Structures: Definition, Classification, and Environmental Applications. Environ. Sci. Technol. 2023, 57, 17169-17177. DOI: 10.1021/acs.est.3c04203.
243. Devi, M. K.; Yaashikaa, P. R.; Kumar, P. S.; Manikandan, S.; Oviyapriya, M.; Varshikaa, V.; Rangasamy, G. Recent Advances in Carbon-Based Nanomaterials for the Treatment of Toxic Inorganic Pollutants in Wastewater. New J. Chem. 2023, 47, 7655-7667.
244. Sitko, R.; Turek, E.; Zawisza, B.; Malicka, E.; Talik, E.; Heimann, J.; Gagor, A.; Feist, B.; Wrzalik, R. Adsorption of Divalent Metal Ions from Aqueous Solutions Using Graphene Oxide. Dalton Trans. 2013, 42, 5682-5689. https://doi.org/10.1039/C3DT33097D.
245. Liu, L.; Li, C.; Bao, C.; Jia, Q.; Xiao, P.; Liu, X.; Zhang, Q. Preparation and Characterization of Chitosan/Graphene Oxide Composites for the Adsorption of Au(III) and Pd(II). Talanta 2012, 93, 350-357. https://doi.org/10.1016/j.talanta.2012.02.051.
246. Musico, Y. L. F.; Santos, C. M.; Dalida, M. L. P.; Rodrigues, D. F. Improved Removal of Lead(II) from Water Using a Polymer-Based Graphene Oxide Nanocomposite. J. Mater. Chem. A 2013, 1, 3789-3796.
247. Yang, Y.; Xie, Y.; Pang, L.; Li, M.; Song, X.; Wen, J.; Zhao, H. Preparation of Reduced Graphene Oxide/Poly(acrylamide) Nanocomposite and Its Adsorption of Pb(II) and Methylene Blue. Langmuir 2013, 29, 10727-10736. DOI: 10.1021/la401940z.
248. Patel, M.; Lanakapati, H.; Maheria, K. Efficient Removal of Pb^{2+}, Cd^{2+}, and Hg^{2+} from Wastewater Using Advanced Graphene Oxide-Zirconium Hybrid Composite. ACS Appl. Eng. Mater. 2024, 2, 1542-1560. DOI: 10.1021/acsaenm.4c00090.
249. Gou, Q.; Cai, X.; Yan, Z.; Gao, Y.; Tang, J.; Xiao, W.; Cai, J. Highly Selective Pb(II) Adsorption by DTPA-Functionalized Graphene Oxide/Carboxymethyl Cellulose Aerogel. Langmuir 2024, 40, 8002-8014. DOI: 10.1021/acs.langmuir.3c03954.
250. Jabbar, A. A.; Hussain, D. H.; Latif, K. H.; Jasim, A. K.; Al-aqbi, Z. T.; Alghannami, H. S.; Albishri, A. High-Efficiency Adsorption of Uranium from Wastewater Using Graphene Oxide/Graphene Oxide Nanoribbons/Chitosan Nanocomposite Aerogels. ACS Omega 2024, 9, 27260-27268. DOI: 10.1021/acsomega.4c01608.
251. Ortiz-Quiñonez, J. L.; Cancino-Gordillo, F. E.; Pal, U. Removal of Cr(III) Ions from Water Using Magnetically Separable Graphene-Oxide-Decorated Nickel Ferrite Nanoparticles. ACS Appl. Nano Mater. 2023, 6, 18491-18507. DOI: 10.1021/acsanm.3c03618.
252. Bagbi, Y.; Solanki, P. R. Fabrication of Mesoporous Silica Nanoparticle-Decorated Graphene Oxide Sheets for the Effective Removal of Lead (Pb^{2+}) from Water. ACS Omega 2024, 9, 304-316. DOI: 10.1021/acsomega.3c05228.
253. Pan, N.; Zhou, F.; Nie, X.; Ma, C.; Lei, Y.; Lei, H.; Li, L. One-Step Synthesis of Silver-Decorated Reduced Graphene Oxide Nanocomposites for Effective Elimination of Iodide Anions from Water. ACS ES&T Water 2024, 4, 719-734. DOI: 10.1021/acsestwater.3c00733.
254. Thakur, K.; Kandasubramanian, B. Graphene and Graphene Oxide-Based Composites for Removal of Organic Pollutants: A Review. J. Chem. Eng. Data 2019, 64, 833-867. https://doi.org/10.1021/acs.jced.8b01057.
255. Abd-Elhamid, A.I., Elgoud, E.M.A., Emam, S.S. et al. Superior adsorption performance of citrate modified graphene oxide as nano material for removal organic and inorganic pollutants from aqueous solution. Sci Rep 202j2, 12, 9204. https://doi.org/10.1038/s41598-022-13111-6.

 doi:10.20944/preprints202510.0466.v1

256. Ghadim, E. E.; Manouchehri, F.; Soleimani, G.; Hosseini, H.; Kimiagar, S.; Nafisi, S. Adsorption Properties of Tetracycline onto Graphene Oxide: Equilibrium, Kinetic and Thermodynamic Studies. PLoS One 2013, 8, 79254.
257. Kyzas, G. Z.; Bikiaris, D. N.; Seredych, M.; Bandosz, T. J.; Deliyanni, E. A. Removal of Dorzolamide from Biomedical Waste- waters with Adsorption onto Graphite Oxide/Poly(Acrylic Acid) Grafted Chitosan Nanocomposite. Bioresour. Technol. 2014, 152, 399-406.
258. Sun, L.; Yu, H.; Fugetsu, B. Graphene Oxide Adsorption Enhanced by in Situ Reduction with Sodium Hydrosulfite to Remove Acridine Orange from Aqueous Solution. J. Hazard. Mater. 2012, 203-204, 101-110.
259. Hosseinabadi-Farahani, Z.; Hosseini-Monfared, H.; Mahmoodi, N. M. Graphene Oxide Nanosheet: Preparation and Dye Removal from Binary System Colored Wastewater. Desalin. Water Treat. 2015, 56, 2382−2394.
260. Leão, M. B.; Fernandes, A. N.; Jauris, C. F. de M. Nanocarbon Dimensionality and Oxidation Degree Influence the Sorption of Atenolol: Implications for Water Treatment. ACS Appl. Nano Mater. 2024, 7 (7), 8307–8317. DOI: 10.1021/acsanm.4c01085.
261. Pervez, M. N.; Jiang, T.; Mahato, J. K.; Ilango, A. K.; Kumaran, Y.; Zuo, Y.; Zhang, W.; Efstathiadis, H.; Feldblyum, J. I.; Yigit, M. V.; Liang, Y. Surface Modification of Graphene Oxide for Fast Removal of Per- and Polyfluoroalkyl Substances (PFAS) Mixtures from River Water. ACS ES&T Water 2024, 4 (7), 2968–2980. DOI: 10.1021/acsestwater.4c00187.
262. Pramanik, A.; Kolawole, O. P.; Gates, K.; Kundu, S.; Shukla, M. K.; Moser, R. D.; Astarlioglu, M. U.; Al-Ostaz, A.; Ray, P. C. 2D Fluorinated Graphene Oxide (FGO)-Polyethyleneimine (PEI) Based 3D Porous Nanoplatform for Effective Removal of Forever Toxic Chemicals, Pharmaceutical Toxins, and Waterborne Pathogens from Environmental Water Samples. ACS Omega 2023, 8 (47), 44942–44954. DOI: 10.1021/acsomega.3c06360.
263. Agrawal, F.; Gupta, K.; Kaushik, J.; Tripathi, K. M.; Choudhary, S. K.; Sonkar, S. K. Graphene Incorporated Sugar Derived Carbon Aerogel for Pyridine Adsorption and Oil–Water Separation. Langmuir, Article ASAP. DOI: 10.1021/acs.langmuir.4c01591.
264. Lv, T.; Wu, F.; Zhang, Z.; Liu, Z.; Zhao, Y.; Yu, L.; Zhang, J.; Yu, C.; Zhao, C.; Xing, G. TiVCTX MXene/Graphene Nanosheet-Based Aerogels for Removal of Organic Contaminants from Wastewater. ACS Appl. Nano Mater. 2024, 7 (7), 7312–7326. DOI: 10.1021/acsanm.4c00038.
265. He, N.; Zhao, X.; Li, Z.; Shi, T.; Li, Z.; Guo, F.; Li, W. Polydopamine Enhanced Interactions of Graphene Nanosheets to Fabricate Graphene/Polydopamine Aerogels with Effectively Clear Organic Pollutants. Langmuir 2024, 40 (18), 9592–9601. DOI: 10.1021/acs.langmuir.4c01591.
266. Natasha; Khan, A.; Rahman, U. ; U. Sadaf; Yaseen, M.; Abumousa, R. A.; Khattak, R.; Rehman, N.; Bououdina, M.; Humayun, M. Effective Removal of Nile Blue Dye from Wastewater using Silver-Decorated Reduced Graphene Oxide. ACS Omega 2024, 9 (17), 19461–19480. DOI: 10.1021/acsomega.4c00973.
267. Kabir, M. H.; Hossain, M. S.; Rahman, M. M.; Ashrafuzzaman, M.; Hasan, M.; Pabel, M. Y.; Islam, D.; Bashar, M. S.; Faruque, T.; Yasmin, S. Green Reduction of Waste-Battery-Derived Graphene Oxide by Jute Leaves and Its Application for the Removal of Tetracyclines from Aqueous Media. ACS Sustainable Resource Management 2024, 1 (8), 1812–1823. DOI: 10.1021/acssusresmgt.4c00181.
268. Herath, T. M.; Zhang, B.; Dwinandha, D.; Fujii, M. Elucidating Adsorption Mechanisms and Characteristics of Emerging Aromatic Organic Contaminants to Graphene Material by Quantum Chemical Calculation Integrated with Interpretable Machine Learning. ACS ES&T Water, Article ASAP. Publication Date (Web): August 2, 2024. DOI: 10.1021/acsestwater.4c00219.

 doi:10.20944/preprints202510.0466.v1

269. Homaeigohar, S.; Elbahri, M. Graphene Membranes for Water Desalination. NPG Asia Mater. 2017, 9, e427. https://doi.org/10.1038/am.2017.135.
270. Nam, Y.-T.; Kang, J.-H.; Jang, J.-D.; Bae, J.-H.; Jung, H.-T.; Kim, D.-W. Recent Developments in Nanoporous Graphene Membranes for Organic Solvent Nanofiltration: A Short Review. Membranes 2021, 11, 793. https://doi.org/10.3390/membranes11100793.
271. Han, Q.; Zhang, Z.; Li, L.; Yang, W.; Tao, Y.; Bi, K. Dual-Side Fabrication of Nanopores on Bilayer Graphene Membranes for Selective Ion Transport. J. Phys. Chem. C 2023, 127(46), 22646-22653. https://doi.org/10.1021/acs.jpcc.3c04886.
272. Reddy, P. R.; Reddy, K. A.; Kumar, A. Comparative Retention Analysis of Intercalated Cations Inside the Interlayer Gallery of Lamellar and Nonlamellar Graphene Oxide Membranes in Reverse Osmosis Process: A Molecular Dynamics Study. J. Phys. Chem. B 2024, 128(21), 5218-5227. https://doi.org/10.1021/acs.jpcb.4c01623.
273. Lv, Y.; Dong, L.; Cheng, L.; Gao, T.; Wu, C.; Chen, X.; He, T.; Cui, Y.; Liu, W. Tailoring Monovalent Ion Sieving in Graphene-Oxide Membranes with High Flux by Rationally Intercalating Crown Ethers. ACS Appl. Mater. Interfaces 2023, 15(39), 46261-46268. https://doi.org/10.1021/acsami.3c10113.
274. Wang, Z.; Ma, C.; Xu, C.; Sinquefield, S. A.; Shofner, M. L.; Nair, S. Graphene Oxide Nanofiltration Membranes for Desalination under Realistic Conditions. Nat. Sustain. 2021, 4, 402–408. https://doi.org/10.1038/s41893-020-00674-3.
275. Gong, D.; Liu, X.; Wu, P.; et al. Water Pumping Effect over the Organic Ions Defined Graphene Oxide Membrane Impulses High Flux Desalination. npj Clean Water 2022, 5, 68. https://doi.org/10.1038/s41545-022-00209-7.
276. Zhang, H.; Xing, J.; Wei, G.; et al. Electrostatic-Induced Ion-Confined Partitioning in Graphene Nanolaminate Membrane for Breaking Anion–Cation Co-Transport to Enhance Desalination. Nat. Commun. 2024, 15, 4324. https://doi.org/10.1038/s41467-024-48681-8.
277. Liu, Q.; Toyosi E, O.; Yang, C.; Zhang, R.; Long, M.; Jiang, Z.; Wu, H. Hydrophilic Graphene Oxide Membrane Intercalated by Halloysite Nanotubes for Oil-in-Water Emulsion Separation. ACS Appl. Eng. Mater. 2023, 1(12), 3338-3347. https://doi.org/10.1021/acsaenm.3c00613.
278. Wu, D.; Sun, M.; Zhang, W.; Zhang, W. Simultaneous Regulation of Surface Properties and Microstructure of Graphene Oxide Membranes for Enhanced Nanofiltration Performance. ACS Appl. Mater. Interfaces 2023, 15(44), 52029-52037. https://doi.org/10.1021/acsami.3c14049.
279. Chen, J.; Liu, X.; Ding, Z.; He, Z.; Jiang, H.; Zhu, K.; Li, Y.; Shi, G. Multistage Filtration Desalination via Ion Self-Rejection Effect in Cation-Controlled Graphene Oxide Membrane under 1 Bar Operating Pressure. Nano Lett. 2023, 23(23), 10884-10891. https://doi.org/10.1021/acs.nanolett.3c03105.
280. Ahmad Farid, M. A.; Sabidi, S.; Ruozhu, W.; Lease, J.; Maeda, T.; Tsubota, T.; Andou, Y. Fabrication of Graphene-Based Nanofiltration Membrane from Fractionated Bamboo Lignin for Dye Removal and Desalination. ACS Appl. Eng. Mater. 2023, 1(10), 2791-2808. https://doi.org/10.1021/acsaenm.3c00498.
281. Soomro, F.; Ali, A.; Ullah, S.; Iqbal, M.; Alshahrani, T.; Khan, F.; Yang, J.; Thebo, K. H. Highly Efficient Arginine Intercalated Graphene Oxide Composite Membranes for Water Desalination. Langmuir 2023, 39(50), 18447-18457. https://doi.org/10.1021/acs.langmuir.3c02699.
282. Ali, A.; Vohra, M. I.; Nadeem, A.; Al-Anzi, B. S.; Iqbal, M.; Memon, A. A.; Jatoi, A. H.; Akhtar, J.; Yang, J.; Thebo, K. H. Ultrafast Graphene Oxide-Lignin Biopolymer Nanocomposite Membranes for Separation of Biomolecules, Dyes, and Salts. ACS Appl. Polym. Mater. 2024, 6(8), 4747-4755. https://doi.org/10.1021/acsapm.4c00285.

 doi:10.20944/preprints202510.0466.v1

283. Tiwary, S. K.; Singh, M.; Hasan Likhi, F.; Dabade, S.; Douglas, J. F.; Karim, A. Self-Cross-Linking of MXene-Intercalated Graphene Oxide Membranes with Antiswelling Properties for Dye and Salt Rejection. ACS Environ. Au 2024, 4(2), 69-79. https://doi.org/10.1021/acsenvironau.3c00059.
284. Alemayehu, H. G.; Hou, J.; Qureshi, A. A.; Yao, Y.; Sun, Z.; Yan, M.; Wang, C.; Liu, L.; Tang, Z.; Li, L. Discrimination of Xylene Isomers by Precisely Tuning the Interlayer Spacing of Reduced Graphene Oxide Membrane. ACS Nano 2024, 18(28), 18673-18682. https://doi.org/10.1021/acsnano.4c05461.
285. Schmidt, S. J.; Dou, W.; Sydlik, S. A. Regeneratable Graphene-Based Water Filters for Heavy Metal Removal at Home. ACS ES&T Water 2023, 3(8), 2179-2185. https://doi.org/10.1021/acsestwater.3c00010.
286. Bhol, P.; Yadav, S.; Altaee, A.; Saxena, M.; Kumari Misra, P.; Samal, A. K. Graphene-Based Membranes for Water and Wastewater Treatment: A Review. ACS Appl. Nano Mater. 2021, 4(4), 3274-3293. https://doi.org/10.1021/acsanm.0c03439..
287. Tian, L.; Zhou, P.; Su, Z.; Graham, N.; Yu, W. Surface Microstructure Drives Biofilm Formation and Biofouling of Graphene Oxide Membranes in Practical Water Treatment. Environ. Sci. Technol. 2024, 58(27), 12281-12291. https://doi.org/10.1021/acs.est.4c03363.
288. Khaliha, S.; Bianchi, A.; Kovtun, A.; Tunioli, F.; Boschi, A.; Zambianchi, M.; Paci, D.; Bocchi, L.; Valsecchi, S.; Polesello, S.; Liscio, A.; Bergamini, M.; Brunetti, M.; Navacchia, M. L.; Palermo, V.; Melucci, M. Graphene Oxide Nanosheets for Drinking Water Purification by Tandem Adsorption and Microfiltration. Sep. Purif. Technol. 2022, 300, 121826. https://doi.org/10.1016/j.seppur.2022.121826.
289. Li, X., Yu, J., Wageh, S., Al-Ghamdi, A.A. and Xie, J. Graphene in Photocatalysis: A Review. Small 2016, 12: 6640-6696. https://doi.org/10.1002/smll.201600382.
290. Zhu, D.; Zhou, Q. Action and mechanism of semiconductor photocatalysis on degradation of organic pollutants in water treatment: A review. Environmental Nanotechnology, Monitoring & Management 2019, 12, 100255. https://doi.org/10.1016/j.enmm.2019.100255.
291. Zhang, J.; Xiong, Z.; Zhao, X.S. Graphene–metal–oxide composites for the degradation of dyes under visible light irradiation. J. Mater. Chem. 2011, 21, 3634-3640. https://doi.org/10.1039/C0JM03827J.
292. Zhang, H.; Lv, X.; Li, Y.; Wang, Y.; Li, J. P25-Graphene Composite as a High Performance Photocatalyst. ACS Nano 2010, 4, 380-386. DOI: 10.1021/nn901221k.
293. Huynh, T.P.; Do, T.C.M.V.; Le, P.H. TiO_2 Nanotube Arrays Decorated with Graphene/Graphite Oxide Nanocomposite for the Photocatalytic Degradation of Anticancer Drugs in the Aquatic Environment. *ACS Appl. Nano Mater*. 2024, 7, 20012–20023. https://doi.org/10.1021/acsanm.4c02377.
294. Li, B.; Cao, H. ZnO@graphene composite with enhanced performance for the removal of dye from water. J. Mater. Chem. 2011, 21, 3346-3349. DOI: 10.1039/c0jm03253k.
295. Lu, K.-Q.; Li, Y.-H.; Tang, Z.-R.; Xu, Y.-J. Roles of Graphene Oxide in Heterogeneous Photocatalysis. ACS Materials Au 2021, 1, 37-54. DOI: 10.1021/acsmaterialsau.1c00022.
296. Trivedi, P.A.; Naik, J.B.; Patil, P.B. Exploring graphene and its derivatives for various applications: photocatalysis. Chem. Pap. 2024, 78, 5705-5722. https://doi.org/10.1007/s11696-024-03475-6.
297. Ramos, P.G.; Rivera, H.; Sánchez, L.A. *et al*. Graphene-based Semiconductors for Photocatalytic Degradation of Organic Dye from Wastewater: A Comprehensive Review. Water Air Soil Pollut. 2024, 235, 292. https://doi.org/10.1007/s11270-024-07111-7.
298. Chitkara, M.; Goyalbc, N.; Kumar, A.; Marasamy, L.; Haq, S.; SAldossari, S. A.; Haldhar, R.; Hossain, M. K. Tailoring graphene-oxide and reduced-graphene-oxide with $NaNO_3$ and $CaCl_2$ catalysts with enhanced photo-catalytic degradation of methylene blue dye. RSC Adv., 2024, 14, 8769-8778. DOI: 10.1039/D3RA08256C.

299. Thakur, S.; Badoni, A.; Sharma, P.; Ojha, A.; Swart, H. C.; Kuznetsov, A. Y.; Prakash, J. Standalone Highly Efficient Graphene Oxide as an Emerging Visible Light-Driven Photocatalyst and Recyclable Adsorbent for the Sustainable Removal of Organic Pollutants. Langmuir Article ASAP. DOI: 10.1021/acs.langmuir.4c01727.
300. Durairaj, S., Sridhar, D.; Ströhle, G.; Li, H.; Chen, A. Bactericidal Effect and Cytotoxicity of Graphene Oxide/Silver Nanocomposites. ACS Appl. Mater. Interfaces 2024, 16, 18300-18310. DOI: 10.1021/acsami.3c15798.
301. Jaiswal, K.; Kadamannil, N.N.; Jelinek, R. Carbon nanomaterials in microbial sensing and bactericidal applications. Current Opinion in Colloid & Interface Science 66, 2023, 101719,.https://doi.org/10.1016/j.cocis.2023.101719.
302. Konwarh, R.; Gollavelli, G.; Palanisamy, S. B. Designing novel nanosensors for environmental aspects. Nanofabrication for Smart Nanosensor Applications. Pal, K., Gomes, F., Eds.; Elsevier: location, country, 2020, volume, pp. 51-87. https://doi.org/10.1016/B978-0-12-820702-4.00003-9.
303. Deokar, A. R.; Sinha, M.; Gollavelli, G.; Ling, Y.-C. Antimicrobial Perspectives for Graphene-Based Nanomaterials. Graphene Science Handbook: Applications and Industrialization. Aliofkhazraei, M., Ali, N., Milne, W. I., Ozkan, C. S., Mitura, S., Gervasoni, J. L., Eds.; CRC Press Taylor & Francis, 2016, pp. 488. https://doi.org/10.1201/b19488.
304. Gorle, G.; Gollavelli, G.; Nelli, G,; Ling, Y.-C. Green Synthesis of Blue-Emitting Graphene Oxide Quantum Dots for In Vitro CT26 and In Vivo Zebrafish Nano-Imaging as Diagnostic Probes. Pharmaceutics 2023, 15, 632. https://doi.org/10.3390/pharmaceutics15020632.
305. Kumah, E. A.; Fopa, R. D.; Harati, S. *et al*. Human and environmental impacts of nanoparticles: a scoping review of the current literature. BMC Public Health 2023, 23, 1059. https://doi.org/10.1186/s12889-023-15958-4.
306. Mohan, D., Pittman Jr, C.U. Activated carbons and low cost adsorbents for remediation of tri- and hexavalent chromium from water. J. Hazard. Mater. 2007 137(2), 762-811. https://doi.org/10.1016/j.jhazmat.2006.06.060.
307. Liu, S., et al. (2012).Graphene oxide-based materials for efficient removal of heavy metal ions from aqueous solution: A review. Environ. Pollut. 2019, 252(Pt A), 62-73. https://doi.org/10.1016/j.envpol.2019.05.050.
308. Pérez, S.; Farré, M.; Barceló, D. Analysis, behavior and ecotoxicity of carbon-based nanomaterials in the aquatic environment. Trends Anal. Chem. 2009, 28(6), 820-832. 2648-2653. https://doi.org/10.1016/j.trac.2009.04.001.
309. Seoktae, Kang.; Meagan S, M.; Menachem, Elimelech. Microbial Cytotoxicity of Carbon-Based Nanomaterials: Implications for River Water and Wastewater Effluent. Environ. Sci. Technol. Lett. 2009, 43(7), https://pubs.acs.org/doi/10.1021/es8031506.
310. Zaytseva, O.; Neumann, G. Carbon nanomaterials: production, impact on plant development, agricultural and environmental applications. Chem. Biol. Technol. Agric. 2016, 3:17, 1-26. https://chembioagro.springeropen.com/articles/10.1186/s40538-016-0070-8.
311. Freixa, A.; Acuña, V.; Sanchís, J.; Farré, M.; Barceló, D.; Sabate, S. Ecotoxicological effects of carbon based nanomaterials in aquatic organisms. Sci. Total Environ. 2018, 619-620, 328-337. https://doi.org/10.1016/j.scitotenv.2017.11.095.
312. Pikula, K.; Johari, S.A.; Santos-Oliveira, R.; Golokhvast, K. Joint Toxicity and Interaction of Carbon-Based Nanomaterials with Co-Existing Pollutants in Aquatic Environments: A Review. Int. J. Mol. Sci. 2024, 25, 11798. https://doi.org/10.3390/ijms252111798.

 doi:10.20944/preprints202510.0466.v1

313. Cha, C.; Shin, S.R.; Annabi, N,; Dokmeci, M.R.; Khademhosseini, A. Carbon-Based Nanomaterials: Multifunctional Materials for Biomedical Engineering. ACS Nano 2013, 7(4), 2891-2897. https://pubs.acs.org/doi/10.1021/nn401196a.
314. OSPAR Convention. Precautionary Principle. https://www.ospar.org/convention/principles/precautionary-principle.
315. Goldstein, B.D. The Precautionary Principle Also Applies to Public Health Actions. Am J Public Health. 2001, 91(9), 1358-1361. https://ajph.aphapublications.org/doi/10.2105/AJPH.91.9.1358
316. Pinto-Bazurco, J.F. The Precautionary Principle. 2020. https://www.iisd.org/articles/deep-dive/precautionary-principle.
317. Warshaw, J. The Trend Towards Implementing the Precautionary Principle in US Regulation of Nanomaterials. Dose-Response 2012, 10, 384-396. https://doi.org/10.2203/dose-response.10-030.Warshaw.